In presenting the dissertation as a partial fulfillment of the requirements for an advanced degree from the Georgia Institute of Technology, I agree that the Library of the Institution shall make it available for inspection and circulation in accordance with its regulations governing material of this type. I agree that permission to copy from, or to publish from, this dissertation may be granted by the professor under whose direction it was written, or in his absence, by the Dean of the Graduate Division when such copying or publication is solely for scholarly purposes and does not involve potential financial gains. It is understood that any copying from, or publication of, this dissertation which involves potential financial gain will not be allowed without written permission.

William G. Trawick

THE POLARIZED ULTRAVIOLET ABSORPTION SPECTRA OF SINGLE CRYSTALS OF POLYATOMIC SUBSTANCES AT LOW TEMPERATURE

12 T

A THESIS

Presented to

the Faculty of the Graduate Division

Georgia Institute of Technology

In Partial Fulfillment

of the Requirements for the Degree

Doctor of Philosophy in the School

of Chemistry

By

William George Trawick

December 1954

THE POLARIZED ULTRAVIOLET ABSORPTION SPECTRA OF SINGLE CRYSTALS OF POLYATOMIC SUBSTANCES AT LOW TEMPERATURE

Approved:

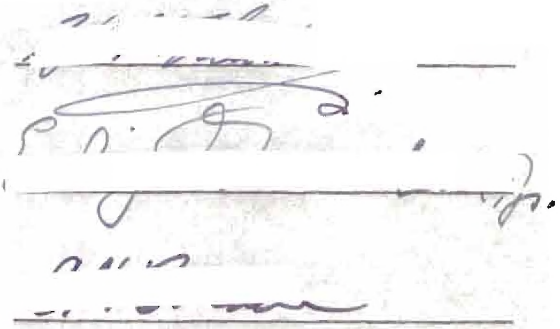

Date Approved by Chairman: December 3, 1954

ACKNOWLEDGMENTS

The author wishes to express his gratitude to Dr. W. H. Eberhardt for suggesting this problem and for the guidance and encouragement that made this thesis possible. He is also indebted to Dr. C. H. Braden and Dr. Erling Grovenstein for reading the manuscript and offering constructive criticism and suggestions. He is indebted to the School of Chemistry for financial aid through Graduate Assistantships and to the Research Corporation for a grant for the summer of 1953. Finally, the author wishes to express his gratitude to his wife for her faith, encouragement, work, and patience in seeing this to its completion.

TABLE OF CONTENTS

LIST OF TABLES

LIST OF ILLUSTRATIONS

Figure | Page

ABSTRACT

A fundamental understanding of the physical and chemical properties of substances can be gained through a knowledge of the electronic structure of the substances. The complexity of the electronic structure for polyatomic molecules necessitates a combined attack by the use of quantum mechanics and special tools in electronic spectra. The added information that can be gained by the use of polarized radiation and oriented molecules is the key to the interpretation presented here for the nitrite ion and some similar substances studied in relation to the nitrite ion.

Quantum mechanical calculations using the linear combination of atomic orbitals approach and sp^2 hybrid atomic orbitals were made for the nitrite ion. An attempt was also made to refine this approximation by the use of valence state ionization potentials for oxygen and nitrogen. The results obtained from these calculations have been compared with energy level schemes suggested by other authors and certain modifications are suggested.

Single crystals of sodium nitrite were grown from aqueous solutions of the salt. Thin natural crystals yielded absorption spectra for radiation polarized parallel to the C_{2v} axis of the ion and perpendicular to the ion. A large crystal was cut and polished to about thirty microns thickness for the absorption spectrum of radiation polarized parallel to the oxygen-oxygen internuclear direction. The crystals were oriented by inspection under a polarizing microscope with the aid of liquids with

their refractive indices the same or almost the same as one of the indices of the crystal.

The source of radiation used was a two and a half kilowatt hydrogen discharge tube. The crystal was placed in a collimated beam from this source and carefully oriented with respect to the beam and a Wollaston polarizing prism. With the Wollaston prism two spectra polarized at right angles to each other were recorded at the same time.

The spectra of sodium nitrite and silver nitrite crystals were recorded at liquid nitrogen temperature and at room temperature. In addition the spectrum of ethyl nitrite was recorded as a gas and spectra in solutions were determined for nitromethane in acidic and neutral ethanol, sodium nitrite in basic and acidic water, and ethyl nitrite in hexane, neutral and acidic ethanol, and neutral and acidic water. These measurements and measurements reported elsewhere for nitrous acid, nitryl chloride, nitrosyl chloride, nitrogen dioxide, dinitrogen tetroxide, ozone, and the nitrate ion were compared. The results of the quantum mechanical calculations and the experimental findings were correlated and interpreted as outlined below.

The absorption band of sodium nitrite which has its maximum near 3500 A appears to have an origin at 3851.4 A and absorbs radiation polarized such that the electric vector vibrates perpendicular to the plane of the nitrite ion. This absorption is believed to be due predominately to a transition in which one of the unshared electrons in an orbital primarily localized on the nitrogen atom is raised to an antibonding π orbital of the ion. This transition is designated $n_N \rightarrow \pi^*$. This assignment is consistent with the fact that the 3500 A band is absent in

nitroalkyls, nitryl chloride and the nitrate ion where the corresponding electrons on the nitrogen are shared with other atoms and hence stabilized. No comparable band is found in crystalline silver nitrite where the crystal structure is similar, but where the internuclear distances and chemical properties suggest a weak electron-pair bond between the silver and the nitrogen atoms. However, absorption in this region is present in nitrous acid and the alkyl nitrites both in solution and in the gas; this absorption is ascribed to a similar transition ($n_N \rightarrow \pi^*$).

The very intense absorption band with its maximum near 2050 A in the sodium nitrite absorbs radiation that is polarized such that the electric vector vibrates parallel to a line joining the oxygen atoms of the nitrite ion. This absorption is assigned to a transition in which an electron in a non-bonding π orbital is raised to an anti-bonding π orbital. This is represented symbolically as $\pi \rightarrow \pi^*$. This transition is comparable to those giving rise to the strong bands in the nitrate ion, nitrogen dioxide, nitryl chloride, the nitroalkyls and the alkyl nitrites at approximately the same region in the spectrum.

The neutral or basic aqueous solutions of the nitrite ion show a weaker band with maximum about 2900 A. This band is believed to underlie the 3500 A band in the crystalline spectrum. Its origin is attributed to raising an electron from a non-bonding orbital, primarily localized on the oxygen atoms, to the anti-bonding π orbital ($n_O \rightarrow \pi^*$). In the crystal this band absorbs radiation polarized with its electric vector perpendicular to the plane of the ion. It serves to broaden the 3500 A band and to complicate the fine structure that is observed at low temperature. This absorption is thought to correspond to bands in the nitrate ion, nitryl

chloride, nitric acid and the nitroalkyls at about the same wave-length. The shift of this band to shorter wave-lengths as the nitrite ion is dissolved has been attributed to interaction of the solvent with these non-bonding electrons on the oxygen atoms. This interaction lowers the energy of the ground state orbital and increases the energy needed for the transition.

A study of the 6020 A absorption band of ozone shows a remarkable similarity to that of the 3500 A band in nitrous acid and alkyl nitrites and thus has been attributed to a non-bonding electron on the central oxygen being raised to the anti-bonding π orbital. By way of summary the assignments for the various bands for a number of substances are listed in a table.

CHAPTER I

INTRODUCTION

Before the discovery of the electron, the concept of the valence bond was represented by a line drawn between the symbols of the elements. This simple idea was of great aid to progress in the field of chemistry even though the nature of the bond was unknown. Some time after the discovery of the electron it was G. N. Lewis who began the modern electronic theory of valence. The development of this theory has come through the theory of quantum mechanics. Quantum mechanics enables one to calculate the distribution of electrons in the simpler systems and from this, the energy of the system in each possible distribution. From these energies and electronic distributions one can determine the size and shape of the system, its chemical properties, and the thermodynamic properties such as heat capacity, entropy, and free energy.

The limit of this usefulness comes in the mathematical solution of the differential equations, and only approximate solutions can be obtained for systems of more than two particles. These approximations become too inaccurate to be of value for most systems. With the quantum mechanical approximations and the energy differences of states determined from spectra one is able to understand the electronic structure of diatomic molecules rather well. From this the physical and chemical properties of a large number of these systems are well known and understood.

The next step is the understanding of triatomic systems. Since

the best approach to the determination of the electronic structure for diatomic molecules is through their spectra, it is reasonable to assume that this method will serve for the more complex systems also. However, a solution is not as easy as for diatomic molecules, for, as Sponer and Teller (18) have said,

> ". . . in spite of much work done, spectroscopy of polyatomic molecules is still in the exploring state. The reasons that band spectra of polyatomic molecules have not yet proved as valuable in the study of molecular structural problems as those of diatomic molecules are well known. The variety of vibrational and rotational frequencies associated with electronic jumps is greater than for diatomic molecules. Furthermore, the anharmonicity of the vibrations does not produce a simple convergence of the bands, it can change their vibrational structure in complicated ways, ... vibrations can interact with rotations in various ways, so that distinction between vibrational and rotational structure of the spectrum becomes difficult. Finally, a polyatomic molecule possesses more possibilities of dissociation . . . and . . . this possibility results in continuous or at least diffuse band spectra, which are less valuable for an analysis than discrete spectra."

This complexity of the spectra necessitates the use of some tools that are not always required for simpler systems. One such tool is the magnetic rotation spectra which allows one to record a simpler spectrum. Another tool, and the one which was used in the work reported here, is that of polarized absorption spectroscopy.

A group theoretical study of the transition probabilities reveals that different transitions absorb (or emit) radiation polarized in different directions with respect to the orientation of the molecule. If all of the molecules are oriented in the same way, then all of the radiation absorbed (or emitted) for a given transition will be polarized as determined by the transition and the orientation of the molecule. Certain crystals contain molecules so oriented. Other crystals contain

molecules oriented in such a manner that only one axis of the molecule lies along a common direction. For the latter type of crystals, only the radiation polarized along this common direction will lead to unambiguous assignment of the direction of dipole moment change. In the case of absorption (or emission) of radiation polarized perpendicular to this axis, the dipole moment change can be along either or both of the axes perpendicular to the axis of unique direction.

Even this polarized spectra can be rather complicated, especially since the crystal field can introduce additional lines due to "term splitting." In the sodium nitrite crystal, however, the selection rules are the same as those for the isolated ion.

The theory of the selection rules in crystals is first discussed by Bethe (2B) and expanded, primarily with regard to infrared work, by Halford and others (3H). Of the polarized infrared absorption spectra reported in the literature that by Newman (4N) of the sodium nitrite crystal is of interest in this work. Polarized ultraviolet absorption spectra have also been reported on a number of substances. Craig and Hobbins (5C) have studied anthracene. Schnepp and McClure (6S) have made assignments to the first two excited singlet electronic states of naphthalene with the help of polarized ultraviolet absorption. Albrecht and Simpson (7A) have studied p-dimethoxybenzene and Lyons (8L) reports absorption by the pyrimidines of plane polarized ultraviolet light. The dichroism of substituted benzenes has been reported by Nakamoto (9N, 10N), and direct evidence for a $n \rightarrow \pi^*$ electronic transition has also been reported by Nakamoto and Suzaki (11N) on the basis of the absorption of polarized ultraviolet by nitro-nitrosobenzene. Studies of

electronic transitions of inorganic substances have been made of platinum and palladium complexes (12Y), praseodymium chloride (13S) and uranium fluorides (14G). All of this experimental work has been reported in the last seven years and most of it in the last three years. There is much activity in the field and it seems to be a promising method of study that will lead one closer to basic understanding of polyatomic molecules.

CHAPTER II

THEORETICAL CALCULATIONS

Quantum Mechanical Calculations.--In order to make assignments for the electronic transitions observed for the nitrite ion some calculations as to the relative energies of the various states must be made. Exact calculations being impossible one must compromise between the roughest of approximations and the most elaborate with the factors of accuracy required and time and effort expended determining the method.

Using the linear combination of atomic orbital (LCAO) approach, a set of molecular orbitals (MO's) can be made up in terms of which the electronic configuration of the nitrite ion and other triatomic systems can be described.

To begin the calculations in as general a manner as is convenient the system may be referred to as AB_2 where the nuclei are arranged symmetrically on an isosceles triangle. The apex angle may be anywhere between 0° and 180°. When the system is represented graphically, the symbols A and B will include the atomic nuclei and all electrons except the valence electrons. Also the assumption is made that these core electrons may be neglected except as they affect the charge on the nuclei.

It will now be assumed that the atomic orbitals (AO's) available on each atom are the three p and the one s orbitals with the same principal quantum number. Suitable changes can be readily made if only the s orbital is to be used on one member of the system. The possibility of using d orbitals will not be considered in this work. These four

orbitals from three atoms will combine to give twelve molecular orbitals.

Simply to use the unhybridized AO's would probably not be a wise choice because a lower energy is likely when hybridized orbitals are used (15C). A hybridized set of orbitals is chosen, so as to preserve the C_{2v} symmetry (16E), having the form

$$\varphi_{Rk} = a_{Rk}s + b_{Rk}p_x + c_{Rk}p_y + d_{Rk}p_z,$$

where $a_{Rk}^2 + b_{Rk}^2 + c_{Rk}^2 + d_{Rk}^2 = 1$, $a_{R1}^2 + a_{R2}^2 + a_{R3}^2 + a_{R4}^2 = 1$, etc., for the kth orbital (1, 2, 3, & 4) on atom R. If this set is chosen such that

$$\varphi_{R1} = a_R s + \frac{1}{\sqrt{2}} p_x - \frac{\sqrt{1 - 2a_R^2}}{\sqrt{2}} p_z ,$$

$$\varphi_{R2} = a_R s - \frac{1}{\sqrt{2}} p_x - \frac{\sqrt{1 - 2a_R^2}}{\sqrt{2}} p_z$$

$$\varphi_{R3} = \sqrt{1 - 2a_R^2}\, s + \sqrt{2}\, a_R p_z , \text{ and}$$

$$\varphi_{R4} = p_y ,$$

the C_{2v} symmetry may be preserved and the hybridization may be varied from none at $a = 0$ to digonal at $a_R = 1/\sqrt{2}$. When $a_R = 1/\sqrt{3}$ the hybridization is trigonal (15C). These hybrids give the atom a two fold rotational axis about φ_{R3}. Just what degree of hybridization is present will depend primarily on the number of electrons and the atoms involved and will vary from system to system.

Assuming an apex angle of near 120° it is possible to represent

the system pictorially as in Fig. 1.[1] This would mean a_R is approximately $1/\sqrt{3}$. $\phi_1, \phi_2, \ldots \phi_6$ are of type φ_{R1} and φ_{R2}, ϕ_7, ϕ_8, and ϕ_9 are of type φ_{R3}, while ϕ_{10}, ϕ_{11}, and ϕ_{12} are of type φ_{R4}.

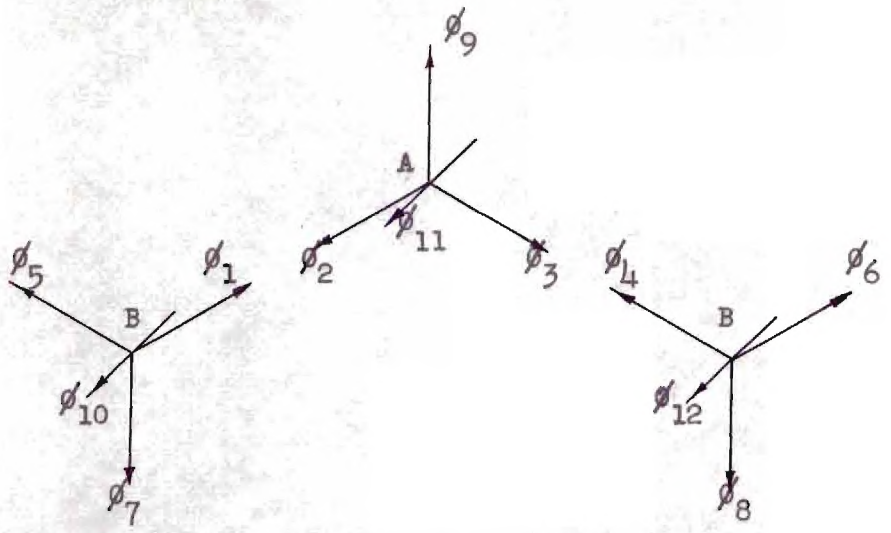

Fig. 1. Graphic Representation of AB_2 of Apex Angle 120°. ϕ_1 thru ϕ_9 are sp^2 Type Hybrids and ϕ_{10}, ϕ_{11}, and ϕ_{12} are pure p_y.

From a consideration of the extent of the overlap and symmetry properties it is convenient to separate these orbitals into the following groups, where the σ orbitals are directed along the internuclear axis, n_A orbitals are unshared orbitals on atom A, and π orbitals are orbitals with a node in the wave function at the plane of the ion:

a. Four σ orbitals of the form $\psi_j = b_{1j}\phi_1 + b_{2j}\phi_2 + b_{3j}\phi_3 + b_{4j}\phi_4$.

b. Four n_O orbitals of the form $\psi_j = b_{5j}\phi_5 + b_{6j}\phi_6 + b_{7j}\phi_7 + b_{8j}\phi_8$.

c. One n_N orbital $\psi_9 = \phi_9$, and

d. Three π orbitals of the form $\psi_j = b_{10j}\phi_{10} + b_{11j}\phi_{11} + b_{12j}\phi_{12}$.

Since there is more overlap in the σ orbitals than in the others,

---

[1] This is a good assumption since the angle in the crystalline sodium nitrite is 115.7 ± 3° (17C).

the splitting of these energy levels will be the greatest and the following symmetry MO's can be written (see Appendix I):

$$\psi_1 = \tfrac{1}{2}(\phi_1 + \phi_2 + \phi_3 + \phi_4)(\sigma), \text{of symmetry } A_1 \text{ (18H)},$$

$$\psi_2 = \tfrac{1}{2}(\phi_1 + \phi_2 - \phi_3 - \phi_4)(\sigma), \text{of symmetry } B_1,$$

$$\psi_3 = \tfrac{1}{2}(\phi_1 - \phi_2 - \phi_3 + \phi_4)(\sigma^*), \text{of symmetry } A_1, \text{ and}$$

$$\psi_4 = \tfrac{1}{2}(\phi_1 - \phi_2 + \phi_3 - \phi_4)(\sigma^*), \text{of symmetry } B_1.$$

To the extent that these MO's are good zero order approximations, the energy levels can be calculated by the formula:

$$E_j = \frac{\int \psi_j^* H \psi_j \, d\tau}{\int \psi_j^* \psi_j \, d\tau} .$$

In terms of integrals over atomic orbitals these energies are:

$$E_1 = \frac{H_{1:1} + H_{1:2} + H_{1:3} + \frac{1}{2}(H_{1:4} + H_{2:3})}{S_{1:1} + S_{1:2} + S_{1:3} + \frac{1}{2}(S_{1:4} + S_{2:3})} .$$

$$E_2 = \frac{H_{1:1} + H_{1:2} - H_{1:3} - \frac{1}{2}(H_{1:4} + H_{2:3})}{S_{1:1} + S_{1:2} - S_{1:3} - \frac{1}{2}(S_{1:4} + S_{2:3})} .$$

$$E_3 = \frac{H_{1:1} - H_{1:2} - H_{1:3} + \frac{1}{2}(H_{1:4} + H_{2:3})}{S_{1:1} - S_{1:2} - S_{1:3} + \frac{1}{2}(S_{1:4} + S_{2:3})} .$$

$$E_4 = \frac{H_{1:1} - H_{1:2} + H_{1:3} - \frac{1}{2}(H_{1:4} + H_{2:3})}{S_{1:1} - S_{1:2} + S_{1:3} - \frac{1}{2}(S_{1:4} + S_{2:3})} .$$

where $H_{ij} = H_{ji} = \int \phi_i^* H \phi_j \, d\tau$ and $S_{ij} = S_{ji} = \int \phi_i^* \phi_j \, d\tau$ and the

assumptions are made that $H_{1:1} = H_{2:2} = H_{4:4}$; $H_{1:2} = H_{3:4}$; $H_{1:3} = H_{2:4}$; $S_{1:1} = S_{2:2}$; $S_{3:3} = S_{4:4}$; $S_{1:2} = S_{3:4}$; and $S_{1:3} = S_{2:4}$. Actually $H_{2:3} = 0$ and $S_{2:3} = 0$.

In a similar way four symmetry orbitals can be written from the four non-bonding oxygen atomic orbitals. The splitting of these energy levels will not be expected to be as great as that of the σ orbitals and to the same approximation can be evaluated as below.

$$\psi_5 = \tfrac{1}{2}(\phi_5 + \phi_6 + \phi_7 + \phi_8),(n_0), \text{ of symmetry } A_1,$$

$$\psi_6 = \tfrac{1}{2}(\phi_5 - \phi_6 + \phi_7 - \phi_8),(n_0), \text{ of symmetry } B_1,$$

$$\psi_7 = \tfrac{1}{2}(\phi_5 - \phi_6 - \phi_7 + \phi_8),(n_0), \text{ of symmetry } A_1 \text{ and}$$

$$\psi_8 = \tfrac{1}{2}(\phi_5 + \phi_6 - \phi_7 - \phi_8),(n_0), \text{ of symmetry } B_1.$$

$$E_5 = \frac{H_{5:5} + H_{5:8} + (H_{5:6} + H_{7:8})/2}{S_{5:5} + S_{5:8} + (S_{5:6} + S_{7:8})/2},$$

$$E_6 = \frac{H_{5:5} - H_{5:8} - (H_{5:6} + H_{7:8})/2}{S_{5:5} - S_{5:8} - (S_{5:6} + S_{7:8})/2},$$

$$E_7 = \frac{H_{5:5} + H_{5:8} - (H_{5:6} + H_{7:8})/2}{S_{5:5} + S_{5:8} - (S_{5:6} + S_{7:8})/2}, \text{ and}$$

$$E_8 = \frac{H_{5:5} - H_{5:8} + (H_{5:6} + H_{7:8})/2}{S_{5:5} - S_{5:8} + (S_{5:6} + S_{7:8})/2}, \text{ where } H_{5:7} = H_{6:8} = 0;$$

$H_{5:5} = H_{6:6} = H_{7:7} = H_{8:8}$; $H_{5:8} = H_{6:7}$; $S_{5:7} = S_{6:8} = 0$;

$S_{5:5} = S_{6:6} = S_{7:7} = S_{8:8}$; and $S_{5:8} = S_{6:7}$.

This leaves the n_N orbital, ψ_9, and the three p_y orbitals. For consideration at this point it will be assumed that there is no interaction

of ψ_9 with other orbitals, but actually it may interact with ψ_5 and ψ_7 because they all are of A_1 symmetry and their energy levels are not widely separated. The π orbitals and their energies are as follows:

$$\psi_{10} = \frac{1}{2}(\phi_{10} + \sqrt{2}\,\phi_{11} + \phi_{12}),\ (\pi_+),\ \text{of symmetry } B_2,$$

$$\psi_{11} = \frac{1}{\sqrt{2}}(\phi_{10} - \phi_{12}),\ (\pi),\ \text{of symmetry } A_2,\ \text{and}$$

$$\psi_{12} = \frac{1}{2}(\phi_{10} - \sqrt{2}\,\phi_{11} + \phi_{12}),\ (\pi^*),\ \text{of symmetry } B_2,$$

$$E_{10} = \frac{H_{10:10} + \sqrt{2}\,H_{10:11} + \frac{1}{2}H_{10:12}}{S_{10:10} + \sqrt{2}\,S_{10:11} + \frac{1}{2}S_{10:12}},$$

$$E_{11} = \frac{H_{10:10} - H_{10:12}}{S_{10:10} - S_{10:12}},\ \text{and}$$

$$E_{12} = \frac{H_{10:10} - \sqrt{2}\,H_{10:11} + \frac{1}{2}H_{10:12}}{S_{10:10} - \sqrt{2}\,S_{10:11} + \frac{1}{2}S_{10:12}},\ \text{where it has been}$$

assumed that $H_{10:10} = H_{11:11} = H_{12:12}$; $S_{10:10} = S_{11:11} = S_{12:12}$; $H_{10:11} = H_{11:12}$; and $S_{10:11} = S_{11:12}$.

Now that approximate expressions for the energies of these one-electron MO's have been made, it would be interesting to ascertain their relative magnitudes for the nitrite ion. In order to make the problem tractable the assumptions are made that the overlap terms are negligible except for $S_{ii} = 1$, the coulomb integrals are all equal,[2] i.e., $H_{1:1} = H_{2:2} = \cdots H_{5:5} = H_{0:0} = H_{N:N} = H^o$, and the exchange integral H_{ij} is proportional to S_{ij}, i.e., $H_{ij} = AS_{ij}$ (19M). The overlap integrals can be evaluated by using Mulliken's tables (20M) if the molecular geometry

---

[2] A qualitative refinement is introduced on page 11.

and the state of hybridization are known. In making these calculations it has been assumed that (a) the hybridization is trigonal, i.e., $a = 1/\sqrt{3}$, (b) the O-N-O angle is 120°, (c) the O-N distance is 1.23 A, and (d) the formal charge on the ion is distributed such that each oxygen atom is 1/2 unit charge negative. Sample calculations of the overlap integrals for the hybrids and a table summarizing them are given in Appendix II. These calculations lead to relative energies in that $E = H^\circ + AS$ (19M), when H° is primarily the coulomb integral. They are presented graphically in Fig. 2 and recorded in terms of the unitless S in Table 1. Placing the eighteen valence electrons in the nine MO's of lowest energy gives a configuration,

$$\psi_1^2, \psi_2^2, \psi_{10}^2, \psi_8^2, \psi_6^2, \psi_9^2, \psi_5^2, \psi_{11}^2, \psi_7^2,$$

which seems consistent with the chemist's picture of the molecule as depicted in Fig. 3. This electronic structure suggests that the transitions observed in the spectra are to ψ_{12}, an anti-bonding π (π^*) MO, from either ψ_5 or ψ_7, non-bonding oxygen (n_O) MO's; ψ_9 a non-bonding nitrogen (n_N) MO; or ψ_{11} a non-bonding π MO. It will be seen later that transitions from ψ_6 and ψ_8 are forbidden on grounds of symmetry considerations.

An improvement of the accuracy of the estimate of the relative energies of the $n_O \rightarrow \pi^*$ and the $n_N \rightarrow \pi^*$ transition would be most desirable in that polarized spectra can not distinguish between these two. By means of a valence state energy calculation as outlined in Appendix III it can be reasoned that the energy for the transition $n_O \rightarrow \pi^*$ is larger than that for the transition $n_N \rightarrow \pi^*$ by about one electron volt.

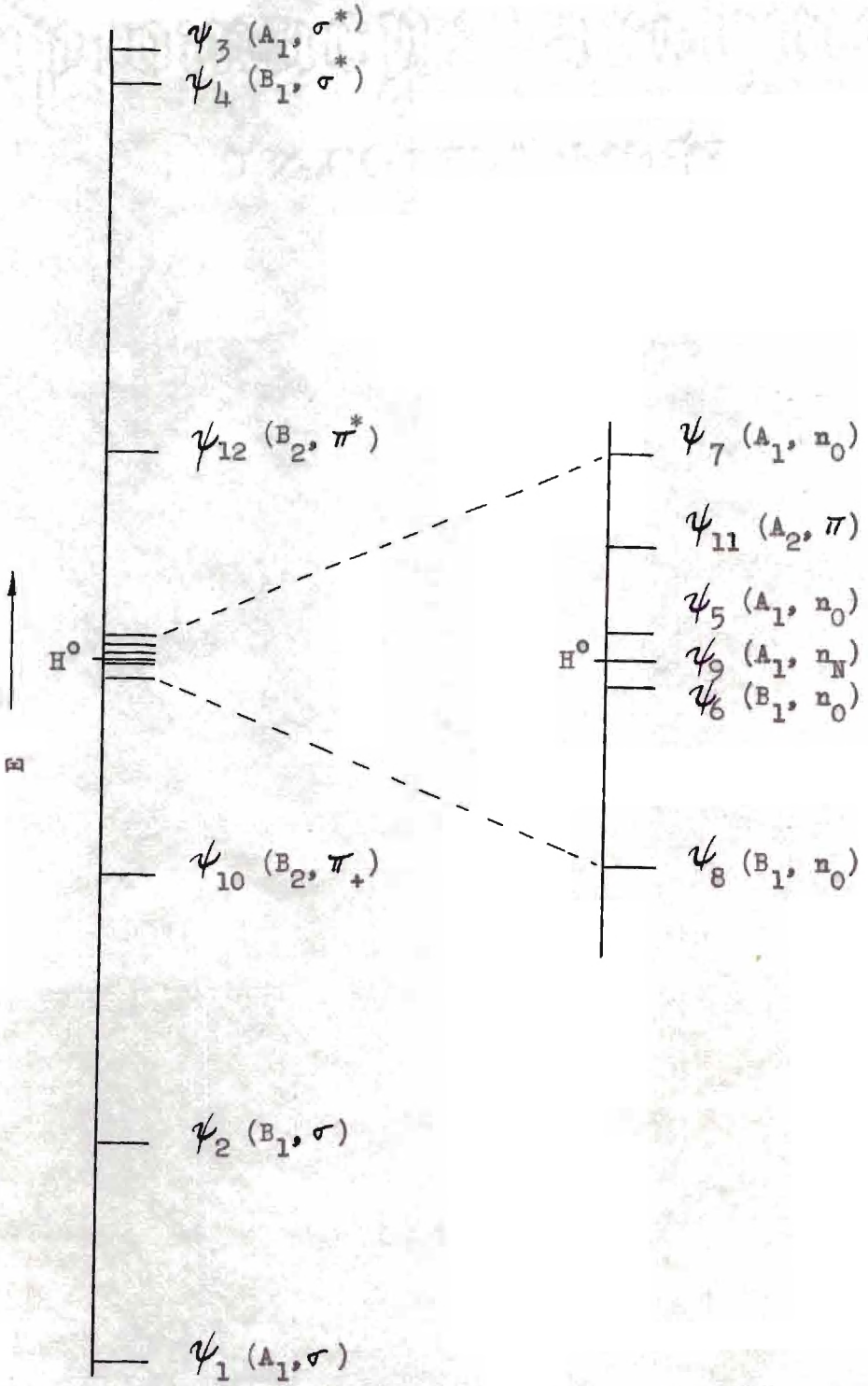

Figure 2. Relative Energies of MO's Estimated from Overlap as Described in the Text. A_1, B_1, A_2, and B_2 are symbols describing the symmetry properties of the wave-functions and σ, n_O, n_N, and π are defined in the text.

Table 1. Relative Energies of MO's Estimated as Described in Text

MO	Symmetry	Energy in terms of S
ψ_1	A_1	-0.78
ψ_2	B_1	-0.54
ψ_3	A_1	0.68
ψ_4	B_1	0.64
ψ_5	A_1	0.003
ψ_6	B_1	-0.003
ψ_7	A_1	0.023
ψ_8	B_1	-0.023
ψ_9	A_1	0.00
ψ_{10}	B_2	-0.24
ψ_{11}	A_2	0.013
ψ_{12}	B_2	0.23

Figure 3
A Chemist's Picture of the Electronic Configuration of the Nitrite Ion

Thus perhaps ψ_9 (n_N) should have a higher energy than indicated in Table 1 and Fig. 2 while ψ_5, ψ_6, ψ_7, and ψ_8 (n_O) should have lower energies.

A consideration of the electronic transition possibilities due to electric dipole absorption shows that $\int \psi_i'^{*} M \psi_j'' \, d\tau$ must be non-vanishing for a transition to be allowable (21S). Here $\psi_i'^{*}$ is the complex conjugate

of the upper state electronic eigenfunction, ψ''_j is the lower state electronic eigenfunction, and M is the dipole moment induced by the radiation. It can be shown that this integral is zero if the integrand transforms in a non-totally symmetric way. On the basis of symmetry it can be shown that the integral vanishes unless the direct product of the transformation properties of the two states contains a term with the same transformation property as that of M. Therefore "a combination between two states is allowed if their direct product contains a term which transforms like . . . (a) translations (along one of the coordinate axes). . . . The direction of this translation determines the direction of the dipole moment connected with the transition" (22S) and is in the direction of the electric vector of the radiation inducing the transition (or being emitted due to the transition).

It must be realized that the selection rules that apply to molecules in the gas phase are modified when those molecules are placed in a field such as that of a crystal lattice. However, in the case of the nitrite ion in sodium nitrite, these selection rules are not modified because the symmetry of the site group is the same as that of the point group (2B, 3H).

The transformation properties of the MO's which describe the

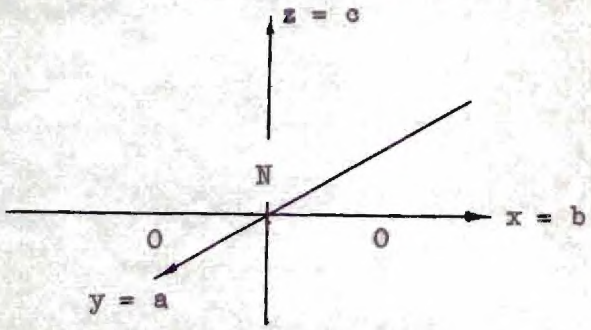

Figure 4
Orientation of the Nitrite Ion in the Coordinate Axes and Crystal Axes

system are determined in Appendix I and recorded also in Table 1 and Fig. 2. Since a translation in the z direction (T_z) has a transformation property represented by A_1, T_x by B_1, and T_y by B_2, the direct product of the symmetry of the combining MO's must be A_1, B_1, or B_2, i.e., A_2 indicates the combination is forbidden. Both Sponer and Teller (21S) and Herzberg (18H) give tables of these direct products. Table 2 is a tabulation of the possible electronic transitions together with the direct product of the transformation properties and the direction of the polarization of the radiation causing the transition. The assignment of axes in the nitrite ion is shown in Fig. 4 and is consistent with that of other workers (17C).[3] The crystal axes a, b, and c correspond to the y, x, and z axes respectively, of the Cartesian coordinates.

Comparison with the Results of Others.--R. S. Mulliken (23M) discussed the triatomic systems in general, and for the eighteen electron system predicted a configuration and energy level scheme as given in Fig. 5 (left). His method was to set up the energy level diagram for the linear system and the angular system with angle of 0° (folded so that terminal atoms are superposed, i.e., diatomic) and to estimate the way the energy levels were smoothly changed from one to the other without crossing of levels of the same symmetry. Mulliken's results and those of this work are compared in Table 5. It will be noticed that the main difference in these results lies in the non-bonding oxygen orbitals (ψ_5, ψ_6, ψ_7, and ψ_8). Calculations herein indicate that these energy levels should be

---

[3] Zeigler (24Z) and Newman (14N) use a notation with b and c interchanged contrary to the convention of Internationale Tabelle (1935). The latter convention is followed by Carpenter (17C).

Table 2. Polarization of Radiation for Transition to Excited Electronic States of Nitrite Ion (18H)

From MO	Symmetry		To MO	Symmetry		Direct Product	Polarization[a]
ψ_7	(n_O)	A_1	ψ_{12}	(π^*)	B_2	B_2	y = a
ψ_{11}	(π)	A_2	ψ_{12}	(π^*)	B_2	B_1	x = b
ψ_5	(n_O)	A_1	ψ_{12}	(π^*)	B_2	B_2	y = a
ψ_9	(n_N)	A_1	ψ_{12}	(π^*)	B_2	B_2	y = a
ψ_6	(n_O)	B_1	ψ_{12}	(π^*)	B_2	A_2	forbidden
ψ_8	(n_O)	B_1	ψ_{12}	(π^*)	B_2	A_2	forbidden
ψ_2	(σ)	B_1	ψ_{12}	(π^*)	B_2	A_2	forbidden
ψ_7	(n_O)	A_1	ψ_4	(σ^*)	B_1	B_1	x = b
ψ_{11}	(π)	A_2	ψ_4	(σ^*)	B_1	B_2	y = a
ψ_5	(n_O)	A_1	ψ_4	(σ^*)	B_1	B_1	x = b
ψ_9	(n_N)	A_1	ψ_4	(σ^*)	B_1	B_1	x = b
ψ_6	(n_O)	B_1	ψ_4	(σ^*)	B_1	A_1	z = c
ψ_8	(n_O)	B_1	ψ_4	(σ^*)	B_1	A_1	z = c
ψ_2	(σ)	B_1	ψ_4	(σ^*)	B_1	A_1	z = c
ψ_7	(n_O)	A_1	ψ_3	(σ^*)	A_1	A_1	z = c
ψ_{11}	(π)	A_2	ψ_3	(σ^*)	A_1	A_2	forbidden
ψ_5	(n_O)	A_1	ψ_3	(σ^*)	A_1	A_1	z = c
ψ_9	(n_N)	A_1	ψ_3	(σ^*)	A_1	A_1	z = c
ψ_6	(n_O)	B_1	ψ_3	(σ^*)	A_1	B_1	x = b
ψ_8	(n_O)	B_1	ψ_3	(σ^*)	A_1	B_1	x = b
ψ_2	(σ)	B_1	ψ_3	(σ^*)	A_1	B_1	x = b

[a]The direction of vibration of the electric vector absorbed or emitted is along y = a, x = b, or z = c.

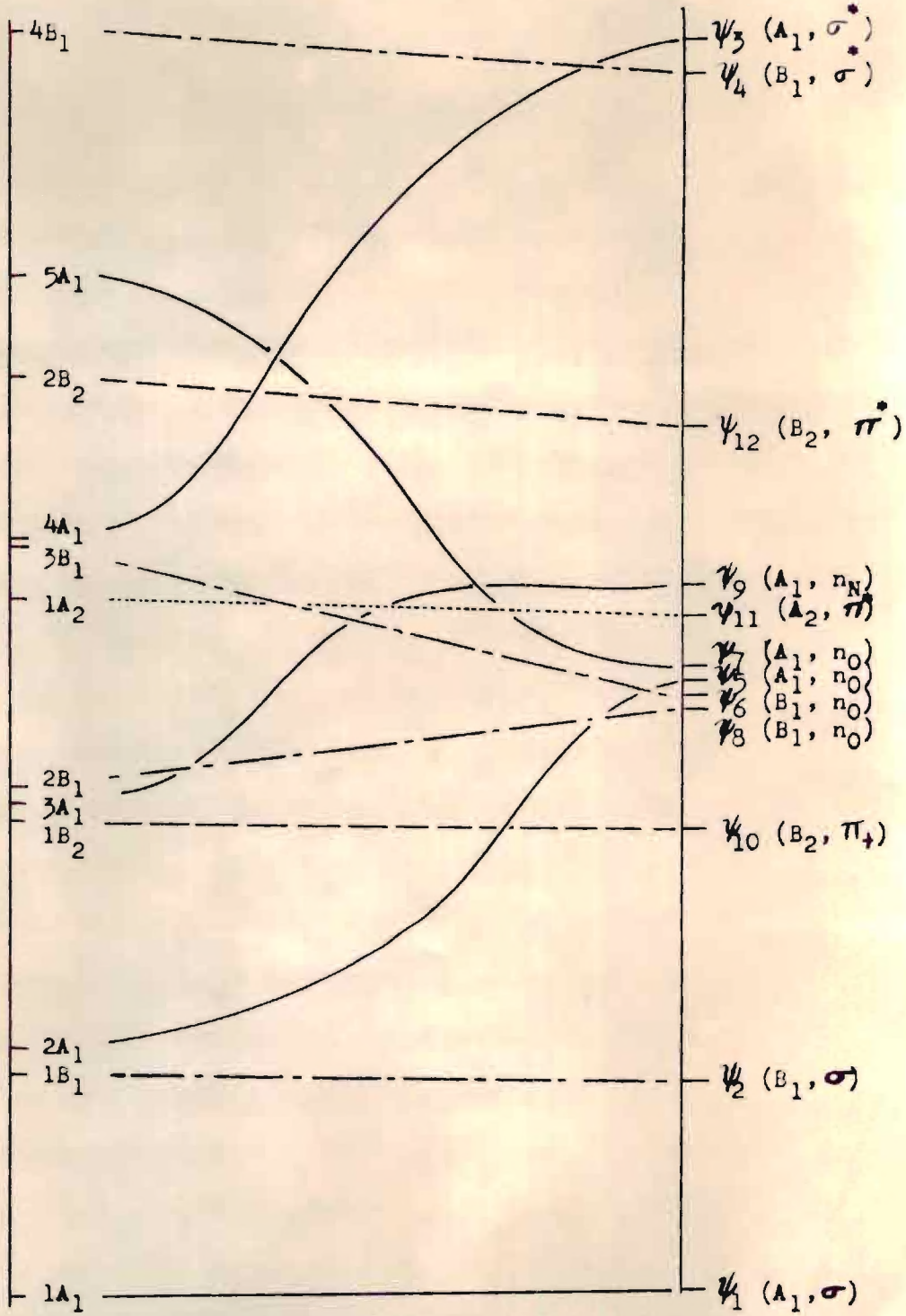

Figure 5. The Energy Level Diagram from Mulliken (23M), on the left, Compared to That of This Work as Described in the Text. Note: Mulliken's symbol b_1 is B_2 in the notation of this work and his b_2 is B_1 here, also his a_1 is A_1, and his a_2 is A_2.

split only a very little. It will be noticed from Fig. 5 that ψ_9, the non-bonding nitrogen orbital, has been raised in energy and that all of the non-bonding oxygen orbitals have been lowered in accordance with the discussion on page 11. The other differences in these energy level diagrams is that Mulliken's $4A_1$[4] is much more stable than the corresponding orbital $(\psi_3)(A_1\sigma^*)$ in this work. Since Mulliken's $3A_1$ is an intermediate designation between a linear $1\pi_u$ and a folded $2a_1$, it corresponds to ψ_9 $(A_1\ n_N)$ instead of the $2A_1$ which is intermediate between $2\sigma_g$ and the 1e'. This would seem to indicate, in agreement with the valence state promotional energy argument (Appendix III), that ψ_9 $(A_1\ n_N)$ should have a higher energy than ψ_5 $(A_1\ n_O)$ to prevent crossing of energy levels of the same symmetry in the hypothetical transition from linear to bent to the superposed system. A difficulty in correlating these energy level diagrams comes with ψ_7 $(A_1\ n_O)$ corresponding to $5A_1$ crossing ψ_3 $(A_1\sigma^*)$ and ψ_9 $(A_1\ n_N)$. Changes are suggested below which would overcome this.

Walsh (25W) presented, in a series of papers, similar energy level schemes for various polyatomic molecules. He did not hybridize the s orbitals on the B atoms and consequently they are of lowest energy. Another significant difference from the diagram given by Mulliken is in the interchange of the position of the linear $3\sigma_g$ and $2\pi_u$ orbitals. This change resulted in Mulliken's $4A_1$ orbital coming from the $2\pi_u$ instead of the $3\sigma_g$. This is consistent with the results presented here; however, this change would necessitate another change to prevent crossing

---

[4] It should be noted that Mulliken's symmetry term symbol b_1 is B_2 in the notation of this work and his b_2 is B_1 here; also $a_1 = A_1$, $a_2 = A_2$.

of A_1 states.

In order to correlate Mulliken's diagram with that of this work and that of Walsh the following changes are suggested:

(a) Interchange the order of Mulliken's $3\sigma_g$ and $2\pi_u$ orbitals as suggested by Walsh. This requires that the linear $2\pi_u$ split to give the folded $2a_1'$ and $1e''$ instead of $3e'$ and $1e''$. $3\sigma_g$ then goes to $3e'$ instead of $2e'$.

(b) Interchange the order of $2e'$ and $2a_1'$. This is necessary as a consequence of (a) to prevent the A_1 orbital of $2\pi_u$ from crossing with the A_1 orbital of $1\pi_u$. The $1\pi_u$ goes (through A_1) to $2e'$ and to $1a_2$ as a result of this change.

H. L. Friedman (26F) agrees with Mulliken's work in the low energy region of the near ultraviolet but postulates that the high energy absorption at 2100 A is due to an electron transfer from the ion to the solvent.

Transitions Predicted.--These calculations lead to the conclusion that the lowest energy transition would be an $n \rightarrow \pi^*$ (polarized along the a axis); perhaps two or three relatively close together. This picture indicates that there would be a $\pi \rightarrow \pi^*$ transition (polarized along b axis) nearby, perhaps lying in the same region of the spectrum with the $n \rightarrow \pi^*$. The accuracy of the estimates made will not permit a definite assignment of these transitions from these considerations alone; other evidence is required at this point. Likewise the electron transfer assignment of Friedman for solutions cannot be denied by assigning the 2100 A band of the crystal to one of the transitions mentioned above.

CHAPTER III

DESCRIPTION OF THE EXPERIMENT

Introduction

In order to determine which transition or transitions are responsible for the various bands of the nitrite ion absorption spectrum, more information is required than that obtained by the calculations of Chapter II. The only conclusive evidence is that obtained from polarized spectra of the oriented molecules at low temperatures. Other evidence, such as the effect of solvents on the spectra (27K) and differences in the spectra of similar substances, can be checked or used to postulate refinements in results already obtained. Thus the first experimental approach is to determine the direction of polarization of the radiation absorbed by a carefully oriented single crystal at low temperatures. The second approach is to study the spectra of the ion in solution and the spectra of other substances.

Polarized absorption spectra were recorded for sodium nitrite, along each of its three axes at room temperature and at liquid nitrogen temperatures. The absorption spectrum of natural crystals of silver nitrite was also studied at room temperature and at 70° absolute. Absorption measurements were also made on sodium nitrite in neutral and acidified aqueous solutions; ethyl nitrite as a gas and in solutions of hexane, ethyl alcohol and water; amyl nitrate as a glass at liquid nitrogen temperature; and nitromethane as a glass at liquid nitrogen

temperature and in ethyl alcohol and water-acid solutions.

Polarization Studies

Crystals, Their Growth and Orientation.--Crystals of sodium nitrite were grown by slow evaporation of the solvent from a thin film of the aqueous solution on quartz microscope slides. Rapid evaporation gave crystals which were too small to be usable. Suitable crystals were obtained by varying the thickness of the film of solution and its concentration. Single crystals as large as one centimeter square and as thin as two microns were grown in this way. Examination of thinner crystals under the microscope showed that they were not continuous but had holes in them. The upper surface of the crystals was not smooth, and as a result some of the light was scattered. This scattering necessitated longer exposure times.

The crystal habit is such that only (010) plates, i.e., crystals having the a and c crystal axes (the yz coordinate plane) in their faces, were obtained. In order to study the absorption of radiation polarized in the direction of the b axis (x coordinate axis) it was necessary to obtain a crystal with the b axis in the plane of the face. Aqueous solutions of sodium nitrite were evaporated slowly at a constant temperature near 20°C. After a month of evaporation from about two hundred milliliters of the saturated solution, single crystals were obtained that were large enough to be cut and polished into (100) plates, i.e., plates having the b and c axes in their faces, as described by Newman and Halford (28N). The lower limit of thickness for these crystals was about thirty microns. Newman and Halford (28N) point out a precaution regarding the optic axes and molecular orientation that should not be overlooked.

The orientation of the crystals was determined by a study of the refractive indices by the Becke line method (29G, 30W) using available liquids of known refractive index. The refractive indices of sodium nitrite reported by Newman (4N) were accepted. They are $n_\alpha = 1.35$, measured along the crystal axis a or the coordinate axis y; $n_\beta = 1.41$, measured along the crystal axis c or the coordinate axis z; and $n_\gamma = 1.62$, measured along the crystal axis b or the coordinate axis x.[1] These indices were not measured exactly but were placed within limits as follows; $1.329 < n_\alpha < 1.359$ by acetone and methyl alcohol, $1.402 < n_\beta < 1.422$ by n-butyl chloride and 1,4-dioxane, and $1.514 < n_\gamma$ by benzene. These measurements were accurate enough to make certain that the crystals were so orientated that the surfaces contained one of the coordinate planes or at most that the face was not inclined to the plane of the axes by an angle great enough to cause any difficulties (See Appendix IV).

The thickness of the crystals was determined by means of interference fringes or colors when the crystals were placed between crossed Nicols of the polarizing microscope (32W). The thicker cut crystals were measured by counting the interference fringes when illuminated by a sodium lamp.

Except for a slight change in the size of the unit cell and a marked change in the metal to nitrogen internuclear distance, silver nitrite has the same crystal structure as sodium nitrite (31W). In

---

[1] The b and c axes of Zeigler's (24Z) notation, which was also used by Newman (4N) and Wycoff (31W), have been exchanged; compare Carpenter (17C).

sodium nitrite the metal to nitrogen distance is 2.61 A while the metal oxygen distance is 2.52 A (17C), but in silver nitrite these distances are 2.04 A and 2.74 respectively (33K). These distances are indicated in Fig. 6.

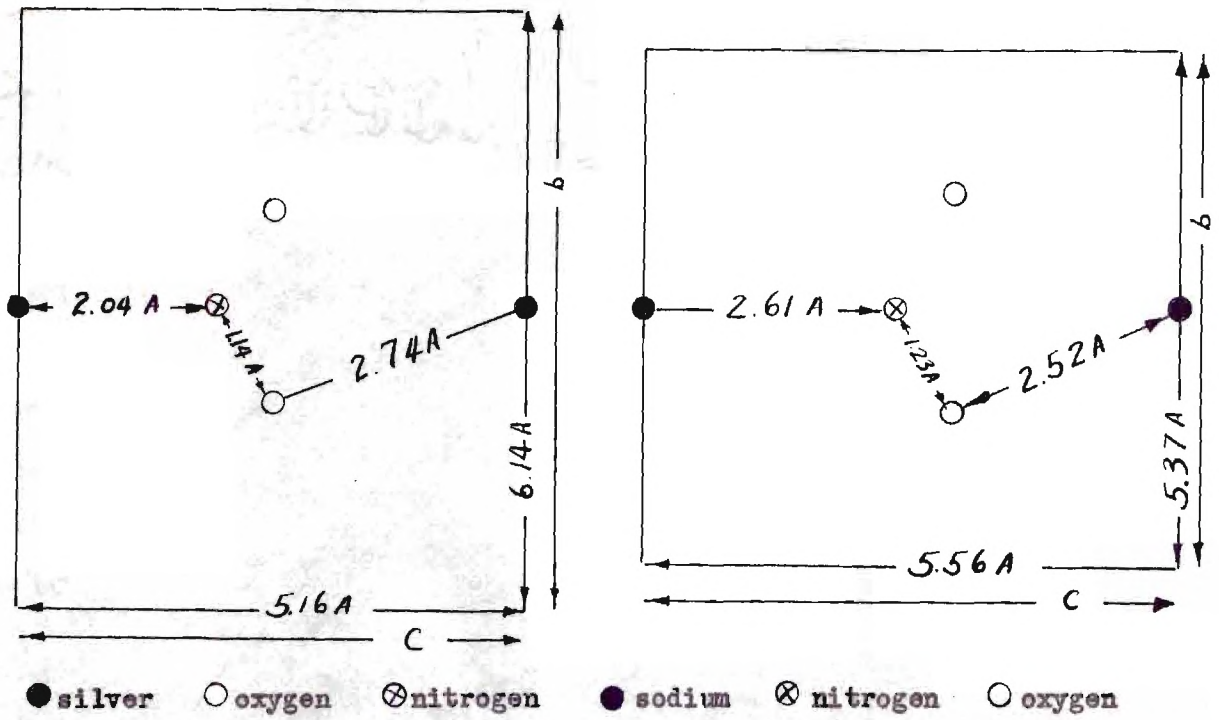

Figure 6. Dimensions in the Crystallographic Unit Cell for Silver Nitrite and Sodium Nitrite for the (100) Planes, i.e., bc Plane. The a Axis is Perpendicular to the Page.

The limited solubility of silver nitrite made it more difficult to secure suitable crystals, but small very thin single crystals were grown in the dark by evaporation of water solutions at 100°C in a humid atmosphere to make the process slower. Only (010) plates, i.e., crystals containing only a and c crystallographic axes (the same convention is used as for sodium nitrite), were obtained and these were too small for polarized absorption techniques. The decomposition due to light was also appreciable.

The necessity for determining with absolute certainty the direction of polarization of the radiation is evident. This was achieved by examination of the microscope polarizer in radiation reflected at Brewster's angle from glass plates. This done for one polarizer the others could be compared to it as a reference. The marking on the quartz wedge, furnished with the microscope, was also confirmed by measuring the refractive indices of a crystal by the Becke line method after assignments were made using the wedge.

Preliminary examinations were made of natural crystals to determine which was the a axis and which the c axis, assuming them to be (010) plates, by means of a quartz wedge and interference colors or fringes (34W). After the absorption spectrum of a crystal was recorded, its orientation was confirmed by the Becke line method for measuring refractive indices. The cut crystal was made from a large crystal oriented by refractive index methods, and the orientation of the polished crystal was checked by the same methods after the spectrographic examination.

Optics and Spectrographs.--The light source used in all the spectrographic absorption work was a water cooled Hanovia hydrogen discharge tube which was made of fused quartz. The electrodes were aluminum cylinders. The power required was five thousand volts alternating current, from a reactive transformer, at one-half ampere. Under prolonged use the windows became coated with aluminum which required that the tube be opened and cleaned with hydrochloric acid. Normal operation was achieved when refilled with dry electrolytic hydrogen at a pressure of about two millimeters of mercury. The length of useful service was markedly increased when a blast of air was directed over the outside of

the tube while in operation.

Polarizers used in the ultraviolet were of two kinds; a Glan-Thompson prism which had been recemented with glycerol to pass this shorter wave-length radiation, and a Wollaston prism with optical contact of the two quartz pieces. The Wollaston prism made it possible to photograph both directions of polarization at the same time by merely separating the two rays by a small angle. These two rays were then thrown onto the upper and lower parts of the slit and the spectra recorded.

The direction of polarization of the Glan-Thompson prisms was determined by comparison with that of the polarizer on the microscope and by observing them in light reflected at Brewster's angle from glass plates. The two beams from the Wollaston were observed through a Glan-Thompson prism of known orientation in order to decide which beam was polarized in a particular direction. It was recognized that the image of the slit is inverted on the film of the spectrograph and in order to confirm the assignment of orientation, the two spectra were observed from the film plane with an eyepiece, as a Glan-Thompson prism was rotated in the optical path just ahead of the Wollaston prism. The spectrum passed was that of light polarized in the same plane as that passing the Glan-Thompson prism. This information thus made it possible to determine unambiguously the direction of polarization of the absorbed and the transmitted radiation in the two rays given by the Wollaston prism.

To orient the crystal with respect to the Wollaston prism an incandescent spot light placed at the film holder of the spectrograph allowed light to emerge from the slit and be collimated by a condensing lens and thus trace out the optical path in the reverse direction. The

Wollaston was placed in this path between crossed polarizers, in this case Glan-Thompson prisms, Fig. 7A, and rotated until the intensity of the two light beams appeared the same (there was a difference of setting for extinction of the two beams of about 1.5°). The Wollaston was then swung out of the optical path and the crystal placed between the crossed polarizers. The crystal was then rotated so as to allow no light to pass through from the spectrograph slit (Fig. 7B). If low temperature spectra were to be recorded this alignment was done with the crystal in its cell and in position; then after the liquid nitrogen had been added to the Dewar flask the alignment was checked and any small correction could be made by rotating the entire cell. When properly located the cell was clamped in position on the optical supports. This done the two Glan-Thompson prisms were removed and the Wollaston returned to its proper position as shown in Fig. 7C.

The low temperature cell shown in Fig. 8 was made from a two hundred milliliter, tall form, electrolytic beaker with side arms of eighteen millimeter outside diameter Pyrex tubing fused on. The windows on the ends of the side arms were of strain-free quartz microscope slides sealed with Apiezon "W" wax onto the ends already ground flat. The copper rod was surrounded closely by an eighteen millimeter Pyrex tubing and secured in position by a brass machine screw which went through a hole in the glass tubing and into a tapped hole in the copper rod. The cell was closed to the moist air by a glass plate which seated itself nicely in stop-cock lubricant on the top of the beaker which had been ground flat. This last seal provided access to the rod for placing or removing the crystals which were mounted, with the quartz plate to which

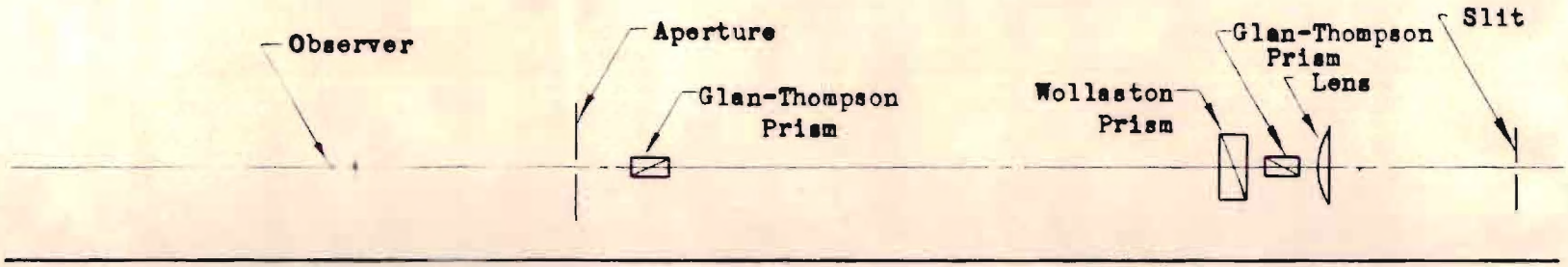

A. Alignment of Wollaston Prism

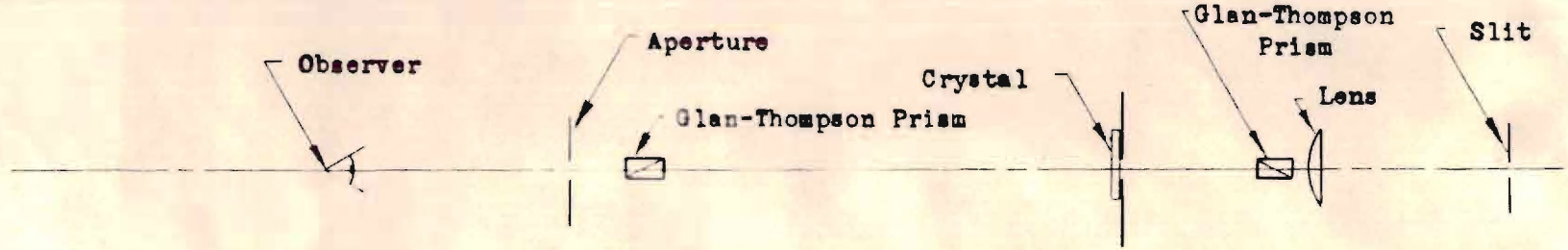

B. Alignment of Crystal

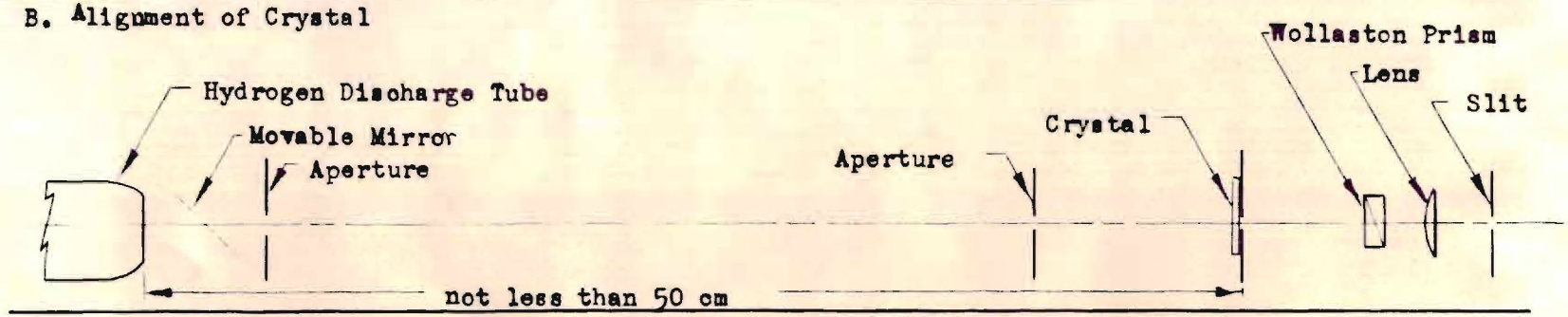

C. Arrangment for Recording Spectrum

Figure 7. Optical Arrangments

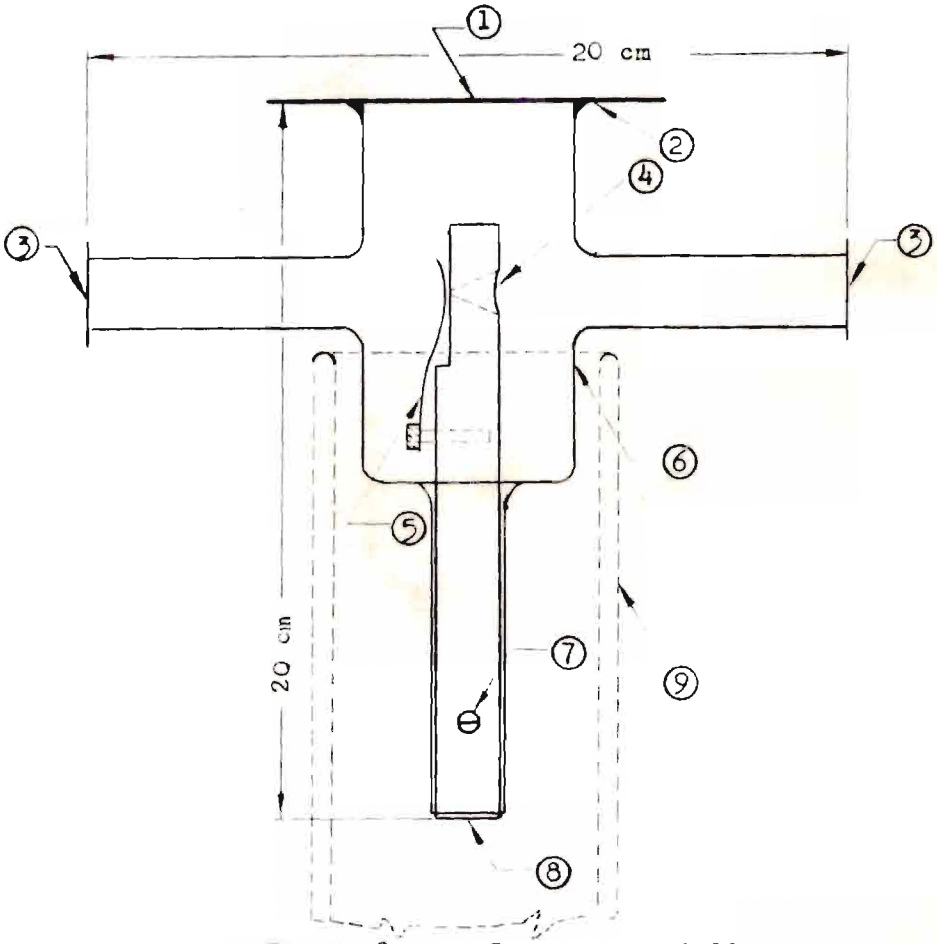

Figure 8. Low Temperature Cell

① Glass Plate. ② Ground joint sealed with stop-cock lubricant. ③ Strain-free quartz plates, sealed on with Apiezon-W. ④ Tapered opening in copper rod. ⑤ Leaf type spring to hold sample against rod. ⑥ 200 ml. tall-form electrolytic beaker with 18 mm. o. d. glass tubes sealed on. ⑦ Machine screw to locate copper rod in cell. ⑧ Copper rod. ⑨ Dewar flask to contain coolant.

they were secured, on the flat side of the copper rod, and held in place by a leaf type spring. The light passed through the quartz plate, the crystal, the hole in the copper rod, and out the other side arm of the cell.

The rather short focal length lens used as a condenser served to reduce the size of the image of the source to about one millimeter yet filled the optics with light, thus making it possible to record one set of spectra in about three millimeters of the lateral space on the film. In this way as many as eight sets of spectra could be put on one thirty-five millimeter film.

The design of the Hanovia hydrogen discharge tube is such that by far the largest part of the light is emitted in a cone with about 2° divergence from an area about four millimeters in diameter. This construction made it possible to omit a collimating lens without losing much light.

The need for the light to be well collimated to prevent absorption of a sizable amount along the axis of the crystal perpendicular to the face was realized. With the arrangement as shown in Fig. 7C this divergence would not have been more than one degree (2 x arc tan. of 4 millimeters (aperture)/ 500 millimeters (aperture to crystal) = 54').

For the purpose of measuring wave-lengths on the absorption spectra an iron arc was placed on each film. This was done by inserting a plane first-surface mirror between the hydrogen discharge tube and the first aperture and removing the crystal; the radiation from the iron arc was thus introduced into the existing optical path where it could be recorded.

Two spectrographs were used; one a small Bausch and Lomb quartz littrow which used two inch by seven inch plates, and the other a Jarrell-Ash JACO-Wadsworth Stigmatic three meter Replica Grating Spectrograph with a 15,000 line per inch replica grating two inches by one and one-half inches. Preliminary work and later work in the shorter wave-length range was done with the Bausch and Lomb instrument, but the Jarrell-Ash spectrograph was used for the fine structure of the low temperature absorptions.

Measurements of wave-lengths were made from a densitometer trace made on a recording densitometer built here, Fig. 9. The film carrier and optical assembly were described elsewhere (35W). The output of the selenium cell placed behind the slit was applied to a d'Arsonval galvanometer which reflected a rectangular image of a light source onto a horizontal "vee"-shaped opening on another selenium cell. The position of the image on the "vee" determined the amount of light reaching the second cell, the output of which was used to drive a Brown Electronik strip-chart recorder. For each revolution of the screw advancing the film a "pip" was placed on the chart so that a second spectrum could be placed alongside the first on the chart without danger of one trace being displaced with respect to the other. It was always possible to measure to better than one angstrom using a film from the Jarrell-Ash spectrograph. When corrected for shift on the film of one spectrum with respect to the other an accuracy of better than 0.1 A was achieved.

Photographic Materials and Exposures.--The film used on the Jarrell-Ash spectrograph was Eastman Kodak 103-F-(3) thirty-five millimeter film. For the shorter wave-length region this was coated with a very thin film

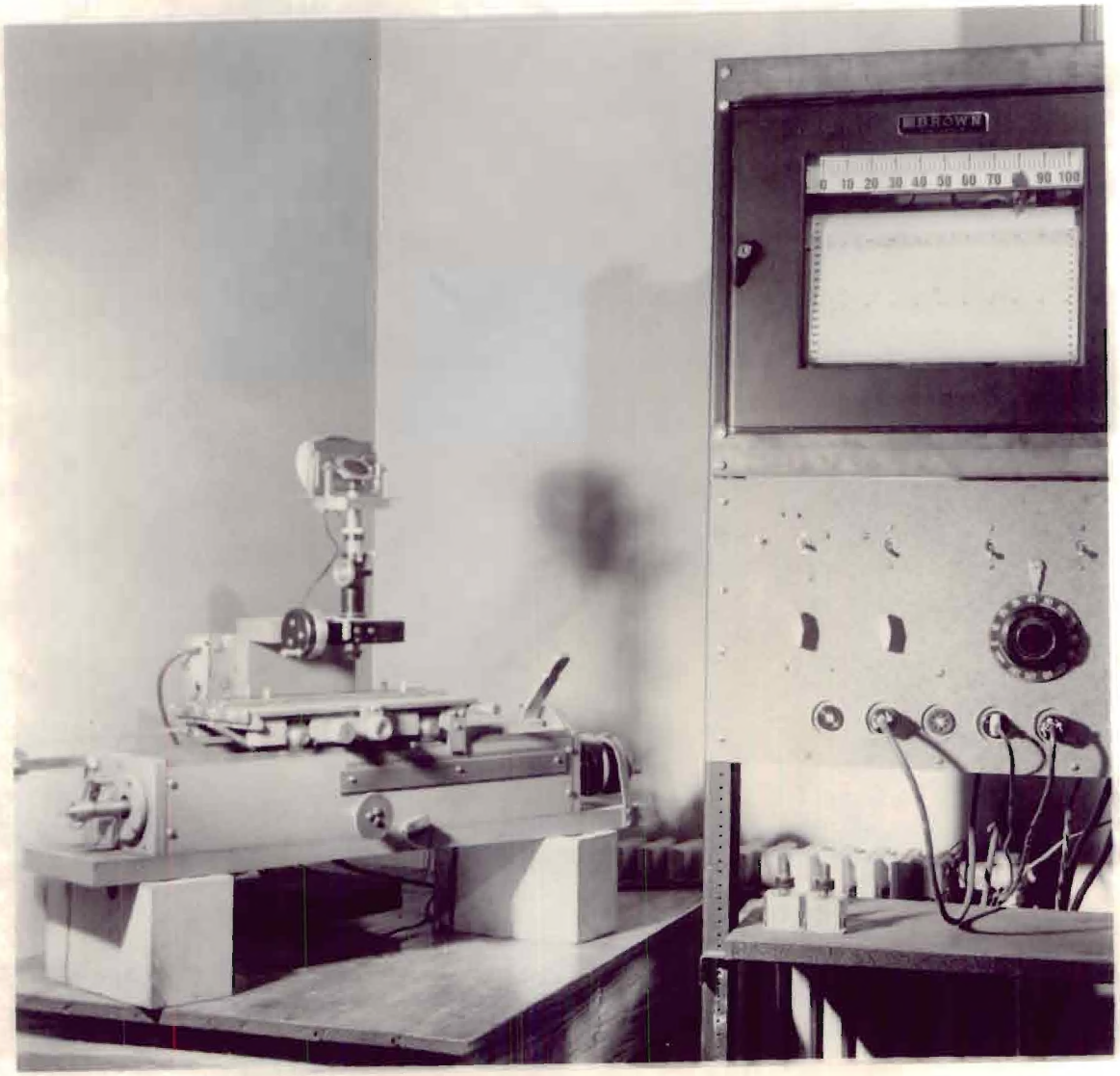

Figure 9. Recording Densitometer

On the left is the film holder which is advanced by a metric screw driven by a syncronous motor through a gear train located on the right end of the assembly. Above the film holder is the microscope and selenium photocell with its adjustable slit. The film is illuminated by a light located behind the assembly. The optical amplifier is located beneath the table (not in view). The controls for the film drive motor, light source, and optical amplifier are located beneath the Brown Electronik strip-chart recorder on the right.

of "Nujol" (36S) for greater sensitivity. For the Bausch and Lomb instrument Eastman Kodak two by ten inch 103-F-(3) X-thin plates cut to seven inches were used at first. Some 103-O-U.V. plates secured for the work were found to be hopelessly streaked so that sheet film was tried and found to be satisfactory. Eastman's Contrast Process Ortho film in five by seven inch sheets was cut to size and sensitized to the ultraviolet by a thin coating of "Nujol".

The film and plates were washed in methyl alcohol to remove the "Nujol" and developed in Kodak D-18 developer as recommended for the film and fixed in Kodak Rapid Liquid Fixer.

The time that the film was exposed to the radiation varied from about thirty seconds for the thin silver nitrite crystals to three hours for the thick sodium nitrite crystals. Slits were about three hundred microns wide except when recording the fine structure at liquid nitrogen temperature and these were made with one hundred micron slits widths.

Other Measurements

Absorption spectra of the following solutions were measured on a Beckman model D. U. spectrophotometer: sodium nitrite in neutral and acid aqueous solutions; ethyl nitrite in hexane, ethyl alcohol, and water solutions; and nitromethane in ethyl alcohol and water-acid solutions. Absorption spectra were also recorded on the Jarrell-Ash spectrograph for gaseous ethyl nitrite and for solid amyl nitrite and nitromethane at liquid nitrogen temperature.

The sodium nitrite was reagent grade purified by recrystallization from aqueous solutions and free from nitrate. The acid used to make the

solution acidic was hydrochloric acid.

The amyl nitrite was purchased in small vials under the trade name "Vaporole" of Burroughs Wellcome and Company. It seemed likely that it was slightly contaminated with decomposition products, but they apparently did not interfere in the region of the spectrum of interest.

The ethyl nitrite was freshly prepared by mixing 14.5 cc of ninety-five per cent ethyl alcohol, 33.0 grams of sodium nitrite and enough water to make 125 cc of solution. This was mixed with a solution of 13 cc of one hundred per cent sulfuric acid, 11 cc of ethyl alcohol and water to make 125 cc. The ethyl nitrite was distilled from this mixture and purified by distilling twice more. This was evaporated directly into the gas cell for vapor measurements and distilled into the hexane and ethyl alcohol for solution measurements.

The solutions were prepared and designated as follows:

Stock solution A: 17.75 grams of hexane was placed in a vessel and ethyl nitrite was distilled in until the weight increased by 1.46 grams. This procedure should have resulted in a concentration of 0.662 moles per liter. From this stock solution the following solutions were prepared:

Solution IA.--Dilute 10 ml. of stock solution A to 25 ml. with hexane.

Solution IIA.--Dilute 5 ml. of solution IA to 20 ml. with hexane.

Solution IIIA.--Dilute 5 ml. of solution IA to 20 ml. with ninety-five per cent ethanol.

Solution IVA.--Dilute 10 ml. of stock solution A to 25 ml. with hexane.

Solution VA.--Dilute 10 ml. of solution IVA to 20 ml. with hexane.

Solution VIA.--Dilute 2.5 ml. of stock solution A to 25 ml. with hexane.

Solution VIIA.--Dilute 2.5 ml. of stock solution A to 25 ml. with ninety-five per cent ethanol.

Solutions VIA and VIIA were prepared at the same time and measurements made at the same time.

Stock solution B: 14.303 grams of ninety-five per cent ethanol was placed in a vessel to which ethyl nitrite was added by distillation to increase the weight 0.443 grams. This should have resulted in a concentration of 0.32 moles per liter. From this stock solution the following solutions were prepared:

Solution IB.--Dilute 2.5 ml. of stock solution B to 25 ml. with ninety-five per cent ethanol.

Solution IIB.--Dilute 2.5 ml. of stock solution B to 25 ml. with water.

Solution IIIB.--Add to 55 drops of solution IB 5 drops of concentrated (12 F) hydrochloric acid.

Solution IVB.--Add to 55 drops of solution IIB 5 drops of concentrated (12 F) hydrochloric acid.

Solution VB.--Dilute 2.5 ml. of stock solution B to 25 ml. with ninety-five per cent ethanol.

Solution VIB.--Dilute 2.5 ml. of stock solution B to 25 ml. with water.

Solution VIIB.--Dilute 10 ml. of solution VB to 25 ml. with ethanol.

Solution VIIIB.--Dilute 10 ml. of solution VIB to 25 ml. with water.

Solutions VB and VIB were prepared and treated as nearly identically as possible. Errors in concentration are discussed in Chapter IV page 50-51.

The nitromethane was obtained from Lyman Morgan and had a boiling range of 101-102°C. Measurements were made in ninety-five per cent ethyl alcohol and a water-acid solvent made with equal volumes of water and concentrated sulfuric acid (about 9 formal).

The spectrum of gaseous ethyl nitrite in an 11.5 centimeter cell was photographed with a one hundred micron slit at pressures from ten millimeters of mercury to one atmosphere. At each pressure a ten second and a one minute exposure were made. Low temperature spectra of amyl nitrite and nitromethane were made through a cell consisting of two quartz slides held fifty microns apart with a brass spacer and clamped against the copper rod of the cell previously described. Amyl nitrite required exposures up to one hour with a three hundred micron slit, while ten minutes with the three hundred micron slit were sufficient for nitromethane.

CHAPTER IV

RESULTS AND DISCUSSION

POLARIZED SPECTRA OF SODIUM NITRITE

The measurements of the absorption spectra of crystalline sodium nitrite at liquid nitrogen temperature (75° absolute) show that there are two regions of absorption: one band with its maximum about 3500 A and another more intense band with its maximum about 2050 A. The 3500 A band consists of numerous rather sharp peaks while the shorter wavelength band is diffuse.

The origin of the 3500 A band is at 3851.4 A as shown in Fig. 10 and Table 3. Rodloff (37R) reported measurements on this absorption at liquid hydrogen temperature (20° absolute) in unpolarized radiation and gave 3818 A as the origin. Rodloff's measurements were made from a spectrum taken on a quartz prism spectrograph and calibrated at only a few points with a mercury arc while the measurements reported here were made from a film from a grating instrument and calibrated with an iron arc. The measurements made in this laboratory are believed to be more accurate and are used in preference to those reported by Rodloff. The details of the measurements made here are given in Appendix V.

The greater resolution of the 3500 A band obtained by Rodloff at 20° absolute is complementary to the measurements made here and his data have been incorporated into the measurements reported in Table 11 by interpolating between points that are evidently the same.

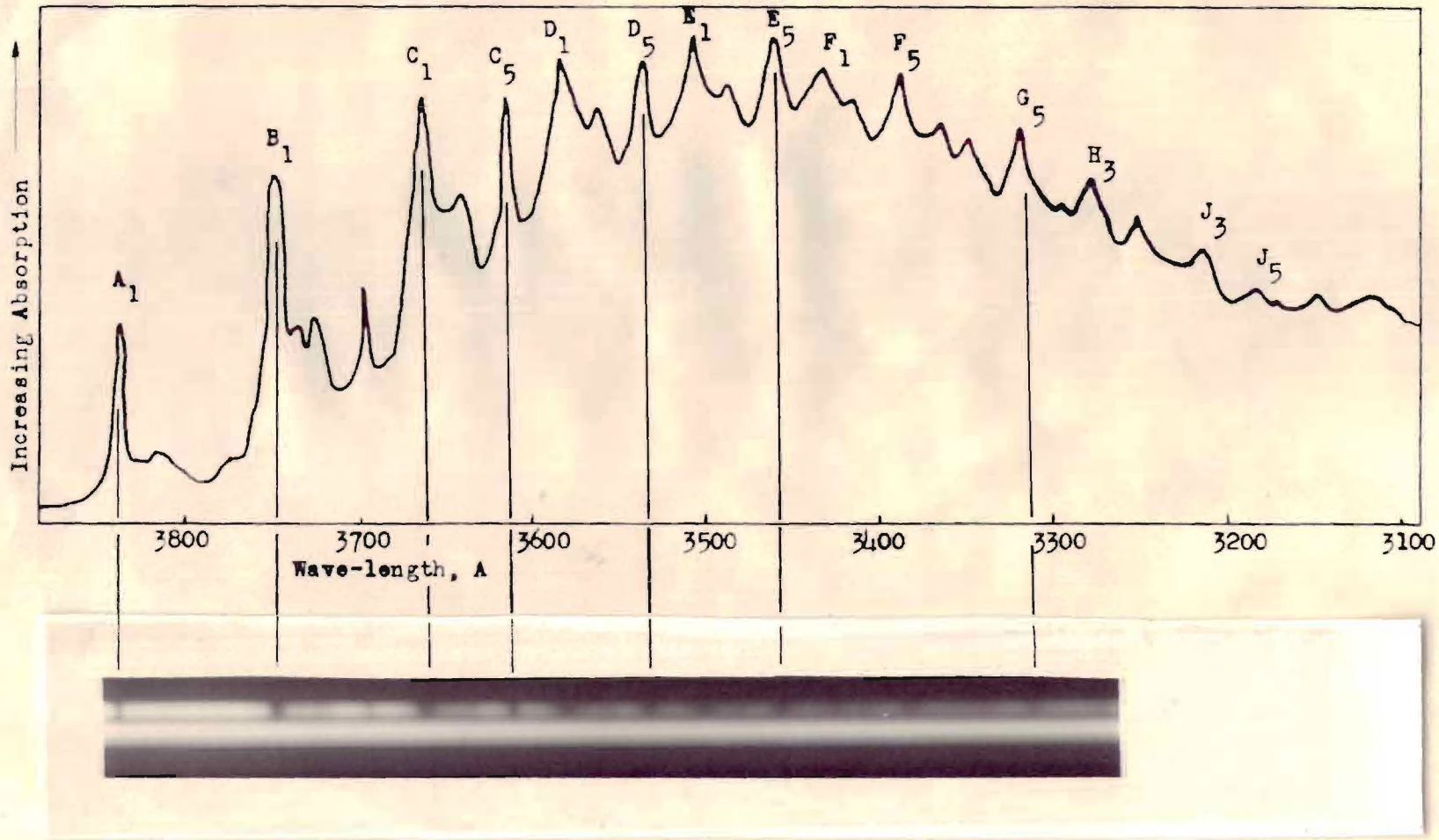

Figure 10. A Densitometer Trace of the Low Temperature 3500 A Absorption Band of Crystalline Sodium Nitrite with Radiation Polarized such that the Electric Vector Vibrates Perpendicular to the Plane of the Nitrite Ion. The photograph shows this region of the spectrum for radiation polarized along the a axis (top) and along the c axis (bottom).

The primary significance of this work is in the use of polarized radiation and carefully oriented single crystals of sodium nitrite. It might have been expected that this rather complex band (3500 A) would resolve itself into two or more simpler bands with different directions of polarization, but such is not the case. It is completely polarized so that the radiation is absorbed when the electric vector vibrates parallel to the a crystallographic axis, i.e., perpendicular to the plane of the ion. No absorption could be detected in this region for radiation polarized in the b or c directions.

The other absorption band in the near ultraviolet begins about 2865 A and reaches its maximum intensity about 2050 A. It shows no fine structure at liquid nitrogen temperature.

The polarization of the radiation absorbed in the long wave-length end of this 2050 A band is such that the electric vector must vibrate parallel to the b axis, i.e., the change in dipole moment is parallel to the line connecting the two oxygen atoms of the ion, Fig. 11. Due to the intensity of the absorption below 2300 A, the low sensitivity of the film, absorption by the quartz optics, and scattering from the crystal surfaces it was not possible to measure the polarization in the thick crystal below this wave-length. A polarization of this direction is consistent with the refractive index (See Appendix VIII).

No attempt was made to measure accurately the absolute molecular extinction coefficients of these two bands, but the maximum extinction coefficient for the shorter wave-length band is estimated to be about eight or ten times as large as the one for the 3500 A band. This estimate is made from films of the spectrum at room temperature where

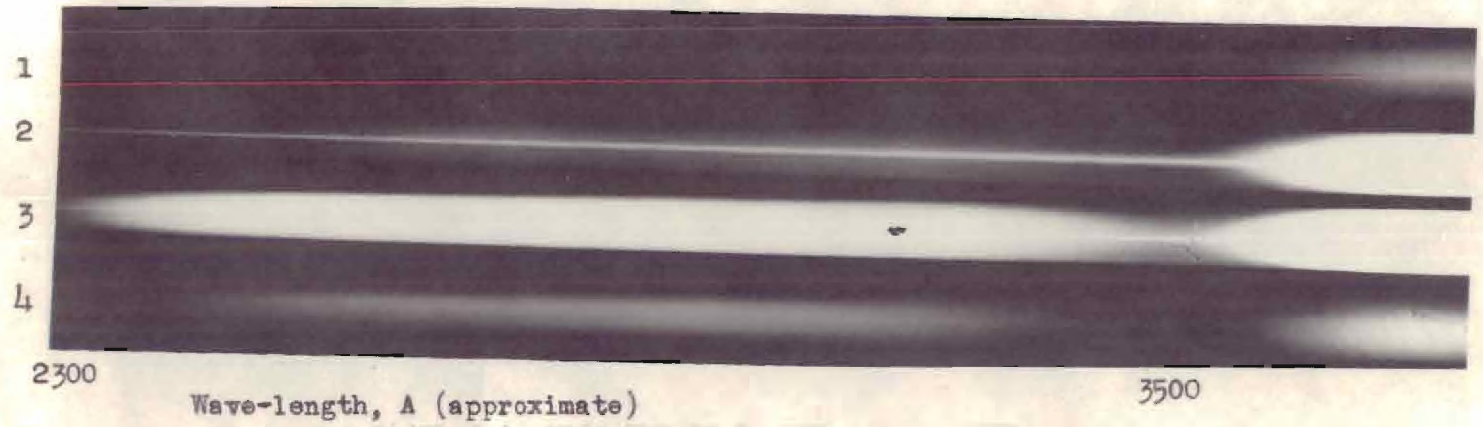

Figure 11. Polarization of the 2050 A Band

The above absorption spectra were recorded at room temperature in a Bausch and Lomb small quartz Littrow spectrograph. The absorption is that of a sodium nitrite crystal cut so that the radiation was perpendicular to the plane of the ion, i. e., the (100) planes. The crystal was about 35 microns thick and 2 mm wide by 3 mm long. The optics were arranged so as to secure as much light as possible. The slit was removed from the spectrograph, thus the entrance aperture was a 3 mm hole. An image of the crystal was focused so as to almost fill this aperature. This arrangment meant that the scattered radiation that contained a component with its electric vector perpendicular to the electric vector passed by the polarizer was a significant part of the total radiation reaching the film. The polarizer used was a Glan-Thompson prism recemented with glycerine, and it was located in the collimated beam in front of the crystal.

Spectrum 1. 5 minute exposure, electric vector vibrating parallel to the b axis of the crystal.
Spectrum 2. 2 hour exposure, electric vector vibrating parallel to the $\bar{b}$ axis of the crystal.
Spectrum 3. 2 hour exposure, electric vector vibrating parallel to the $\bar{c}$ axis of the crystal.
Spectrum 4. 5 minute exposure, electric vector vibrating parallel to the $\bar{c}$ axis of the crystal.

the 3500 A band is diffuse. This estimate seems reasonable in light of the relative intensities of eight to one reported by Maslakowez (38M) for the corresponding bands in potassium nitrite. A rough estimate of the molecular extinction coefficient of the 3500 A band of the crystal gives a maximum of about thirty-four at 3500 A (Fig. 12 and Table 12). This estimate was made at room temperature from a crystal of about eight microns average thickness and large enough to cover the aperture of the Beckman model D. U. spectrophotometer. The fine structure evident at liquid nitrogen temperature is blurred at room temperature so there was no difficulty with slit width. Of course this radiation was unpolarized. This value is comparable to that of the corresponding band in solution but is probably no better than within one hundred per cent of the true value. This uncertainty is due to the lack of uniformity of the thickness, the scattering of light from the rough surface, and the possibility of holes in the crystal. It was not possible to estimate the absorption coefficient of the shorter wave-length band in this way. The optical density of the latter band reaches the practical limit of the instrument about 230 millimicrons. The uncertainty evident in the points recorded (Table 12) is probably due to the fact that the crystal is not in identically the same position for successive measurements. The increased scattering at the shorter wave-length adds to the uncertainty of these points too.

Discussion.--The direction of polarization of the 3500 A band immediately limits the possible transitions involved to four as listed in Chapter II which are

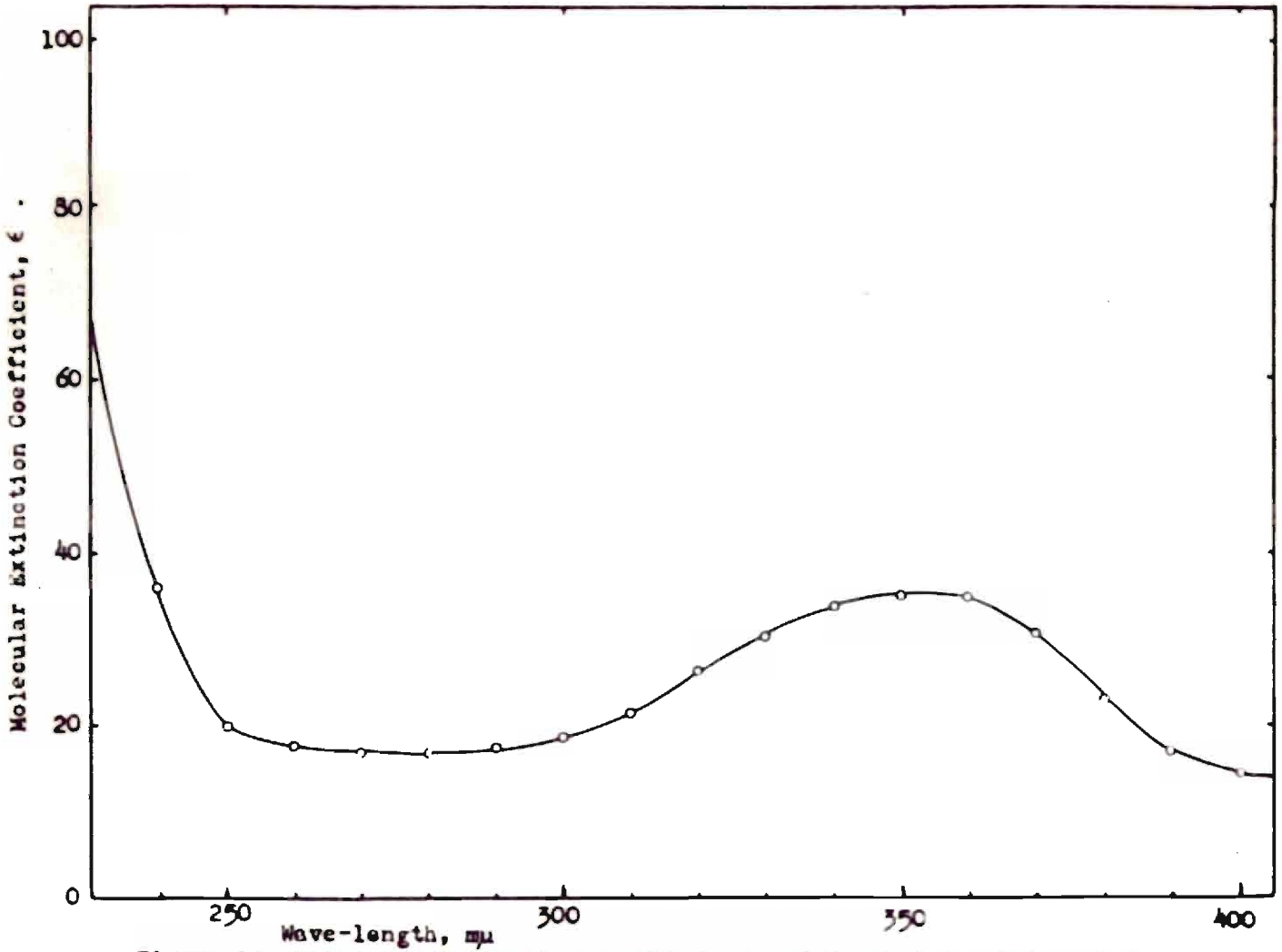

Figure 12. Molecular Extinction Coefficients of Crystalline Sodium Nitrite at Room Temperature (see text).

$\psi_7 \rightarrow \psi_{12}$, $(n_o \rightarrow \pi^*)$;
$\psi_5 \rightarrow \psi_{12}$, $(n_o \rightarrow \pi^*)$;
$\psi_9 \rightarrow \psi_{12}$, $(n_n \rightarrow \pi^*)$;
$\psi_{11} \rightarrow \psi_4$, $(\pi \rightarrow \sigma^*)$.

The complexity of this band suggests either that it consists of more than one of these transitions or that the crystal field causes term splitting (39D). The transition $\psi_{11} \rightarrow \psi_4$ would probably lead to dissociation, and this interpretation is not favored by the existence of fine structure. Also the calculations of Chapter II indicate that the energy for the $\psi_{11} \rightarrow \psi_4$ transition is much too high to be found at this point in the spectrum. On the basis of the above reasoning the $\psi_{11} \rightarrow \psi_4$ transition can be eliminated as a possible source for this 3500 A band. In order to distinguish between the other three bands, additional information is needed.

The polarization of the 2050 A band in the b direction leaves a number of possible transitions that would be responsible for this absorption. The most likely transition, on the basis of calculations in Chapter II, is

$\psi_{11} \rightarrow \psi_{12}$, $(\pi \rightarrow \pi^*)$; but other possibilities

are

$\psi_7 \rightarrow \psi_4$, $(n_0 \rightarrow \sigma^*)$;
$\psi_5 \rightarrow \psi_4$, $(n_0 \rightarrow \sigma^*)$;
$\psi_9 \rightarrow \psi_4$, $(n_N \rightarrow \sigma^*)$;
$\psi_6 \rightarrow \psi_3$, $(n_0 \rightarrow \sigma^*)$;
$\psi_8 \rightarrow \psi_3$, $(n_0 \rightarrow \sigma^*)$;
$\psi_2 \rightarrow \psi_3$, $(\sigma \rightarrow \sigma^*)$.

The high energies of the last six transitions, as calculated in Chapter II, will allow them to be ruled out as sources of the 2050 A band.

There is also a possibility of a charge transfer process, i.e., $Na^+ + NO_2^- \longrightarrow Na + NO_2$, similar to that suggested by Friedman (26F) for the nitrite ion in aqueous solution. The energy inducing this transition in the crystal probably would not need to be polarized in view of the three dimensional crystalline structure (17C). Before eliminating a charge transfer process as the source of the 2050 A band more information is desirable.

OTHER MEASUREMENTS

Silver Nitrite Crystals.--Crystalline silver nitrite shows no appreciable absorption in the 3500 A region; if present at all, it is certainly very weak as compared to the absorption in sodium nitrite at this position in the spectrum. A weak absorption band does begin about 3100 A and either extends into the shorter wave-length region beyond 2400 A or merges with another that does extend into that region. No fine structure is evident in this absorption at liquid nitrogen temperature.

No polarized spectra of silver nitrite were obtained since repeated efforts to grow large single crystals failed. The largest single crystals produced were too small to orient and study spectrographically by the techniques available in this laboratory. To add to the difficulties, the crystals that were secured rapidly darkened on exposure to light. The photo-decomposition is probably responsible for the absorption about 3100 A as reported by Belenky and Juse (40B) for aqueous solutions.

The author has not been able to discover another nitrite with

"bonded" electrons on the nitrogen and the same (C_{2v}) crystal symmetry from which the direction of polarization could be determined.

Nitromethane.--The absorption spectra of nitromethane in ninety-five per cent ethanol and in forty per cent ethanol, thirty per cent water, thirty per cent sulfuric acid (prepared to be about ten formal in hydrogen ions) are shown in Fig. 13 (Table 13). No absorption is observed in the 3500 A region, but there is a weak band with its maximum about 2700 A and a much more intense one beginning just below 2500 A and extending into the vacuum ultraviolet. No fine structure is found in either band. The 2700 A band does exhibit a small solvent effect in that the acidic solution has a lower extinction coefficient (less than 14 as compared to almost 16) and Haszeldine (41H) reports an extinction coefficient of 20 in light petroleum. The wave-length of the maximum also changes from about 2710 A for the acid solution to about 2740 A for the ethanol solution. Haszeldine (41H) reports the maximum in light petroleum to be at 2780 A.

Nitromethane at the temperature of liquid nitrogen does not exhibit any fine structure in the longer wave-length band either. This rapid cooling by liquid nitrogen evidently produced a glass instead of a crystalline mass since the material was quite transparent.

Nitrate Ion.--An aqueous solution of potassium nitrate shows two bands (Fig. 14 and Table 14) (42C), a weak one with its maximum near 3000 A and a more intense one reaching its maximum about 2000 A. No fine structure is present in either band. Krishnan (43K) reports that both of these bands absorb radiation polarized so that the electric vector vibrates parallel to the plane of the nitrate ion. McConnell (44Mc) attributes the 3000 A absorption to an $n \rightarrow \pi^*$ transition on the basis of the intensity

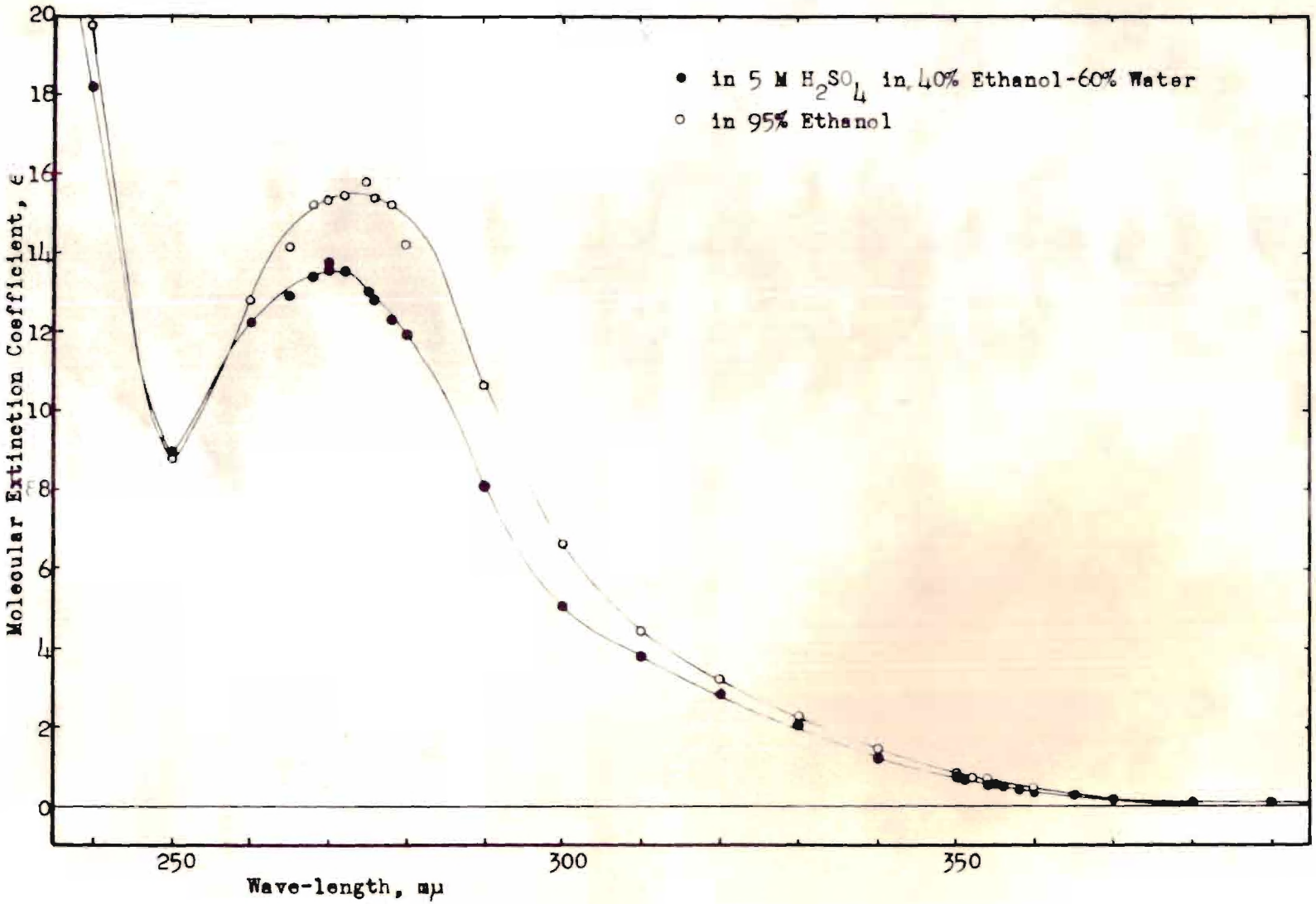

Figure 13. The Absorption Spectrum of Nitromethane

Figure 14. The Absorption Spectrum of an Aqueous Potassium Nitrate Solution (42C)

changes of the bands for NO_3^-, HNO_3, $R\text{-}ONO_2$ and R-N=O. However, since a non-bonding orbital (n) of the nitrate ion or any linear combination of them is symmetric with respect to the plane of the ion and all π orbitals are antisymmetric with respect to the plane of the ion, radiation polarized in the plane of the ion should not induce an $n \rightarrow \pi^*$ transition. Thus either Krishnan's assignment must be wrong or McConnell's reasoning is not substantiated in this instance.

Ethyl Nitrite.--The absorption spectrum of ethyl nitrite was measured as a gas and in five solvents as follows:

a. normal hexane,

b. ninety-five per cent alcohol,

c. ninety-five per cent ethyl alcohol, one formal in hydrochloric acid,

d. water, and

e. water one formal in hydrochloric acid.

These spectra are recorded in Tables 15 and 16 and Figs. 15 and 16. The gaseous absorption is compared with that reported by Purkis and Thompson (45P). Qualitatively all of these spectra are similar in that there is an absorption maximum about 3600 A with some fine structure and a much more intense band with its maximum near 2200 A.

No great effort was made to measure accurately the absolute extinction coefficient of the ethyl nitrite but care was taken to measure the relative absorption in the different solutions. For the purposes of this work the absolute value of the extinction coefficient is not required, but the relative change of this absorption coefficient in the different solvents is significant. Hydrogen bonding or "solvation" of

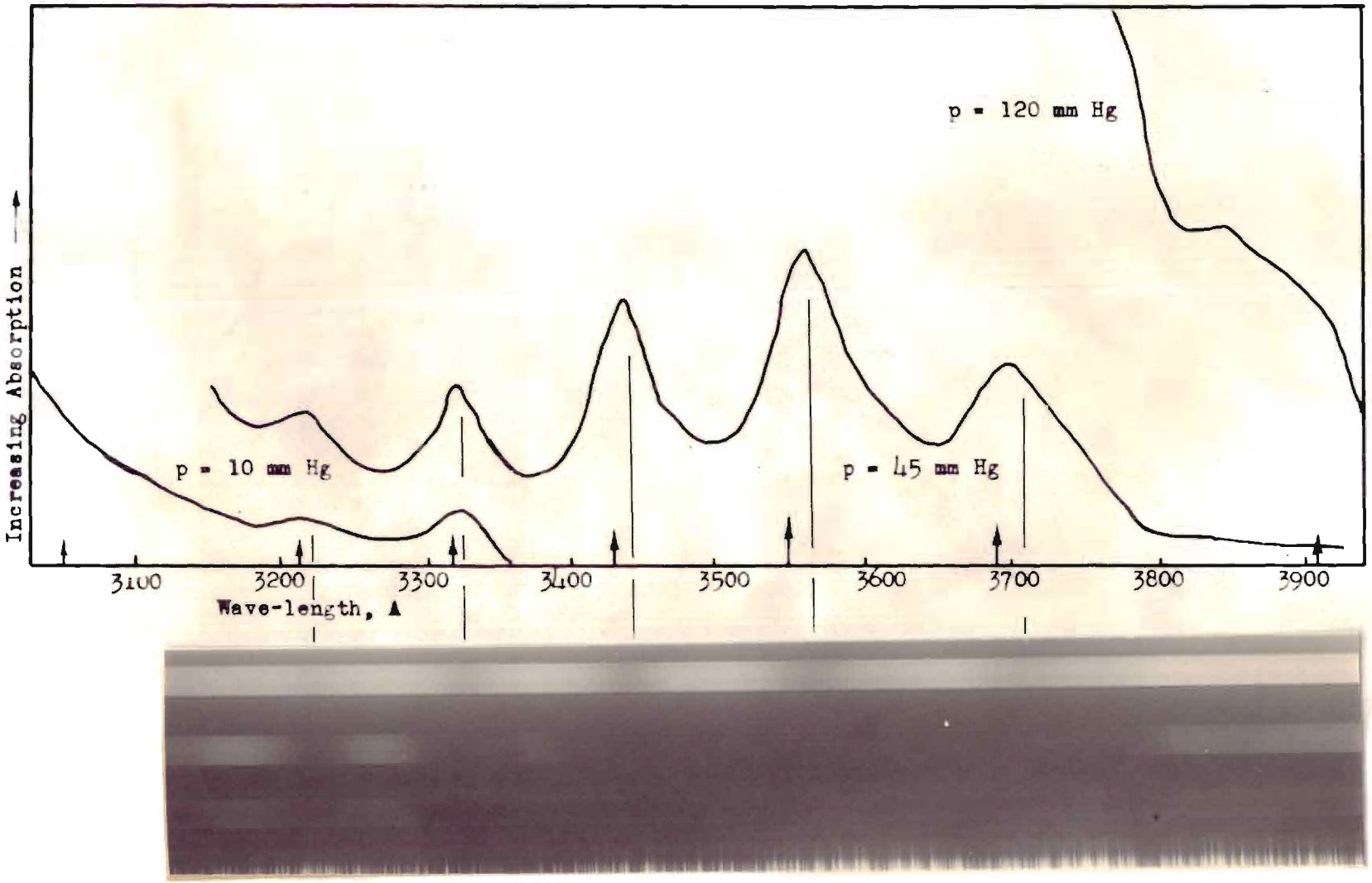

Figure 15. The Absorption Spectrum of Ethyl Nitrite Gas (The arrows, ↑, indicate the position of absorption maxima reported by Purkis (45P))

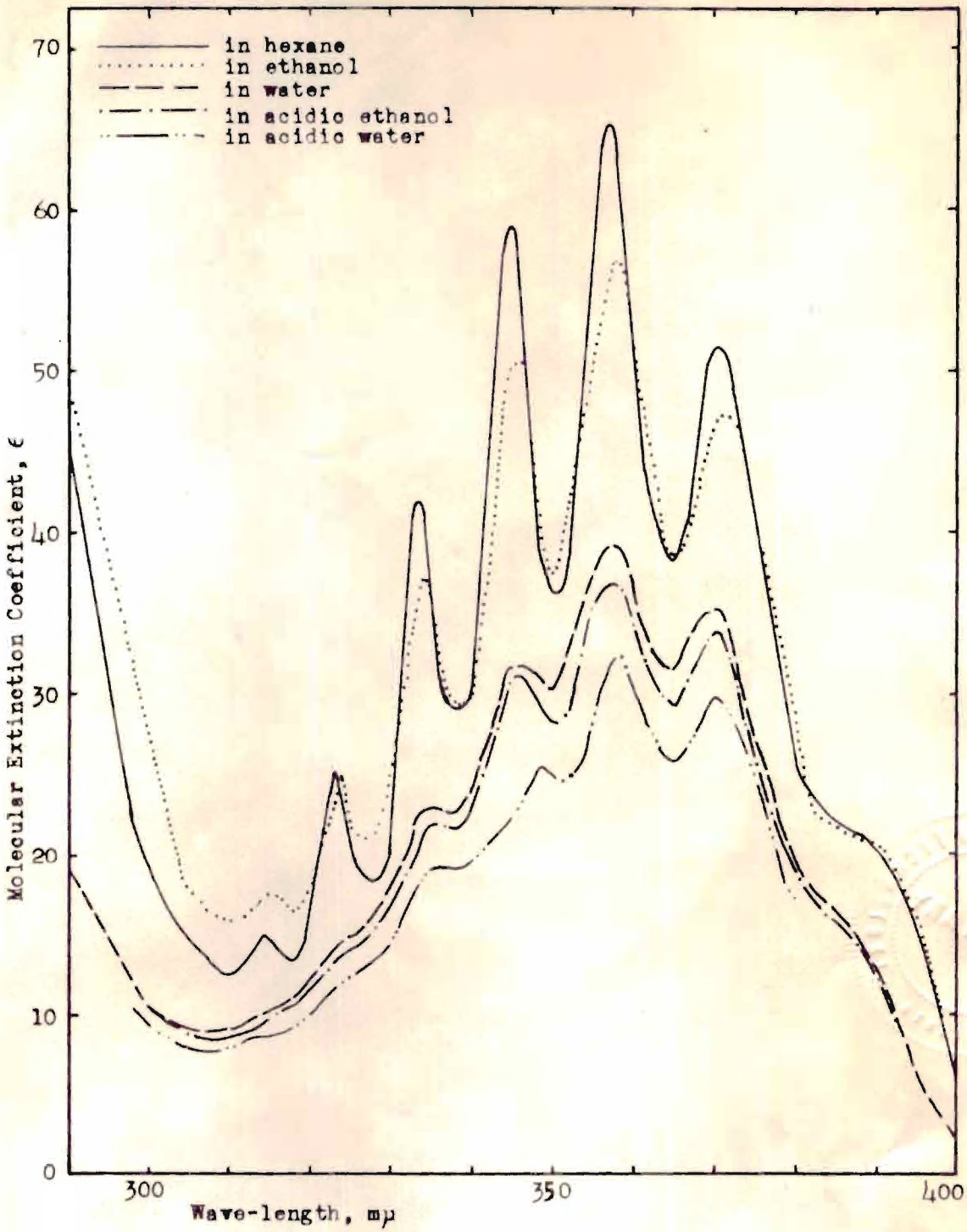

Figure 16. Absorption Spectrum of Solutions of Ethyl Nitrite (see text)

the "non-bonding" nitrogen electrons on some of the molecules would lead to a decrease in absorption due to the $n_N \rightarrow \pi^*$ transition. The greatest difficulty in obtaining an absolute extinction coefficient was in determining the concentration of the stock solutions. The second stock solution (B), in ethyl alcohol, was deemed more accurate for several reasons, namely, greater care in preparation and less tendency to evaporate due to the greater solubility of the ethyl nitrite in alcohol. The error is estimated to be not over twenty per cent and perhaps within ten per cent. Though no exceptional purity was claimed for the ethyl nitrite the method of preparation (see Chapter III, p. 33) indicates that any error introduced here would be rather small as compared to the error introduced by the uncertainty of the concentration. The possibility of decomposition was realized but successive measurements indicated this to be small. The loss of ethyl nitrite during dilution seems to be the greatest source of error, and this loss is greater from the hexane and aqueous solutions.

Because of the greater care used in preparing stock solution B, the greater solubility of ethyl nitrite in the alcohol, the identical handling of solution VB (ethanolic) and VIB (aqueous), and the agreement of the extinction coefficient with that reported by Haszeldine (55.5 as compared to 45 for butyl nitrite in ethanol and 87 in light petroleum at 357 and 356 millimicrons), (41H) the measurements on these two solutions were considered standard. Measurements of extinction coefficients from other ethanolic and aqueous solutions were assumed to have an unknown concentration and adjusted so as to agree with VB and VIB, respectively, at 357-358 millimicrons. The averages of these different runs are plotted in Fig. 16.

Calculations of the extinction coefficients made from measurements on solution VIA were adjusted by making its apparent concentration the same as that for solution VIIA (ethanolic), because these two solutions were made in the same way from the same stock solution and handled similarly. The other hexane solutions were adjusted to agree at 370 millimicrons. The acidic ethanolic solution, IIIB, and the acidic aqueous solutions IVB were adjusted by changing the apparent concentration of solutions IB and IIB (the solutions from which they were made by addition of acid) to correct for the dilution due to added acid. The results of these calculations are given in Table 16. For comparison, the concentrations of the solutions as estimated from preparation and the concentrations estimated by absorption are tabulated also (Table 16).

Amyl Nitrite.--Amyl nitrite, cooled rapidly to the temperature of liquid nitrogen, formed a transparent solid believed to be a glass and gave the spectrum shown in Fig. 17 and Table 17. The absorption spectrum is similar to that for ethyl nitrite; a very intense diffuse band with its maximum near 2000 A or slightly longer wave-length and a weaker band of seven maxima with the strongest reaching its maximum at 3446 A. For comparison the maxima of the gas reported by Purkis and Thompson (45P) are shown in Table 17 and indicated as lines on Fig. 17.

Sodium Nitrite Solutions.--The absorption of sodium nitrite solutions in one-tenth formal aqueous hydrochloric acid and one-tenth formal sodium hydroxide are given in Table 18 and the region from 2500 A to 4100 A is shown in Fig. 18. There are two bands in both cases; the more intense reaching its maximum about 2000 A and the weaker one located in the 3500 A

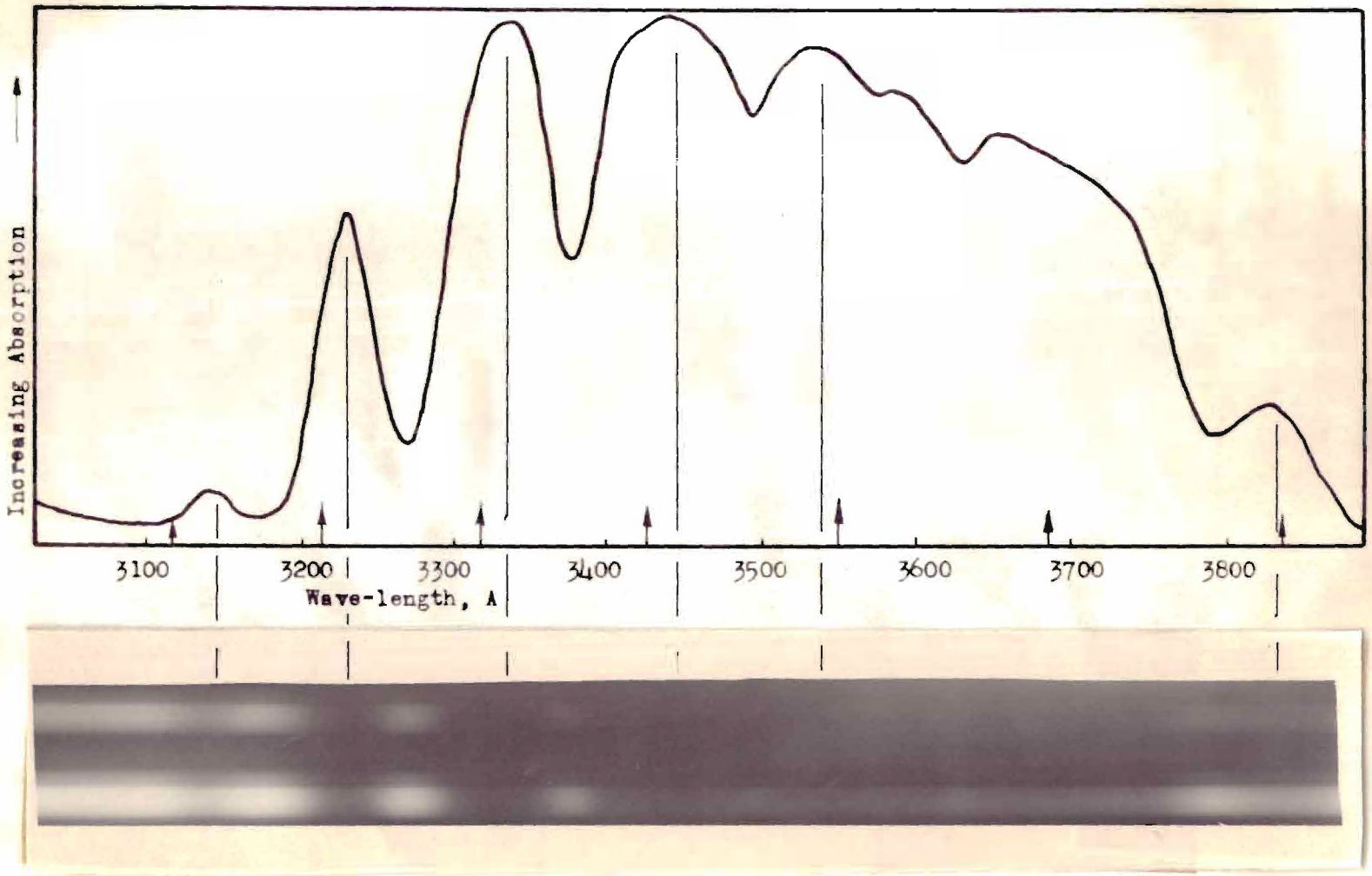

Figure 17. The Absorption Spectrum of Amyl Nitrite Glass (Arrows, ↑, indicate the position of the absorption maxima reported by Purkis and Thompson (45P))

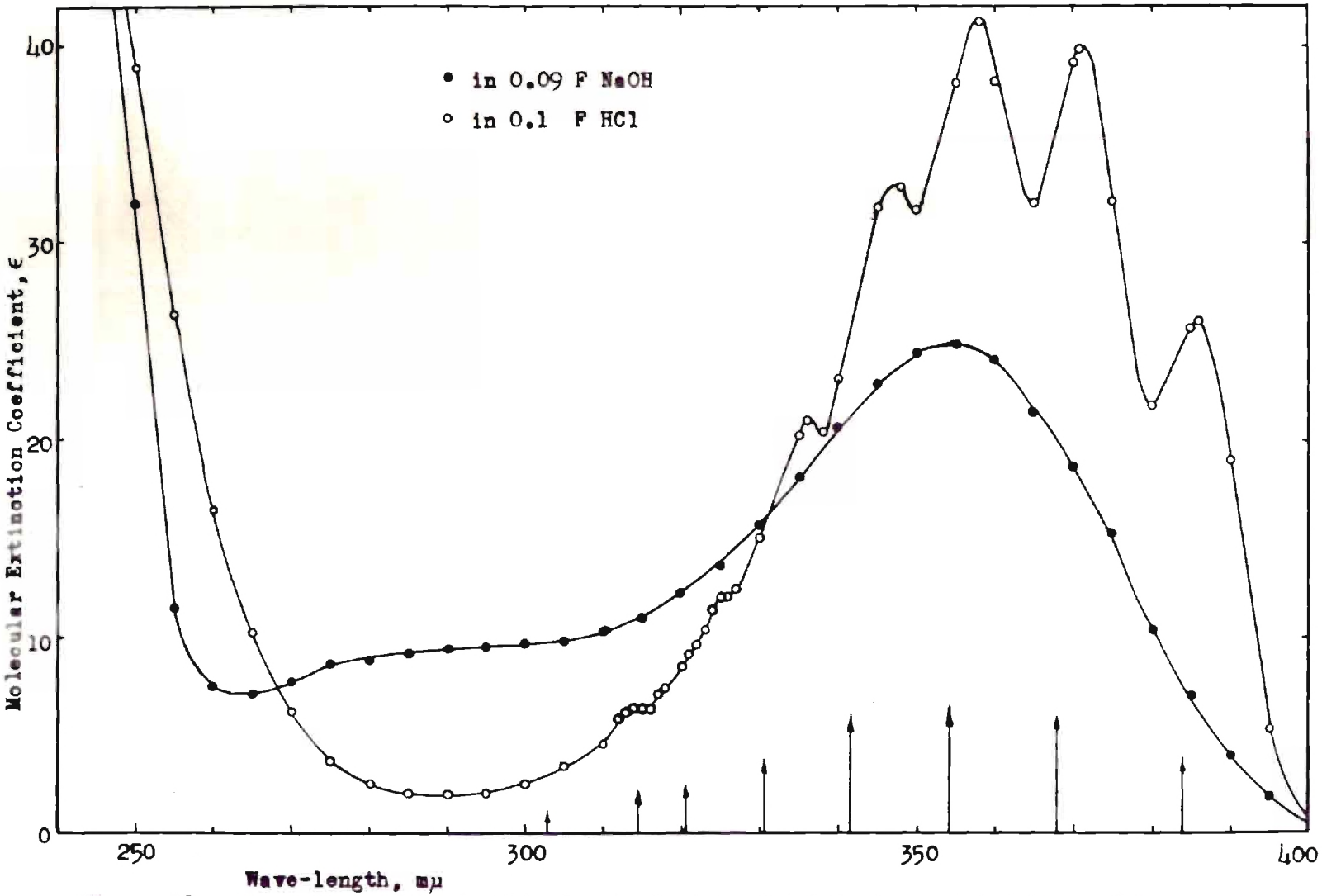

Figure 18. Absorption of Sodium Nitrite in Basic and Acidic Aqueous Solutions (The arrows, ↑, represent the absorption maxima of nitrous acid reported by Tarte (467))

region. Closer observation of the basic solution reveals no fine structure. The maximum of the 3500 A band is about 3550 A. A third band, weaker than either of the other, appears with a maximum about 2900 A and overlapping the band on either side.

The acidic solution of sodium nitrite gives the absorption spectrum of nitrous acid which consists of a band of five or six maxima at about 358 and 371 millimicrons. For comparison the absorption maxima given by Tarte (46T) for gaseous nitrous acid are shown on Fig. 18 as lines and are listed in Table 19. Similar results are given by Kortum (47K). There is no evidence of a third band between this 3500 A region and the 2000 A band. The maximum molecular absorption coefficient of the band at 3500 A is greater in the acidic solution than in the basic solution by a ratio of about three to two. There is a change of the ratio of the extinction coefficients of the 2000 A band to the 3500 A band on solution. In the crystal this ratio is about eight or ten to one, but in solution the ratio is about three hundred to one.

Nitrosyl Chloride.--Goodeve and Katz (48G) give the absorption spectrum for nitrosyl chloride gas shown in Fig. 19 and Table 20. It is possible that the diffuse band at 3350 A and the more intense band at 1970 A are comparable to those bands of the alkyl nitrites at similar places in the spectrum.

Nitryl Chloride.--Eberhardt (49E) and Athey (50A) report that the absorption spectrum of nitryl chloride gas shows two bands in the 2000 A - 4000 A region also. A very intense band reaches its maximum somewhere below 2400 A and a weaker band has a maximum about 3000 A; neither shows any fine structure.

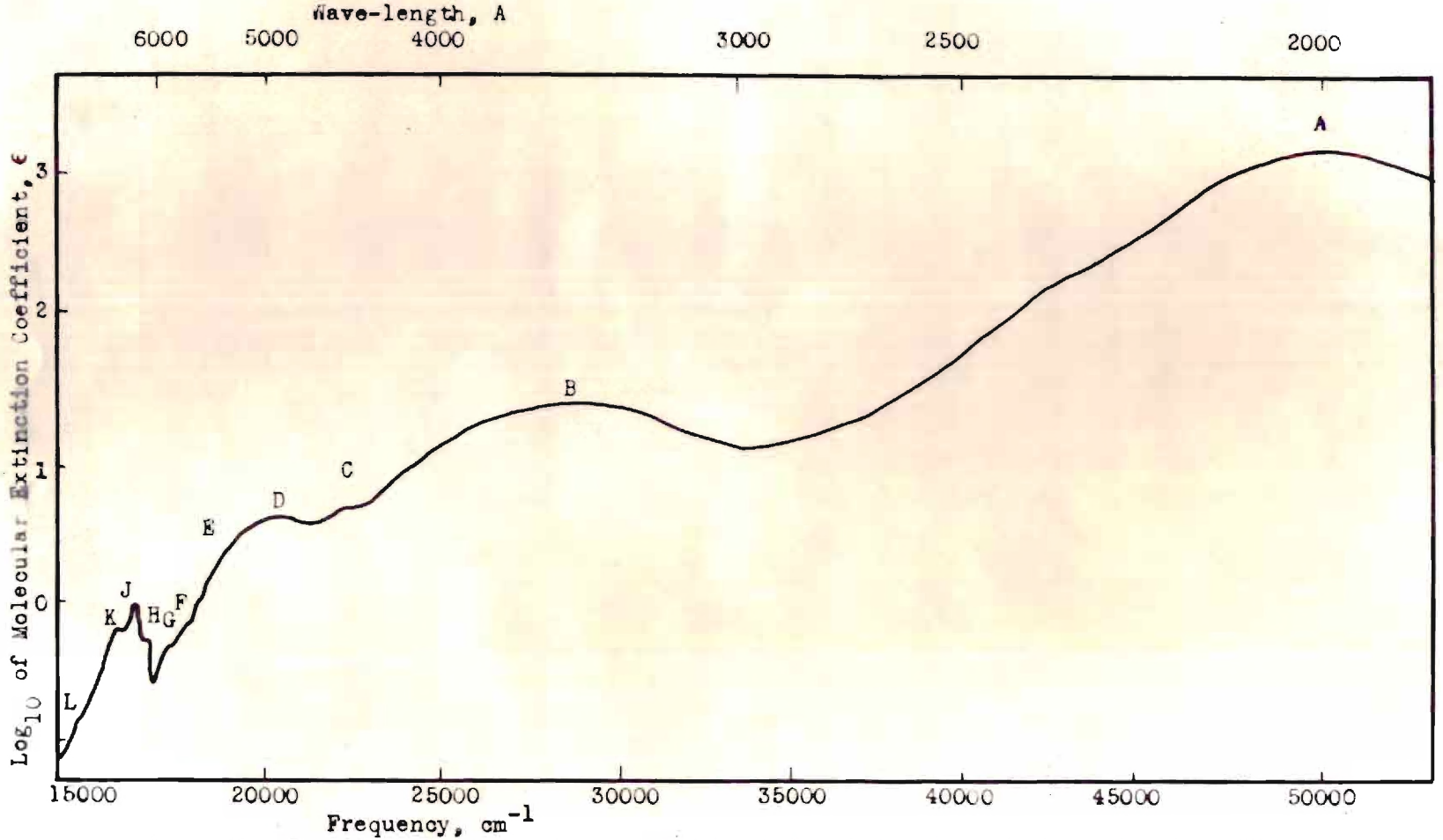

Figure 19. The Adsorption Spectrum of Nitrosyl Chloride after Goodeve and Katz (48G)

Ozone.--Vigroux (51V) has summarized the absorption spectrum of ozone, a system isoelectronic with the nitrite ion. There is a very intense band about 2500 A (Fig. 20 and Table 21) and one not so intense with a maximum about 6000 A (Fig. 21 and Table 21). The one at 2500 A shows some fine structure superposed on the long wave-length end which has its origin at 3514 A. The 6000 A band also shows several maxima (Fig. 21).

Nitrogen Dioxide.--Nitrogen dioxide exhibits two regions of absorption of interest. Harris and King (52H) report that the strong absorption band beginning at 2491 A is polarized along the axis of symmetry of the approximate symmetric rotor, i.e., parallel to a line joining the oxygen atoms. This suggests that it is a $\pi \rightarrow \pi^*$ transition. The region between 4000 A and 9000 A probably contains two or more electronic transitions but has not yielded to detailed analysis.

DISCUSSION OF SODIUM NITRITE ABSORPTION BANDS

The only conclusive evidence presented here is the polarization of the radiation absorbed by the nitrite ion, however, by reasoning based on absorptions in similar substances it is believed that a definite assignment can be made for the transition giving rise to the absorptions. This reasoning is presented below.

The 3500 A Band.--The 3500 A band in crystalline sodium nitrite seems to be predominately due to a transition whereby one of the electrons of ψ_9, which is primarily localized on the nitrogen atom and not shared by other atoms, is promoted to ψ_{12}, an antibonding π orbital. The absorption due to transition, $\psi_9 \rightarrow \psi_{12}$ ($n_N \rightarrow \pi^*$), in the crystal seems to be complicated by a weaker underlying transition $\psi_7 \rightarrow \psi_{12}$ ($n_O \rightarrow \pi^*$). Added complication

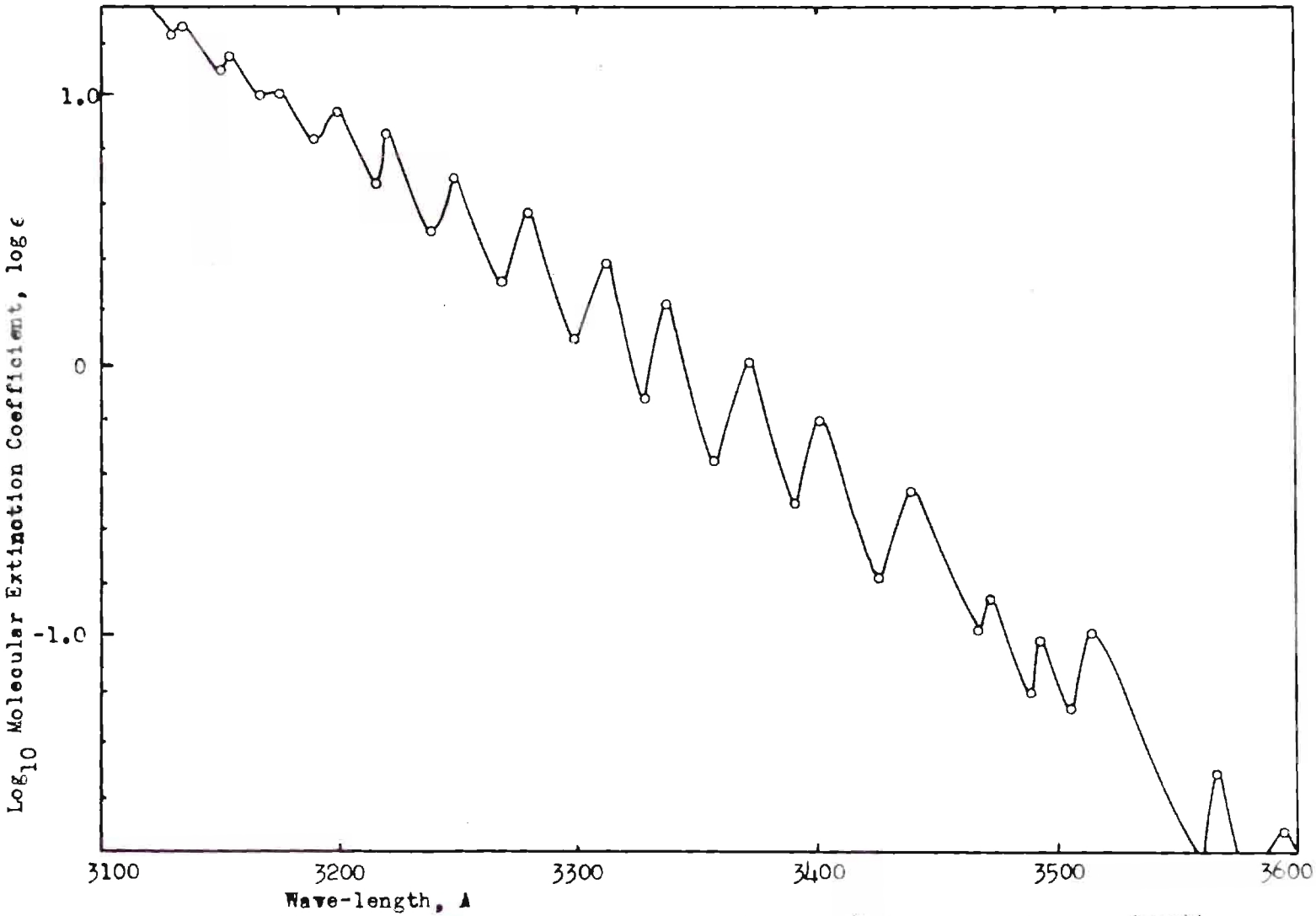

Figure 20. A Portion of the 2550 A Band of Ozone (Points from Vigreux (51V))

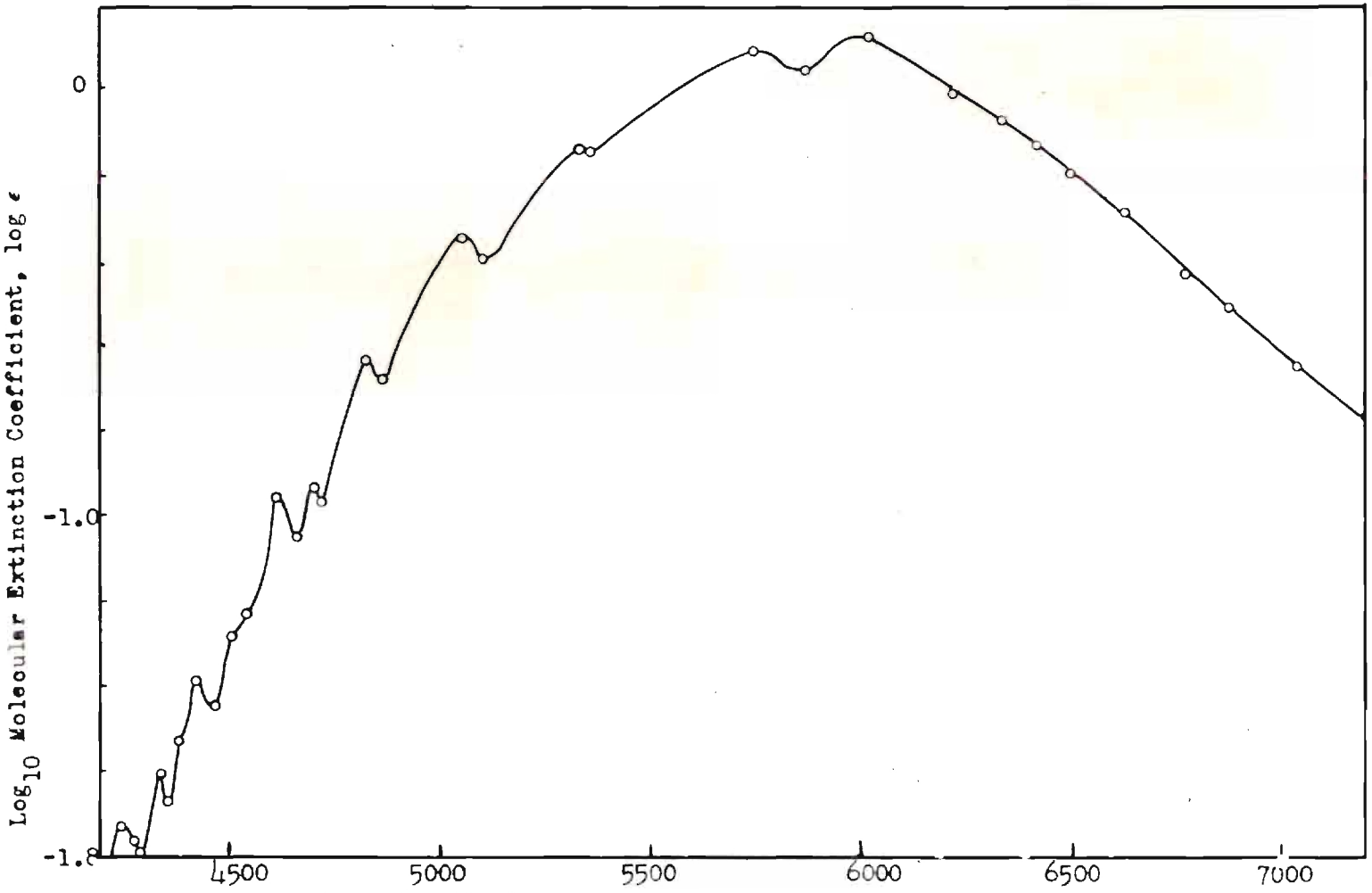

Figure 21. The 6020 A Band of Ozone (Points from Vigreux (51V))

of this band may come from splitting in the crystal field (39D). This second transition promotes an electron which is in a molecular orbital localized on the oxygens and designated as a non-bonding oxygen electron. The grounds for this assignment are given below.

The absence of a band at 3500 A in silver nitrite where, though crystal structure is the same except for spacing, there seems to be an electron pair bond between the nitrogen atom and the silver atom. The tendency for silver to form the $[Ag(NO_2)_2]^-$ complex (53N) seems to verify the existence of this bond. This electron pair bond would stabilize the "non-bonding" electrons on nitrogen and thus shift the absorption due to transitions involving these electrons farther into the ultraviolet.

Likewise, in nitromethane, where there is certainly a bond between carbon and nitrogen that uses the orbital of the NO_2 group comparable to ψ_9 of the ion no absorption is found at 3500 A. No non-bonding nitrogen orbitals exist in the nitrate ion since the bonds to the oxygen atoms would require all three of the sp^2 orbitals. As would be expected there is no absorption in the 3500 A region in the nitrate ion.

On the other hand the alkyl nitrites, nitrous acid, nitrosyl chloride, ozone and nitrogen dioxide have absorptions that could be attributed to a transition comparable to the $n_N \rightarrow \pi^*$.

The question arises as to the possibility that one of the remaining pair of non-bonding electrons on the alkyl nitrites and nitrous acid would give rise to an $n_O \rightarrow \pi^*$ transition. Of course all of these non-bonding orbitals will be combined to give a set of molecular orbitals, as was the case in the nitrite ion though neglected there. However the

orbital that has the greatest contribution from oxygen AO's (n_O) will be more stable in R-O-N=O than in the nitrite ion due to a decrease in formal charge on the oxygen from - 1/2 to zero. This would tend to shift the absorption farther into the ultraviolet. This concept is in agreement with the fact that formic acid shows no absorption until the wavelength is about 2500 A or less (54G). In the case of formic acid the "n_N" electrons are stabilized by the hydrogen attached to the carbon.

A comparison of the 3500 A band of nitrous acid and ethyl nitrite with the 6000 A band of ozone shows a striking similarity (Fig. 22). The extensive absorption of nitrogen dioxide may well be due, in part, to a comparable transition in that molecule. Dinitrogen tetroxide shows no absorption above 4000 A (55H).

The 3350 A band in nitrosyl chloride suggests that it is due to this same type transition. The intensities of all of these bands are of the right magnitude for an $n \rightarrow \pi^*$ transition (27K).

The position of the bands in the more similar of these substances, namely nitrite ion (λ_{max} 3550 A), nitrous acid (λ_{max} 3570 A), ethyl nitrite (λ_{max} 3570 A), and nitrosyl chloride (λ_{max} 3350 A), also suggests that the transition is of the same origin in all of them. All of the bands in ozone and nitrogen dioxide (see below) seem to be shifted to longer wave-lengths.

Nakamoto (11N) ascribes the band at 760 millimicrons in m-nitronitrosobenzene to an $n_N \rightarrow \pi^*$ transition of a non-bonding electron on the nitroso-nitrogen to a π orbital of the molecule. The longer wavelength is not surprising in view of the fact that the π orbital involves the benzene ring also.

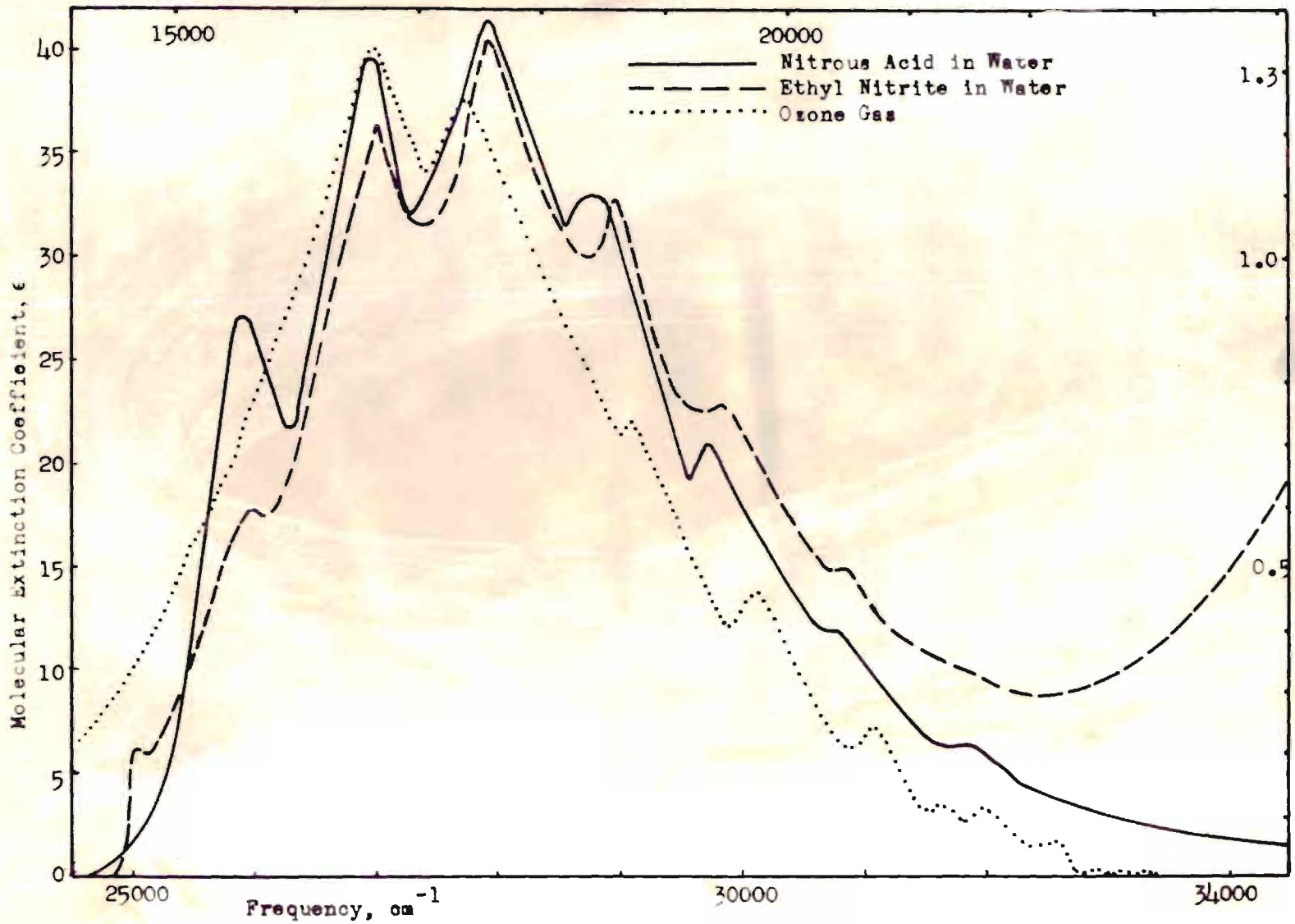

Figure 22. Comperison of 3500 A Band in Nitrous Acid and Ethyl Nitrite with 6020 A Band in Ozone (Above and to the Right are the Scales for Ozone)

The existence of a weaker absorption at about 2900 A in aqueous sodium nitrite is believed to be due to a transition $\psi_7 \rightarrow \psi_{12}$ ($n_0 \rightarrow \pi^*$). This band is believed to underlie the 3500 A band in the crystalline sodium nitrite. Since it involves an electron on an oxygen atom which is essentially unshared by a second atom it is not surprising that it would undergo a "blue shift" (44Mc) on dissolving in water. These electrons must be quite basic since nitrous acid is formed when protons react with the nitrite ion. In nitrous acid the hydrogen is attached to an oxygen instead of the nitrogen atom. This assignment seems to be verified by the absence of this third band in nitrous acid and the alkyl nitrites (R-ONO). The weak bands in silver nitrite, nitromethane, and nitryl chloride are probably due to a non-bonding oxygen electron being raised to an antibonding π orbital since there are no "free" electrons on the nitrogen atom. The absorption in nitromethane shows a solvent effect as expected for a $n \rightarrow \pi^*$ transition (44Mc).

An absorption band due to the $n_0 \rightarrow \pi^*$ transition in ozone is probably the one beginning at 3514 A. In nitrogen dioxide a comparable transition probably gives rise to some of the absorption in the 4000 A to 9000 A region. This extensive band between 9000 A and 4000 A has not yielded to separation into individual electronic transitions. Since there should be two such transitions involving non-bonding oxygen electrons these transitions could be the origin of a second and third band in this region of the nitrogen dioxide spectrum. In N_2O_4 there is no absorption above 4000 A (55H) and the two bands with maxima near 2600 and 3400 A are probably due to non-bonding oxygen electrons jumping to an antibonding π molecular orbital. A longer wave-length than found in nitromethane

would be expected due to the antibonding π in the N_2O_4 involving a larger part of the molecule and thus having lower energy. A shorter wave-length then in nitrogen dioxide is probably due to a higher energy of the non-bonding orbitals as the O-N-O angle becomes more nearly 180° (25W). The nitryl chloride absorption band with its maximum about 2900 A is probably to be ascribed to the raising of a non-bonding oxygen electron to an anti-bonding π orbital.

The 2050 A Band.--Primarily on the basis of its polarization the very intense absorption band of the nitrite ion at 2050 A is assigned as a $\pi \rightarrow \pi^*$ transition ($\psi_{11} \rightarrow \psi_{12}$) and is comparable to similar bands in nitrous acid, alkyl nitrites, nitroalkyls, silver nitrite, nitryl chloride, nitrosyl chloride (λ_{max} 1970 A), ozone (λ_{max} 2550 A), nitrogen dioxide (λ_{max} 2491 A), and nitrate ion (λ_{max} 2000 A). All of these bands are very intense as would be expected for $\pi \rightarrow \pi^*$ transitions (27K). The rotational analysis of the nitrogen dioxide band at 2491 A (52H) indicates the electronic transition is polarized properly for a $\pi \rightarrow \pi^*$ ($\psi_{11} \rightarrow \psi_{12}$) transition.

The possibility of a charge transfer being the origin of this band can be further discounted. Rabinowitch (56R) assigns this band in sodium nitrate to such a process, but states that the molecular extinction coefficient should reach or exceed 10^4. The intensity of the absorption in the crystal, on the basis of Rabinowitch's intensity requirements, is not a charge transfer ($\log \epsilon_{max} \approx 2.5$ for $NaNO_2$ as compared to $\log \epsilon_{max} = 4.05$ for $NaNO_3$). However, the increased intensity of this band in solution could be, at least in part, due to a charge transfer (see Appendix VII).

Thermodynamic data for the process

$$NaNO_{2\,(solid)} \rightarrow Na_{(gas)} + NO_{2(gas)}$$

indicate the energy would be equivalent to about 2380 A (see Appendix VII). The energy for the process in aqueous solution

$$NO^{-}_{2(aqueous)} + H_2O_{(liquid)} \rightarrow NO_{2(gas)} + H_{(gas)} + OH^{-}_{(aqueous)}$$

corresponds to about 2880 A. It is reasonable to assume that the energy difference for the charge transfer process in solution and in the crystal is of the same order of magnitude as that indicated by the thermodynamic data. This would place the absorption in the crystal about 7000 cm^{-1} above that in solution or about 1800 A if the 2050 A band in solution is assumed to be due to charge transfer. On the basis of thermodynamic calculations outlined in Appendix VII strontium nitrite is the most likely substance considered which would give a charge transfer spectra in the crystal above 2000 A. Silver nitrite is not ionic, judging from the previous reasoning, and the process could not be readily described as a charge transfer.

Comparison of the Band Separations.--Perhaps the best way to compare the various bands in the different substances is to compare the differences in the energy of the transitions. The accompanying figure depicts the significance of these numbers.

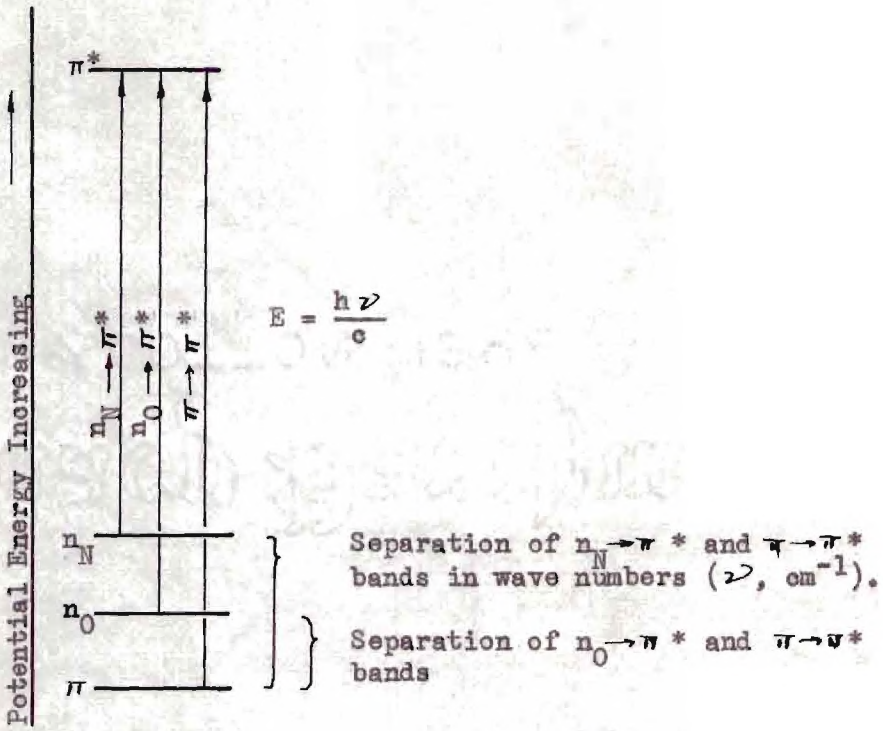

Figure 23. Promotional Energy and Band Separation Diagram

The way that the separation of these bands changes from one substance to another is an indication of the relative stabilities of these orbitals. These separations are listed in Table 3.

If it is assumed that the difference in energy of the n_N and π orbitals is 13000 cm^{-1} for the typical triatomic system and the difference between the n_O and π orbitals is 8000 cm^{-1} then any deviation from these values should give insight into the behavior of these orbitals under various conditions.

A separation of the $n_N \rightarrow \pi^*$ and $\pi \rightarrow \pi^*$ transitions smaller than 13,000 cm^{-1} could be due to

(1) stabilization of the n_N orbital by

(a) increase in its s-character as the O-N-O angle decreases (25W) or

Table 3. Comparison of Band Separation*

Substance	A	B
Nitrite Ion (crystal)	9040 cm^{-1}	7603 cm^{-1}
Nitrite Ion (solution)	13400	8500
Silver Nitrite (crystal)		3000
Nitrous Acid	13000	
Ethyl Nitrite	13000	
Amyl Nitrite (glass)	>7000	
Nitrosyl Chloride	3100	
Ozone	12400	600
Nitrogen dioxide	-	15000
Dinitrogen Tetroxide		12500
Nitryl Chloride		9500
Nitro-nitrosobenzene	9200	

*For the origins as estimated, see Chapter V.

Column A is a measure of the energy difference of the n_N and π^* orbitals expressed in wave numbers (cm^{-1}, ν).

Column B is a measure of the energy difference of the n_O and π^* orbitals.

(b) increase in "effective" nuclear charge of the nitrogen atom,

(2) destabilization of the π^* orbital by

(a) a decreased number of atoms involved (conjugation), or a combination of these. A separation larger than this value could be due to a change of the above in the opposite direction.

A separation of the n_O and π orbitals by an energy larger than 8000 cm^{-1} could be due to

(1) destabilization of the n_O orbital by

(a) less overlap with other n_O orbitals due to increased O-N-O angles (25W), or

(b) decrease in the interaction of these orbitals with a solvent,

(c) decrease in the effective nuclear charge as more electrons are "concentrated" on the oxygen atoms,

(2) stabilization of the π orbital as a result of greater conjugation, or any combination of these effects. A decrease in the energy separation could be ascribed to the reversal of these effects.

The separation of the n_N and π orbitals for crystalline sodium nitrite smaller than 13000 cm^{-1} is probably due primarily to an increase in s-character of the n_N as the O-N-O angle decreases in the crystal field.

The small separation of the n_O and π orbitals in silver nitrite may suggest that there is not such a high concentration of electrons on the oxygen since the substance is probably not as ionic as sodium nitrite.

The 7000 cm^{-1} separation tabulated for amyl nitrite may not be correct since it was estimated from a curve not too suitable for such an estimate. Purkis and Thompson (45P) report its absorption as almost identical with that of ethyl nitrite.

The small separation of the n_N and π in nitrosyl chloride is probably due to increased effective charge of the nitrogen nucleus as the chlorine atom "withdraws" electrons. Also the π orbital is probably destabilized due to lack of a vacant p-orbital on chlorine.

In ozone it would be expected, on the basis of increased nuclear charge, that the n_O and π orbitals would be more widely separated than in the nitrite ion but it seems to be in the opposite direction. However, if the $n_O \rightarrow \pi^*$ transition that corresponds to the one in the nitrite ion ($\psi_7 \rightarrow \psi_{12}$) at 3100 A in solution were at about 6000 A, underneath the $n_N \rightarrow \pi^*$ type band, and the band at 3514 A were assigned to a transition

corresponding to $\psi_5 \rightarrow \psi_{12}$ ($n_0 \rightarrow \pi^*$) this would be reasonable. This $\psi_5 \rightarrow \psi_{12}$ ($n_0 \rightarrow \pi^*$) transition is assumed to be hidden by the $\pi \rightarrow \pi^*$ transition in the nitrite ion and other substances.

The large separation of the n_0 and π orbitals in the nitrogen dioxide and dinitrogen tetroxide suggests destabilization of the n_0 orbital in NO_2 due to larger O-N-O angle and the stabilization of the π orbital in N_2O_4 due to conjugation over a larger system.

The smaller separation of the n_N and π orbitals in nitro-nitrosobenzene indicates that the n_N orbital is stabilized more than the π orbital. The stabilization of the n_N orbital is probably due to a combination of increased s-character of the orbital and increased effective nuclear charge due to electron "withdrawing" power of benzene ring. Of course the π orbital should be stabilized due to conjugation with the benzene ring.

CHAPTER V

CONCLUSIONS AND RECOMMENDATIONS

Conclusions.--Crystalline sodium nitrite at a temperature of 75° absolute was found to have an absorption band containing much fine structure with its origin at a wave-length of 3851.4 A. The absorbed radiation must have its electric vector vibrating perpendicular to the plane of the ion. This band was interpreted as having as its origin two electronic transitions in which non-bonding electrons of the nitrite ion are raised to an anti-bonding π molecular orbital. The transition involving the electrons on the nitrogen atom of the ion was assumed to have its origin at 3851.4 A while the transition involving the non-bonding oxygen electrons required slightly more energy. Though no detailed analysis of the fine structure was possible the basis for this assignment is in comparison with spectra of similar substances such as silver nitrite, nitromethane, nitryl chloride, which have no absorption at this point in the spectrum; and ethyl nitrite, nitrous acid, and nitrosyl chloride, which do have absorption at this point. These assignments are consistent with quantum mechanical calculations for the nitrite ion made on the basis of overlap integrals and valence state promotional energies.

An aqueous solution of sodium nitrite showed no fine structure but gave an absorption band with its maximum at about 355 millimicrons which has been ascribed as a transition in which a non-bonding nitrogen electron is raised to an anti-bonding π orbital ($n_N \longrightarrow \pi^*$). In addition another weaker band with its maximum near 2950 A is attributed to the non-bonding

oxygen to anti-bonding π transition ($n_O \rightarrow \pi^*$). This band is thought to be superposed on the short wave-length part of the $n_N \rightarrow \pi^*$ band in the crystalline spectrum thus making a detailed analysis of the fine structure more difficult. It also served to broaden the band in the spectrum of the crystalline sodium nitrite.

The polarization of the much more intense band of the nitrite ion, which has its maximum about 2050 A, is parallel to a line joining the oxygen atoms. This fact and evidence from the spectra of nitrogen dioxide and other similar substances has led to the assignment of this absorption to an electron passing from a non-bonding π orbital (ψ_{11}) to an anti-bonding π orbital (ψ_{12}).

Assignment of the transitions in similar substances is summarized in the table below. Factors leading to these assignments were polarization (when known), similarity of fine structure, solvent effects, position in the spectrum, and intensities.

Table 4. The Assignment of Absorption Band Origins in the Nitrite Ion and Some Similar Substances

Substance	A		B		C	
	Origin[a]	ϵ_{max}[b]	Origin[a]	ϵ_{max}[b]	Origin[a]	ϵ_{max}[b]
Nitrite Ion (crystal)	3851 A	35	3650 A	?	2860 A	350
Nitrite Ion (aq. soln.)	3900	25	3280	10	2560	7500
Silver Nitrite (crystal)	----	--	3100	10*	2860*	?
Nitrous Acid	3850	39	----	--	2560	>1000
Ethyl Nitrite (hexane soln.)	3850	65	----	--	2560	>1000
Amyl Nitrite (glass)	3850	50*	----	--	3000	1120
Nitrosyl Chloride	3340	33	----	--	3000	2550
Ozone	6250	1.33	3520	0.6	3514	2700
Nitrogen Dioxide	?	?	4000	34	2500	?
Dinitrogen-Tetroxide	----	--	3640	34	2500	?
Nitrate Ion (aq. soln.)	----	--	3220	7.3	2700	22000
Nitryl Chloride	----	--	3600	10	2670	3000
Nitromethane	----	--	3100	16	2560	?
Nitro-nitrosobenzene	>7700	1.1			4500	2.2

Column A is for bands assigned to $n_N \rightarrow \pi^*$ transitions. Column B is for $n_O \rightarrow \pi^*$ transitions. Column C is for $\pi \rightarrow \pi^*$ transitions.

[a] The origin is given in terms of wave-length, A, of the radiation inducing the transition.

[b] The maximum molecular extinction coefficient for the band is given under ϵ_{max} when it is known.

*Values so marked are not more than a rough estimate.

Recommendations.--Some of the measurements reported in this work, though accurate enough for the purpose of this effort, are not altogether satisfactory in other respects. Therefore some suggestions for further work are enumerated below.

The absolute value of the molecular extinction coefficient of ethyl nitrite in various solvents, similar to the ones reported here, should be measured.

Some technique should be developed by which large single crystals of silver nitrite can be grown and oriented for study in polarized ultraviolet radiation to confirm the conclusions reported herein.

The effect of increasing the hydrogen ion concentration on the intensity of the nitrous acid absorption in the region around 3500 A should also be checked with precautions to be sure that any change is not due to loss of nitrous acid by evaporation.

The polarization of the longer wave-length absorption of the nitrate ion should be checked to be sure that Krishnan's assignment is correct.

Further study should be made of the fine structure of the nitrite ion absorption in the low temperature spectrum of the crystal. A detailed analysis of this band would be a great aid in a more complete understanding of this triatomic system.

APPENDIX I

CONSTRUCTION OF SYMMETRY ORBITALS

From four AO's one can construct four and only four MO's of the form (15C)

$$\psi_j = b_{1j}\phi_1 + b_{2j}\phi_2 + b_{3j}\phi_3 + b_{4j}\phi_4$$

but with four AO's it is possible to make more than this number and still maintain suitable numerical values for the coefficients, i. e., $b_{1j}^2 + b_{2j}^2 + b_{3j}^2 + b_{4j}^2 = 1$. To simplify the construction assume equal contribution from each AO in every MO, i.e., $b_{1j}^2 = b_{2j}^2 = b_{3j}^2 = b_{4j}^2 = 1/4$ and the following MO's can be written:

$$\psi_a = \frac{1}{2}(\phi_1 + \phi_2 + \phi_3 + \phi_4),$$

$$\psi_b = \frac{1}{2}(\phi_1 + \phi_2 + \phi_3 - \phi_4),$$

$$\psi_c = \frac{1}{2}(\phi_1 + \phi_2 - \phi_3 + \phi_4),$$

$$\psi_d = \frac{1}{2}(\phi_1 - \phi_2 + \phi_3 + \phi_4),$$

$$\psi_e = \frac{1}{2}(-\phi_1 + \phi_2 + \phi_3 + \phi_4),$$

$$\psi_f = \frac{1}{2}(\phi_1 + \phi_2 - \phi_3 - \phi_4),$$

$$\psi_g = \frac{1}{2}(\phi_1 - \phi_2 + \phi_3 - \phi_4),$$

$$\psi_h = \frac{1}{2}(-\phi_1 + \phi_2 + \phi_3 - \phi_4),$$

The only MO's that are suitable are those which can be represented by an irreducible representation from those of the symmetry determined by the location of the nuclei, i.e., C_{2v} (58E). To determine which MO's are suitable and which are not, their behavior when certain transformations are made must be determined. The same results come out of the secular equation but it is easier to construct the MO's by inspection as indicated in this Appendix. Under transformations corresponding to the elements of the group, C_{2v}, the eigenfunction must remain unchanged except for its sign which may or may not change. Sufficient to characterize the behavior of the C_{2v} group are the transformations of rotation about the z-axis by 180°, C_2, and reflection in the plane of the ion, σ_{xz}. Since AO's ϕ_1, ϕ_2, ϕ_3, and ϕ_4 are cylindrically symmetric with respect to the line joining the nuclei, they are symmetric with respect to reflection in the plane of the ion, that is, they do not change sign on reflection in this plane. They do change under the operation C_2 however and ϕ_1 is transformed into ϕ_4, ϕ_2 is transformed into ϕ_3, ϕ_3 into ϕ_2 and ϕ_4 into ϕ_1. These and the other AO's are listed in Table 5 along with the function resulting from the operations C_2 and σ_{xz}. It is obvious from the table that only ϕ_9 is a suitable orbital and thus there is need for the linear combination of AO's.

From the behavior of the AO's the behavior of the MO's made from them can be deduced, for instance, ψ_a undergoing the operation C_2 gives $\frac{1}{2}(\phi_4 + \phi_3 + \phi_2 + \phi_1)$ or ψ_a. Applying this principle to all of the MO's written on the preceding page shows that only four are symmetry orbitals. These are shown in Table 5 along with the symbolic representation for their transformation properties. The other linear combinations, ψ_5 to

Table 5. Transformation Properties of AO's and MO's with Representations for MO's

Atomic Orbitals			Molecular Orbitals			
Orbital	Symmetry Operation		Orbital	Symmetry Operation		
ϕ_i	$C_2\phi_i$	$\sigma_{xz}\phi_i$	ψ_j	$C_2\psi_j$	$\sigma_{xz}\psi_j$	Representation*
ϕ_1	ϕ_4	ϕ_1	$\psi_a = \psi_1$	ψ_a	ψ_a	A_1
ϕ_2	ϕ_3	ϕ_2	ψ_b	ψ_e	ψ_b	none
ϕ_3	ϕ_2	ϕ_3	ψ_c	ψ_d	ψ_c	none
ϕ_4	ϕ_1	ϕ_4	ψ_d	ψ_c	ψ_d	none
ϕ_5	ϕ_6	ϕ_5	ψ_e	ψ_b	ψ_e	none
ϕ_6	ϕ_5	ϕ_6	$\psi_f = \psi_2$	$-\psi_f$	ψ_f	B_1
ϕ_7	ϕ_8	ϕ_7	$\psi_g = \psi_4$	$-\psi_g$	ψ_g	B_1
ϕ_8	ϕ_7	ϕ_8	$\psi_h = \psi_3$	ψ_h	ψ_h	A_1
ϕ_9	ϕ_9	ϕ_9	ψ_5	ψ_5	ψ_5	A_1
ϕ_{10}	$-\phi_{12}$	$-\phi_{10}$	ψ_6	$-\psi_6$	ψ_6	B_1
ϕ_{11}	$-\phi_{11}$	$-\phi_{11}$	ψ_7	ψ_7	ψ_7	A_1
ϕ_{12}	$-\phi_{10}$	$-\phi_{12}$	ψ_8	$-\psi_8$	ψ_8	B_1
			ψ_9	ψ_9	ψ_9	A_1
			ψ_{10}	$-\psi_{10}$	$-\psi_{10}$	B_2
			ψ_{11}	ψ_{11}	$-\psi_{11}$	A_2
			ψ_{12}	$-\psi_{12}$	$-\psi_{12}$	B_2

*The term symbols used to indicate transformation properties are defined by Herzberg (18H).

ψ_{12} can be constructed in a similar manner; they are as follows:

$$\psi_5 = \tfrac{1}{2}(\phi_5 + \phi_6 + \phi_7 + \phi_8),$$

$$\psi_6 = \tfrac{1}{2}(\phi_5 - \phi_6 + \phi_7 - \phi_8),$$

$$\psi_7 = \tfrac{1}{2}(\phi_5 - \phi_6 - \phi_7 + \phi_8),$$

$$\psi_8 = \tfrac{1}{2}(\phi_5 + \phi_6 - \phi_7 - \phi_8),$$

$$\psi_9 = \phi_9,$$

$$\psi_{10} = \tfrac{1}{2}(\phi_{10} + \sqrt{2}\,\phi_{11} + \phi_{12}),$$

$$\psi_{11} = \tfrac{1}{\sqrt{2}}(\phi_{10} - \phi_{12}), \text{ and}$$

$$\psi_{12} = \tfrac{1}{2}(\phi_{10} - \sqrt{2}\,\phi_{11} + \phi_{12}).$$

APPENDIX II

CALCULATION OF OVERLAP INTEGRALS

The evaluation of the overlap integrals $S_{AB} = \int \psi_A^* \psi_B \, d\tau$ used in this work is based on the overlap integral tables of Mulliken (20M). However since the atomic orbitals that are used herein are hybridized orbitals which are not embraced by Mulliken's tables, suitable linear combinations have been made. Consider the following general example: Proceed to calculate the overlap integral of the hybridized AO's, $\overline{A}$ on atom A and $\overline{B}$ on atom B at the usual angles as indicated in Fig. 24, where $\overline{A} = a_s s_A + a_z Z_A$, $\overline{B} = b_s s_B + b_z Z_B$, and s_A, s_B are

Figure 24. Vector Representation of Hybridized AO's.

s-orbitals on atoms A and B respectively, and Z_A, Z_B are p-orbitals directed along $\overline{A}$ and $\overline{B}$ respectively.

Define a new set of AO's, Y'_A, Z'_A, Y'_B and Z'_B, represented pictorially in Fig. 25, then $\overline{A} = a_s s_A + a'_z Z'_A + a'_y Y'_A$ and $\overline{B} = b_s s_B + b'_z Z'_B + b'_y Y'_B$.

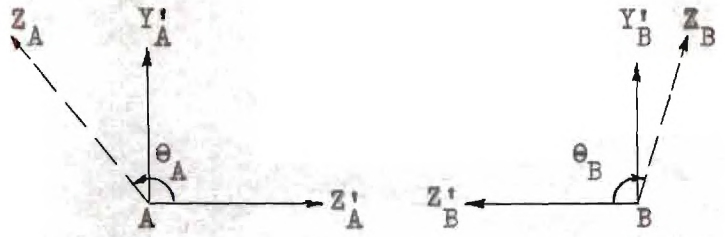

Figure 25. Vector Representation of Non-hybridized AO's.

Treating Z, Z', and Y' as vectors (57C), $Z_A = Z'_A \cos\theta_A + Y'_A \sin\theta_A$ and $Z_B = Z'_B \cos\theta_B + Y'_B \sin\theta_B$. This gives

$$\bar{A} = a_s s_A + a_z(\cos\theta_A Z'_A + \sin\theta_A Y'_A)$$

$$\bar{B} = b_s s_B + b_z(\cos\theta_B Z'_B + \sin\theta_B Y'_B) \quad \text{and}$$

$$S_{AB} = \int AB\,d\tau = a_s b_s \int s_A s_B\,d\tau + a_s b_z \cos\theta_B \int s_A Z'_B\,d\tau + a_z b_s \cos\theta_A \int s_B Z'_A\,d\tau +$$

$$a_z b_z(\sin\theta_A \sin\theta_B \int Y'_A Y'_B\,d\tau + \cos\theta_A \cos\theta_B \int Z'_A Z'_B\,d\tau).$$ The terms $\int s_A Y'_B\,d\tau = \int s_B Y'_A\,d\tau = 0$ and $\int Z'_A Y'_B\,d\tau = \int Y'_A Z'_B\,d\tau = 0$ because of orthogonality and have been dropped.

From this formula the overlap integrals used herein will be calculated. To illustrate with the system of the nitrite ion the following assumptions were made: (a) the hybridization is trigonal, i.e., $a = \frac{1}{\sqrt{3}}$, (b) the O-N-O angle is 120°, (c) the O-N distance is 1.23 A, and (d) the formal unit negative charge on the ion is distributed such that each oxygen atom is - 1/2 and the nitrogen atom is neutral. Using Mulliken's notation (20M), $\mu_N = 1.95$ and $\mu_O = 2.19$ (the average of μ_O and μ_{O^-}). From this values for $p_{AB} \equiv (\mu_A + \mu_B)R/2a_H$ and $t_{AB} \equiv (\mu_A - \mu_B)/(\mu_A + \mu_B)$ were calculated, where R is the inter-nuclei distance and a_H is the first

Bohr atomic radius for hydrogen.

For overlap between AO's on oxygen and nitrogen $p_{ON} = 4.80$, $t_{ON} = 0.058$ and $t_{NO} = -0.058$. From Mulliken's tables for $p = 4.80$ $S_{2s,2s}$ for $t = 0.0$, $S = 0.330$ and for $t = 0.1$, $S = 0.331$; interpolating for $t = 0.058$, $S = 0.331$. Similarly the other S's are found and the results recorded in Table 6 along with values found for oxygen-oxygen overlap for which $t = 0$ and $p = 8.8$.

Table 6. Overlap for Non-hybridized AO's in the Nitrite Ion (20M).

$S_{A,B} = \int \phi_A^* \phi_B d\tau$	oxygen-nitrogen	oxygen-oxygen
$S_{2s,2s}$	0.331	0.039
$S_{2s,2p_z}$	0.380	0.053
$S_{2p_z,2s}$	0.332	0.053
$S_{2p_z,2p_z}$	0.322	0.071
$S_{2p_x,2p_x}$	0.183	0.013

The following is an illustration of the calculation of the overlap of ϕ_1 with ϕ_2, i.e., $S_{1,2}$, where $\theta_A = \theta_B = 0$, $\sin \theta_a = \sin \theta_B = 0$, and $\cos \theta_A = \cos \theta_B = 1$. Assuming trigonal hybridization, i.e., $a_s = b_s = 1/\sqrt{3}$, and $a_z = b_z = \sqrt{2}/\sqrt{3}$, $S_{1,2}$ becomes

$$S_{1,2} = \frac{0.331}{3} + \frac{\sqrt{2}}{3}(1)(0.380) + \frac{\sqrt{2}}{3}(1)(0.332) + \frac{2}{3}(0)(0.183) + \frac{2}{3}(1)(0.322) = 0.110 + 0.335 + 0.215 = 0.660.$$

Likewise the others have been calculated and the results are tabulated in Table 7.

Table 7. Overlap for Hybridized AO's in the Nitrite Ion

$S_{i,j} = i,j = \int \phi_i^* \phi_j d\tau$	θ_A [a]	θ_B [a]	$S_{i,j}$
Oxygen-Nitrogen			
1,2; 4,3	0	0	0.660
1,3; 1,9; 4,2; 4,9	0	120 or 240	0.070
5,2; 7,2; 8,3; 6,3	120 or 240	0	0.104
5,3; 6,2	120	240	0.096
7,9; 8,9	240	120	0.096
5,9; 6,9	120	120	0.088
7,3; 8,2	240	240	0.088
10,11; 12,11	-	-	0.183
Oxygen-Oxygen			
1,4	30	30	0.094
7,8	270	270	0.021
5,6	150	150	-0.002
5,8; 6,7	150	270	-0.013
5,4; 1,6	60	150	-0.013
7,4; 1,8	60	270	0.027
10,12	-	-	0.013

[a] θ_A and θ_B are angles as indicated in Figs. 24 and 25.

APPENDIX III

VALENCE STATE PROMOTIONAL ENERGIES

The molecular orbital calculation carried out in Chapter II has as its primary consideration the interaction of the electrons and the nuclear framework and indeed the coulomb integral was assumed to be the same for electrons about the nucleus of the oxygen as for the electrons about the nitrogen. Of course this approximation is not good and the calculation in this Appendix is an attempt to refine this approximation.

The two transitions that are of interest in this respect are the $n_N \longrightarrow \pi^*$, resulting in excited state A, and the $n_O \longrightarrow \pi^*$, resulting in excited state B. In order to ascertain the energy of these transitions a circuitous route must be taken which is outlined below.

Beginning with the atoms in the ground state there are two hypothetical paths that can be followed to arrive at the two different excited states as follows:

For the transition $n_N \longrightarrow \pi^*$, the first path consists of three steps:

(a) the separated atoms in their ground state (X_a) going to the separated atoms in their valence state as found in the molecule in its ground state (X_v),

(b) the separated atoms in their valence state (X_v) combining to give the molecule in its ground state (X_m), and

(c) the transition $n_N \longrightarrow \pi^*$ which gives the excited state (A).

The second path consists of two steps:

(a) the separated atoms in their ground state (X_a) going to the separated atoms in the valence state found in the excited molecule (A_a) and

(b) the atoms in the excited valence state (A_a) combining to give the molecule in its excited state (A_m).

These two paths could be outlined symbolically as follows:

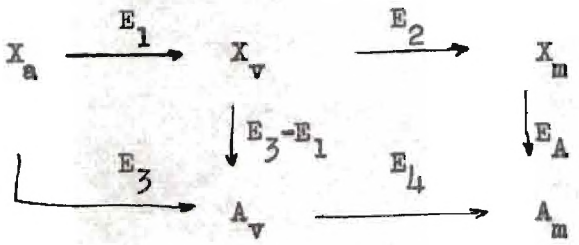

where the energies of the various transitions are designated as indicated by the symbols adjacent to the arrows.

A similar scheme for the transition $n_0 \rightarrow \pi^*$ is

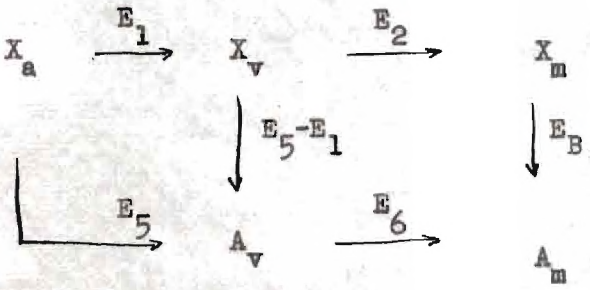

The difference in the energy E_B and E_A is the value that is desired, therefore, since

$$E_A = E_3 + E_4 - E_1 - E_2 \text{ and}$$
$$E_B = E_5 + E_6 - E_1 - E_2,$$
$$E_B - E_A = E_5 + E_6 - E_3 - E_4 .$$

But it will be assumed that E_4 and E_6 are equal and then

$$E_B - E_A = E_5 - E_3 .$$

Mulliken (59M) has listed some valence state energies, but the valence states that he gives do not include those for hybridized orbitals. Using a linear combination of the atomic orbitals to make hybrids the promotional energies can be calculated just as they were for the non-hybridized orbitals.

Writing the hybridized orbitals as in Chapter II, p. 6

$$\phi_{R1} = a_R s + \frac{1}{\sqrt{2}} p_x - \frac{\sqrt{1-2a_R^2}}{\sqrt{2}} p_z ,$$

$$\phi_{R2} = a_R s - \frac{1}{\sqrt{2}} p_x - \frac{\sqrt{1-2a_R^2}}{\sqrt{2}} p_z ,$$

$$\phi_{R3} = \sqrt{1-2a_R^2}\, s + \sqrt{2}\, a_R p_z , \text{ and}$$

$$\phi_{R4} = p_y ,$$

will permit a description of the valence state of an atom in terms of hybridized orbitals. The following configurations can be written[1]

I. $\phi_{R1}^1, \phi_{R2}^1, \phi_{R3}^2, \phi_{R4}^1$

II. $\phi_{R1}^1, \phi_{R2}^1, \phi_{R3}^1, \phi_{R4}^1$

III. $\phi_{R1}^2, \phi_{R2}^2, \phi_{R3}^2, \phi_{R4}^2$

IV. $\phi_{R1}^2, \phi_{R2}^1, \phi_{R3}^1, \phi_{R4}^1$

V. $\phi_{R1}^1, \phi_{R2}^1, \phi_{R3}^1, \phi_{R4}^2$

VI. $\phi_{R1}^2, \phi_{R2}^1, \phi_{R3}^1, \phi_{R4}^2$

---

[1]The calculation outlined here follows the calculation made in detail by Eberhardt (60E).

It should be noted here that configuration I corresponds closely to the valence state of the nitrogen atom in the ion in its ground state and in state B_m. Configuration III corresponds to oxygen in the ion in its ground state and in state A_m, V to nitrogen in state A_m and VI to oxygen in state B_m.

The energies of these configurations can be written as a sum of coulomb, exchange, and repulsion integrals; for example the energy for configuration I is

$$E_I = I_1 + I_2 + 2I_3 + I_4 + J(12) + 2J(13) + J(14) + 2J(23) + J(24) + 2J(34) + 2J(33) - 1/2K(12) - K(13) - 1/2K(14) - K(23) - 1/2K(24) - K(34).$$

The notation used here is the same as that used by Eyring, Walter, and Kimball (61E) except that hybridized orbitals are used here instead of the unhybridized atomic orbitals.

According to the reasoning above the energy needed is E_3, however it is easier to calculate $E_3 - E_1$, i.e., the energy of the transition $X_v \longrightarrow A_v$, than it is to calculate E_3 ($X_a \longrightarrow A_v$) and the results are just as useful. As a result of the foregoing argument it can be assumed that the transition $n_N \longrightarrow \pi^*$ involves energy equal to $E_V - E_I$ and the transition $n_O \longrightarrow \pi^*$ involves energy equal to $E_{VI} - E_{III}$. To evaluate the integrals, in terms of which the energy differences are expressed, it is necessary to expand the integrals in terms of non-hybridized atomic orbitals in real form. This necessitates conversion of the integrals J and K in exponential form to J's and K's in real form. The results obtained by Eberhardt (60E) for this conversion are presented in Table 8.

Table 8. Hybridized Integrals Expressed in Terms of Non-hybrid Integrals[a]

Hybridized Integrals	Value in Terms of Non-hybrid Integrals[b]
$J(11) = J(22)$	$= F_o^{c} + 2a^2(1-a^2)F_1 + (4 - 8a^2 + 4a^4)F_2$
$J(33)$	$= F_o + 4a^2(1-2a^2)F_1 + 16\,a^4\,F_2$
$J(44)$	$= F_o + 4F_2$
$J(12)$	$= F_o - 2a^4\,F_1 + (2 + 4a^2 + 4a^4)\,F_2$
$J(13) = J(23)$	$= F_o - 2a^2(1 - 2a^2)F_1 + 2a^2(1 - 4a^2)F_2$
$J(14) = J(24)$	$= F_o - 2\,(1 - a^2)\,F_2$
$J(34)$	$= F_o - 4a^2\,F_2$
$K(12)$	$= 2a^2(1 - a^2)\,F_1 + (3 - 6a^2 + 4a^4)\,F_2$
$K(13) = K(23)$	$= (1 - 3a^2 - 4a^4)\,F_1 + (7a^2 - 8a^4)\,F_2$
$K(14) = K(24)$	$= a^2\,F_1 + 3\,(1 - a^2)\,F_2$
$K(34)$	$= (1 - 2a^2)\,F_1 + 6a^2\,F_2$
$I_1 = I_2$	$= I_p - a^2(I_p - I_s)$
I_3	$= I_s + 2a^2(I_p - I_s)$
I_4	$= I_p$

[a] These results were obtained from Eberhardt (60E).

[b] The notation used is that of Eyring, Walter and Kimball (61E) with the exception of F_o = their F^o, $F_1 = 1/3\,F^1 = 1/3\,G^1$, $F_2 = 1/25\,F^2 = 1/25\,G^2$, $I_s = I(2,0;2,0)$, and $I_p = I(2,1;2,1)$.

[c] The assumption that there is only one value of F_o is made in these calculations, i.e., it is assumed that the repulsion between two electrons is the same for electrons in s and p orbitals as for electrons in two p orbitals.

From Table 8 and the energies expressed as a sum of integrals as was mentioned above it can be demonstrated that

$$E_A = (I_p - I_s)(1 - 2a^2) + F_1 (1 - 4a^2 + 4a^4) + F_2 (-3 + 8.5\, a^2 - 4a^4) \text{ and}$$

$$E_B = (I_p - I_s)\, a^2 + F_1(0.5a^2 + 2a^4) + F_2(-4.5a^2 - 4a^4).$$

For trigonal hybridization $a = 1/\sqrt{3}$ and

$$E_A = 1/3\ (I_p - I_s) + 0.1111F_1 + (-0.6111)F_2 \text{ and}$$

$$E_B = 1/3\ (I_p - I_s) + 0.2888F_1 - 4.6388\ F_2.$$

It should be noted at this point that E_A involves changes on the nitrogen atom only while E_B involves changes on the oxygen atom only and as a result the I's, F_1's and F_2's must be evaluated for nitrogen for use in E_A and for oxygen for use in E_B.

Using the values of these integrals as recorded in Table 9 the results recorded below can be obtained.

$$E_A = 1/3\ (12.6 \text{ e.v.}) + 0.1111\ (2.54 \text{ e.v.}) - 0.6111\ (0.25)$$
$$= 4.20 + 0.28 - 0.15 = 4.33 \text{ e.v.}$$

$$E_B = 1/3\ (16.8 \text{ e.v.}) + 0.2888\ (3.54 \text{ e.v.}) - 4.6388\ (0.36 \text{ e.v.})$$
$$= 5.60 + 1.02 - 1.67 = 4.95 \text{ e.v.}$$

$$E_B - E_A = 0.62 \text{ e.v.} \quad \text{or } 5000 \text{ cm}^{-1}.$$

Table 9. Estimated Values for the Integrals $I_p - I_s$, F_1, and F_2

Integral	Value for Nitrogen	Value for Oxygen
$I_p - I_s$	12.6 e.v.[a]	16.8 e.v.[b]
F_1	2.54 e.v.[c]	3.54 e.v.[d]
F_2	0.25 e.v.[e]	0.36 e.v.[f]

[a]This evaluation is made from the following states from Mulliken's Table III (59M):

N (s^2xyz,V_3), 1.33 e.v. and (sx^2yz,V_3), 13.86 e.v.
N (s^2x^2y,V_1), 3.06 e.v. and (sx^2y^2,V_1), 15.69 e.v.
The average value is 12.6 e.v.

[b]This value is made as above from the following states:

O (s^2xyz,V_3), 1.85 e.v. and (sx^2yz,V_3), 18.88 e.v.
O (s^2x^2y,V_1), 4.29 e.v. and (sx^2y^2,V_1), 21.57 e.v.
O^- (s^2x^2yz,V_2), 0.67 e.v. and (sx^2y^2z,V_2), 17.08 e.v.
The average value with equal weight for the O^- and O is 16.8 e.v.

[c]F_1 is evaluated from the relationship the $^2D\ (sp^4) - {}^4P\ (sp^4) = F_1 + 6F_2$ (see Mulliken's Table II (59M). Mulliken estimates $^2D\ (sp^4)$ for nitrogen to be 14.96 e.v. (13.86 + 1.10 e.v.) above the ground state (^4S) (Table III of reference 59M) and Bacher and Goudsmit (62B) give 10.92 e.v. (117345 - 29192 cm^{-1}) for the $^4P\ (sp^4)$. Thus $F_1 + 6F_2 = 4.04$ e.v. and if $F_2 = 0.25$ e.v. (see below), $F_1 = 2.54$ e.v.

[d]F_1, as above, is evaluated from $^2D\ (sp^4) - {}^4P\ (sp^4) = F_1 + 6F_2$. Bacher and Goudsmit give this energy to be 5.70 e.v. (163027 - 117025 cm^{-1}) (62B) and $F_1 = 3.54$ e.v. where $F_2 = 0.36$ e.v. (see below).

[e]Mulliken (Table III, reference 59M) estimates $G_2 = F_2 = \frac{8922\ cm^{-1}}{4.5}$ or 0.25 e.v. for nitrogen.

[f]Mulliken (Table III, reference 59M) estimates $G_2 = F_2 = \frac{13113\ cm^{-1}}{4.5}$ or 0.36 e.v.

APPENDIX IV

INCLINATION OF A CRYSTAL PLANE TO A FACE

A light ray that travels through an anisotropic crystalline substance such that the electric vector does not vibrate parallel to one of the crystal axes will have a refractive index different from that measured along the crystal axes. It will be intermediate between the refractive indices of the axes that lie in the same plane as the electric vector (or its components).

For example, suppose that a crystal of sodium nitrite contained the a axis in its face, but the perpendicular to this axis is neither the b nor c axis though it lies in a plane containing them. Designate the angle between the c axis and the face by θ as indicated in Fig. 26.

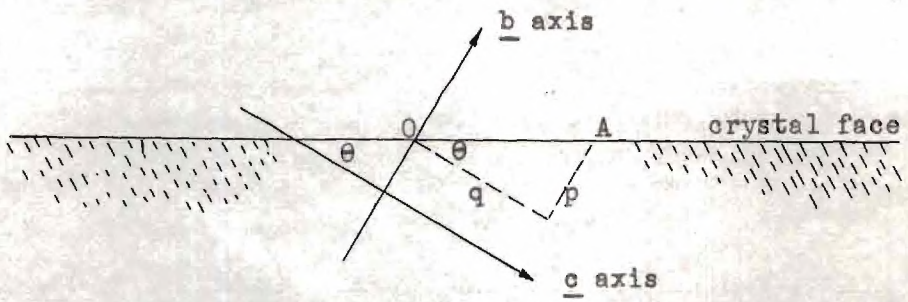

Figure 26. The Angle of the Crystal Axis to the Face of the Crystal.

The equation for the indicatrix in the plane of the b and c axes (63W) is

$$\frac{p^2}{n_\gamma^2} + \frac{q^2}{n_\beta^2} = 1$$

where p and q are as indicated in Fig. 26. Then it can be written that

$$p = AO \sin \theta = n' \sin \theta$$

$$q = AO \cos \theta = n' \cos \theta$$

where n' is the refractive index of the substance to radiation which has an electric vector vibrating parallel to OA. For sodium nitrite n_β = 1.41 and n_γ = 1.62 and n' is not greater than 1.422 in the case studied in this work. Therefore θ cannot be greater than its value in the equation

$$\frac{(1.422 \sin \theta)^2}{(1.62)^2} + \frac{(1.422 \cos \theta)^2}{(1.41)^2} = 1$$

$$0.7705 \sin^2\theta + 1.0171 \cos^2\theta = 1$$

$$\cos^2\theta = 0.93068$$

$$\cos \theta = 0.96472$$

$$\theta = 15.2^\circ$$

Similar calculations can be made for other possible orientations of the crystal.

The magnitude of the absorption of a ray vibrating parallel to the face and perpendicular to the a axis would be equal to

$$\epsilon(\nu) = \sin^2\theta \, \epsilon_b(\nu) + \cos^2\theta \, \epsilon_c(\nu)$$

where $\epsilon_b(\nu)$ and $\epsilon_c(\nu)$ are the absorption coefficients for electric vectors of frequency ν vibrating parallel to the b and c axes respectively.

APPENDIX V

WAVE-LENGTH MEASUREMENTS

Since there was a disagreement between the wave-length of the absorption of sodium nitrite measured in this laboratory and that reported by Rodloff (37R) it was essential that the method be thoroughly reliable. The technique developed is simple and straight forward. It overcomes the two main difficulties encountered here, namely, correct identification of the calibration lines and the shift of the film or plates as it is moved from the position for the absorption to that for the calibration spectrum.

To assure correct identification of the many lines of the iron spectrum the densitometer trace was fastened to a wall and the film placed in a projector and enlarged so there was a one-to-one correlation of the lines on the film and the lines of the trace. It is much easier to compare a photograph or projection of a spectrum to the ones recorded in wave-length tables than to try to pick out a certain line from a trace. To check this assignment, after two such lines were tentatively identified, the number of angstroms per inch was determined and the wave-length of a number of prominent lines measured. These measured wave-lengths were then compared with values recorded in the M. I. T. Tables (64H).

The scale used was inches because the paper on which the trace was made was marked off in inches. An architect's scale with 50 divisions per inch was used to measure to a fraction of an inch. The error involved here was not more than 0.02 inch.

To correct for any shift in the film in moving it for recording the next spectrum, the wave-length of one of the intense hydrogen emission lines was measured with the iron spectrum as a reference. Any difference found in this measured and reported wave-length is applied as a correction to the wave-length of the absorption spectrum.

The following table summarizes the results of one such measurement. The points given are chosen at random and are only a few of the ones checked.

The difference of - 0.60 A was used to correct the absorption measurements made from spectrum #17 of this film. Similar techniques were used on all other spectra.

Table 10. Measurement of Wave-Length of H_γ Emission

Scale Reading[a]	Wave-length (Measured)	Wave-length (Recorded)	Difference
1.87 inches		4299.241 A	
12.18		4375.932	
Iron Lines			
0.81	4291.356 A	4291.466 A	0.110 A
1.18	4294.108	4294.128	0.020
1.70	4297.976	4298.040	0.066
1.87	4299.241	4299.241	0
2.70	4305.415	4305.455	0.040
3.03	4307.870	4307.906	0.036
3.22	4309.283	4309.380	0.097
4.00	4315.085	4315.087	0.002
5.45	4325.871	4325.765	- 0.006
5.63	4327.210	4327.098	- 0.212
6.98	4337.252	4337.049	- 0.203
9.04	4352.575	4352.737	0.162
11.05	4367.526	4367.582	0.056
11.33	4369.609	4369.774	0.165
12.18	4375.932	4375.932	0
13.19	4383.445	4383.547	0.102
13.84	4388.280	4387.897	- 0.383
13.97	4389.247	4388.411	- 0.836
H_γ			
7.52	4341.27 A	4340.47 A	- 0.80 A
	4341.07 (by interpolation) (from error at 6.98 inches)		- 0.60

[a]These measurements were made from Trace #1 of film #44 (lowest speed of densitometer). Iron lines were from spectrum #11 and H_γ from spectrum #17. The first two lines recorded in the table were used as calibration lines to give 7.4385 A per inch of scale. 0.00 inches correspond to 4285.331 A.

APPENDIX VI

TABLES

Table 11. Absorption Maxima in the 3500 A Band of Crystalline Sodium Nitrite at Low Temperature

Wave-length	Frequency[b]	Designation (Rodloff)	Wave-length (Rodloff)
3851 A	25960 cm^{-1}	A_1	3818 A
(3842)[a]	26021	A_2	3810
3822	26157	A_3	3790
(3791)	26371	A_5	3760
3762	26574	B_1	3730
3757	26609	B_2	3725
3746	26688	-	-
3735	26766	B_3	3704
(3718)	26889	B_4	3687
3706	26976	B_5	3675
(3697)	27041	B_6	3666
(3881)	27159	C_1	3650
3672	27225	C_2	3640
3650	27390	C_3	3620
3623	27594	C_5	3595
(3610)	27693	C_6	3582
3592	27832	D_1	3563
3571	27995	D_3	3540
3543	28217	D_5	3517
3536	28272	D_6	3508
3515	28441	E_1	3483
(3500)	28563	E_3	3469
3493 (unresolved)			
(3488)	28662	E_4	3457
3466	28843	E_5	3437
3436	29095	F_1	3405
(3425)	29189	F_3	3395
3420 (unresolved)			
(3415)	29274	F_4	3385
3392	29473	F_5	3365
3368	29683	-	-
3352	29824	G_3	3327
3323	30085	G_5	3300
3300	30294	-	-
3281	30470	H_3	3262
3253	30732	H_5	3235
3215	31095	J_3	3200
3186	31378	J_5	3175
3149	31747	-	-
3115	32093	-	-

[a]Wave-lengths in ( ) were interpolated from Rodloff's measurements (37R).

[b]Frequency, cm^{-1}, was taken from Keyser's tables (65K), as were all frequencies of this work.

Table 12. Estimate of the Molecular Extinction Coefficient for a Single Crystal of Sodium Nitrite on a Beckman Model D.U. Spectrophotometer

Wave-length mμ	Slit Width mm	Optical Density D	Extinction Coef. ϵ
400	0.09	0.343	14.1
390	0.09	0.402	16.5
380		0.552	22.7
370		0.745	30.6
360		0.835	34.3
350		0.851	35.0
340		0.812	33.4
330	0.09	0.726	29.8
320	0.12	0.624	26.0
310		0.510	21.0
300		0.442	18.2
290		0.416	17.1
280		0.409	16.8
270	0.12	0.405	16.6
260	0.17	0.413	17.0
250		0.467	19.2
240		0.858	35.3
230		1.42	58.4
		1.77	72.7
220	0.17	1.70 **	70.
		1.78	73
210	0.75	1.82	75
		2.02	83
200	2.00	1.50	62
		1.69	70
202	2.00	1.83	75
203	2.00	1.70	70
		1.85	76
204	1.30	1.76	72
		1.84	76
205	1.00	1.75	72
		1.88	77
206		1.75	72
		1.94	80
207		2.0	82
		1.98	81
208	0.75	1.72	71
		1.95	80
209		1.82	75
		2.00	82
210		1.54	63
		2.00	82

Table 12. (Concluded).

Wave-length mμ	Slit Width mm	Optical Density D	Extinction Coef. ε *
340	0.1	0.800	32.9
342		0.802	33.0
344		0.824	33.8
346		0.820	33.7
348		0.838	34.4
350		0.844	34.6
352		0.835	34.3
354		0.844	34.5
356		0.844	34.6
358		0.844	34.6
360		0.851	35.0
365		0.818	33.6
370		0.760	31.2

*The average thickness of the crystal was estimated to be eight microns by the interference method. With a density of 2.168 g/cc this gives a concentration of 31.4 moles/liter and a path length of 8×10^{-4} cm. $\epsilon = D/c \times l$

**The difference in optical density is believed to be due primarily to the fact that the crystal could not be positioned in exactly the same place for successive measurements. Measurements below 230 mμ have little significance.

Table 13. Absorption Spectrum of Nitromethane

Wave-length mμ	Optical Density, D Solution I	I*	II	II*	Extinction Coefficient, ε I (ave.)	II (ave.)
400	0.002	0.000	0.002	0.000	0.07	0.07
390	0.002	0.003	0.001	0.002	0.07	0.03
380	0.000	0.009	0.000	0.015	0.02	0.05
370	0.005	0.038	0.006	0.048	0.15	0.18
365		0.064		0.079	0.22	0.27
360	0.009	0.098	0.013	0.119	0.28	0.42
358		0.116		0.142	0.39	0.48
356		0.136		0.165	0.46	0.56
355		0.145		0.175	0.49	0.59
354		0.160		0.188	0.54	0.64
352		0.186		0.216	0.63	0.73
350	0.020	0.208	0.027	0.246	0.69	0.87
340	0.036	0.377	0.043	0.412	1.25	1.42
330	0.059	0.590	0.067	0.643	1.99	2.21
320	0.085	0.843	0.094	0.914	2.86	3.13
310	0.112	1.128	0.130	1.25	3.80	4.32
300	0.151		0.198		5.11	6.70
290	0.240		0.313		8.12	10.60
280	0.355		0.419		12.0	14.2
278	0.368		0.451		12.4	15.2
276	0.382		0.456		12.9	15.4
275	0.385		0.457		13.0	15.8
272	0.401		0.455		13.5	15.4
270	0.405		0.455		13.7	15.3
268	0.399		0.450		13.5	15.2
265	0.385		0.416		13.0	14.1
260	0.362		0.379		12.2	12.8
250	0.266		0.262		9.0	8.8
240	0.539		0.585		18.2	19.8
230	>2		>2		>70	>70

Solution I was 0.0296 mole/l. of nitromethane in 5 M H_2SO_4 in 40% ethyl alcohol-60% water.
Solution I* was 0.296 mole/l. of nitromethane in 5 M H_2SO_4 in 40% ethyl alcohol-60% water.
Solution II was 0.0296 mole/l. of nitromethane in 95% ethyl alcohol.
Solution II* was 0.296 mole/l. of nitromethane in 95% ethyl alcohol.

Table 14. Spectrum of Potassium Nitrate in Aqueous Solution*

Wave-length mμ	Optical Density D	Abs. Coef. ϵ	$\text{Log}_{10}\epsilon$	Conc. Moles/l	Slit Width mm
201	0.438	21900	4.3404	0.00002	1.95
205	0.423	21100	4.3243		1.17
208	0.391	19600	4.2923		0.82
210	0.356	17800	4.2504		0.75
215	0.266	13300	4.1239		0.50
220	0.168	8400	3.9243	0.00002	0.50
220	0.772	3860	3.5866	0.0002	0.344
225	0.399	2000	3.3010		0.278
230	0.184	920	2.9638		0.240
235	0.085	430	2.6335	0.0002	0.207
235	0.745	372	2.5705	0.002	0.210
236	0.510	255	2.4065		0.200
238	0.336	168	2.2253		0.200
240	0.232	116	2.0645		
242	0.156	78	1.8921		
244	0.097	48.5	1.6857		0.200
246	0.075	37.5	1.5740		0.150
247	0.053	26.5	1.4232		0.150
248	0.040	20.0	1.3010	0.002	0.145
250	0.868	8.68	0.9385	0.100	0.165
252	0.561	5.61	0.7490		0.149
254	0.381	3.81	0.5809		0.142
256	0.261	2.61	0.4166		0.138
258	0.194	1.94	0.2878		0.133
260	0.154	1.54	0.1875		0.130
262	0.145	1.45	0.1614		0.125
264	0.148	1.48	0.1703		0.122
266	0.158	1.58	0.1987		0.121
270	0.196	1.96	0.2923		0.096
275	0.274	2.74	0.4378		0.108
280	0.350	3.50	0.5441		0.085
285	0.453	4.53	0.6561		0.096
290	0.580	5.80	0.7634	0.100	0.078
295	0.659	6.59	0.8189		0.086
300	0.700	7.00	0.8451		0.070
301	0.727	7.27	0.8615		0.084
302	0.729	7.29	0.8627		0.083
303	0.717	7.17	0.8555		0.081
305	0.705	7.05	0.8482		0.080
310	0.620	6.20	0.7924		0.074
315	0.499	4.99	0.6981	0.100	0.073

Table 14. (Concluded)

Wave-length mμ	Optical Density D	Abs. Coef. ϵ	$\log_{10}\epsilon$	Conc. Moles/l	Slit Width mm
320	0.327	3.27	0.5145	0.100	0.068
325	0.201	2.01	0.3032	0.100	0.070
325	0.885	1.77	0.2480	0.500	0.072
330	0.450	0.900	$\bar{1}$.9542		0.070
335	0.206	0.412	$\bar{1}$.6149	0	0.070
340	0.092	0.184	$\bar{1}$.2648		0.070
350	0.022	0.044	$\bar{2}$.6435	0.500	0.070

*Measurements made in this laboratory by Wu-chieh Cheng (42c).

Table 15. Absorption Maxima for Ethyl Nitrite Gas

Wave-length A	Frequency cm^{-1}	Scale on Trace Inches*	Frequency Reported by Purkis and Thompson (45P)
			33680
			32788
3218	31066	6.3	31104
3319	30120	8.6	30148
3343	29120	11.3	29154
3558	28098	14.2	28169
3691	27085	17.3	27100
3844	26007	20.85	25582

*These measurements were made from Trace #2 of Film #57. Curve #1 is photometered from spectrum #13 of that film--10 sec. exposure, 100u slit, 120 mm. Hg pressure, 11.5 cm path length. Curve #2 is from spectrum #25--1 min. exposure, 100u slit, 45 mm. Hg pressure, 11.5 cm path length. Curve #3 is from spectrum #31--1 min. exposure, 100u slit, 10 mm. Hg pressure, 11.5 cm path length. Curve #4 is from spectrum #9--iron arc with 30u slit.

Calibration data: 3100.4 (doublet) = 3.59 inches
3647.8 = 16.30 inches, 1 inch = 43.034 A
3475.5 = 12.32 inches (calc. 3475.6 A)

Table 16. Absorption Measurements on Ethyl Nitrite Solutions

Wave-length mμ	Optical Density, D, of Solutions IA	IIA	IIIA	IVA	VA	VIA	VIIA
400	1.30	0.306	1.82		0.110		
395	2.35	0.657	0.474		0.287		
390	2.50	0.843	0.65		0.36		
388			0.672				
386			0.692				
385			0.700		0.395		
382			0.742				
380	2.61	1.07	0.876		0.461		
378			1.04				
375			1.33		0.741		
374			1.42		0.791	0.642	0.629
373			1.47		0.842	0.687	0.662
372			1.52		0.890	0.721	0.682
371			1.56		0.912	0.742	0.691
370	2.65	1.85	1.53		0.912	0.738	0.681
369			1.48		0.878	0.704	0.651
368			1.40				
367			1.32		0.738		
366			1.25				
365			1.23		0.677		
364			1.25				
363			1.32		0.727		
362			1.41				
361			1.50		0.812		
360		1.83	1.64	1.90	0.920	0.748	0.748
359			1.72		1.00	0.830	0.807
358			1.80		1.12	0.910	0.851
357			1.79		1.16	0.941	0.848
356			1.72		1.11	0.900	0.797
355			1.63		1.02	0.814	0.729
354			1.47				
352			1.22		0.695		
350		1.45	1.19		0.645		
349			1.25				
348			1.35		0.728		
347			1.49		0.813		
346			1.62		0.964		
345			1.63		1.05		
344			1.58		1.02		
342			1.23		0.763		
340		1.22	0.958		0.537		
338							

Table 16. (continued)

Wave-length mμ	Optical Density, D, of Solutions IA	IIA	IIIA	IVA	VA	VIA	VIIA
336			1.02		0.550		
335			1.13				
334			1.18		0.738		
333			1.13		0.732		
332			1.01		0.643		
330						0.310	
328					0.336	0.251	
326					0.352	0.272	
325			0.699				
324					0.441	0.304	
323					0.448		
322					0.402	0.225	
320					0.295	0.194	
318					0.254	0.174	
316					0.271	0.186	
315			0.479				
314					0.294	0.184	
312					0.258	0.167	
310					0.238	0.161	
308					0.247		
306					0.265	0.183	
305					0.307		
304					0.282		
300					0.345		0.246
295					0.550		
285					1.10		
280							

Table 16. (continued)

Wave-length mμ	Optical Density of Solutions IB	IIB	IIIB	IVB	VB	VIB	VIIB	VIIIB
410	0.05	0.033						
400	0.100	0.086	0.077					
395	0.576	0.225	0.202					
390	0.788	0.484	0.431	0.305				
388								
386								
385	0.861	0.640	0.556					
382	1.03							
380	1.02	0.695	0.597	0.529	0.890	0.635	0.378	0.148
378	1.23	0.794						
376	1.44	0.930			1.23	0.840		
374	1.61	1.11	0.972		1.42	1.02		
372	1.72	1.24	1.09	0.950	1.50	1.11	0.634	0.228
371	1.71	1.25			1.51	1.12	0.651	0.285
370	1.72	1.29	1.12	0.982	1.50	1.12	0.642	0.282
369		1.26			1.44	1.11	0.622	0.272
368	1.60	1.24	1.07	0.933	1.37	1.68		
366	1.47	1.18						
365			0.972	0.849	1.24	1.00		
364	1.48	1.14			1.777	1.17		
362	1.62	1.19						
361								
360	1.81	1.32	1.13				0.703	0.284
359		1.34			1.75	1.22		
358	2.00	1.43	1.22	1.68	1.78	1.27	0.788	0.305
357	2.00	1.41			1.78	1.25	0.782	0.305
356	1.91	1.42	1.20		1.72	1.21	0.742	0.294
355		1.33						
354	1.68	1.32	1.16		1.48	1.11		
352	1.58	1.10						
350	1.49	1.08	0.937	0.822	1.23	0.958	0.512	0.226
349								
348								
347		1.10						
346					1.63	1.05	0.641	0.244
345	1.81	1.12	1.03	0.898	1.63	1.05	0.696	0.242
344					1.57	1.02	0.649	0.232
342								
340		0.862						
338	1.09	0.830	0.721	0.621	0.957	0.732	0.392	0.168

Table 16. (continued)

Wave-length mμ	Optical Density of Solutions IB	IIB	IIIB	IVB	VB	VIB	VIIB	VIIIB
336		0.818						
335		0.825						
334	1.38	0.831	0.725	0.622	1.21	0.732	0.500	0.163
333		0.808						
332								
330		0.669			0.800	0.593	0.332	0.128
328	0.781	0.583	0.507	0.443	0.690	0.517		
326		0.542						
325			0.465	0.410				
324		0.538			0.797	0.476		
323	0.865		0.450	0.393	0.765	0.462		
322		0.490						
320		0.436						
318	0.593	0.388	0.343	0.308	0.528	0.357		
316		0.370			0.558	0.342		
315								
314	0.610	0.356	0.313	0.281	0.559	0.325		
312		0.340			0.512	0.311		
310		0.327	0.288	0.258				
308								
306								
305		0.332	0.297	0.262	0.560	0.312		
304								
300		0.390	0.344	0.306	0.683	0.361	0.288	0.072
290		0.693			1.23	0.638	0.513	0.112
280					2	1.23	1.03	0.218
270							1.80	0.438
260							2.0	0.841
250								1.46
240								
230								
220								
210								
200								

Table 16. (continued)

Wave-length mμ	Molecular Extinction Coefficients VIA	VA	VB	IIIA	VIIA	VIIB	IB
410							1.4
405							2.8
400		6.2		5.6			7.2
395		16.1		14.6			16.0
390		20.3		19.9			21.8
388				20.8			
386				21.4			
385		22.1		21.6			24.0
382				22.9			
380		25.8	27.8	27.0		26.6	28.4
378				32.0			34.0
376			38.4				39.9
375		41.6		40.8			
374	44.3	44.3	44.3	43.7	41.1		44.7
373	47.6	47.1		45.3	43.2		
372	49.8	49.7	46.8	46.9	44.5	42.8	47.7
371	51.2	51.0	47.1	48.1	45.1	45.8	47.5
370	51.0	51.0	46.8	47.1	44.5	45.1	47.7
369	48.7	49.1	44.9	45.5	42.6	43.7	
368			42.7	43.0			44.3
367		41.3		40.6			
366				38.6			40.7
365		37.8	38.6	37.9			
364			51.5	38.6			41.0
363		40.8		40.6			
362				43.5			45.0
361		45.5		46.1			
360	51.8	51.6		50.3	48.7	49.6	51.1
359	57.6	56.0	54.6	53.0	52.9		
358	62.9	62.7	55.5	55.5	55.5	55.5	55.5
357	65.1	65.0	55.5	55.5	55.5	55.2	
356	62.2	62.1	53.7	53.0	51.9	52.3	53.1
355	56.1	57.1		50.2	47.5		
354			46.2	45.3			46.7
352		39.0		37.5			43.8
351		36.4					41.3
350		36.1	38.4	36.5		36.0	
349				38.6			
348		40.8		41.6			
347		45.5		45.8			
346		54.0	50.9	49.7		48.7	
345		58.8	50.9	50.5		49.0	50.2

Table 16. (continued)

Wave-length mμ	Molecular Extinction Coefficients VIA	VA	VB	IIIA	VIIA	VIIB	IB
344		57.1	49.0	48.7		45.7	
342		42.7		37.9			
340		30.2		29.6			
338			29.9			27.6	30.2
336		30.8		31.4			
335				34.9			
334		41.3	37.7	36.3		35.2	38.4
333		41.0		34.9			
332		36.0		31.0			
330	20.5		24.9			23.3	
328	17.4	18.9	21.5				21.7
326	18.9	19.7					
325				21.5			
324	21.0	24.7	24.9				
323			23.9				23.9
322	15.6	23.8					
320	13.4	16.5					
318	12.1	14.3	16.5				16.4
316	12.8	15.2	17.4				
315				14.8			
314	12.7	16.5	17.5				17.0
312	11.5	14.5	16.0				
310	11.2	13.4					
308		13.8					
306	12.6	14.9					
305		17.2	17.5				
304		15.8					
300		19.3	21.3		17.0	20.3	
295		30.8				36.2	
285		59.7	38.4		53.0		
Apparent Conc.	.0145	0.0179	0.032	0.033	0.0145	0.0137	0.0367
Estimated Conc.	.0265	0.0331	0.032	0.0662	0.0265	0.013	0.032

Table 16. (continued)

Wave-length mμ	Molecular Extinction Coefficients VIB	IIB	VIIIB	IIIB	IVB
405		0.9			
400		2.4		2.3	
395		6.2		6.07	
390		13.3		13.0	
385		17.7		16.7	
380	19.7	19.6	19.3	17.9	16.0
378		21.9			
376	26.3	25.7			
374	31.9	30.8		29.2	
372	34.8	34.6	36.5	32.8	28.6
371	35.0	34.5	37.2		
370	35.0	36.2	36.6	33.6	29.6
369	34.8	34.8	35.3		
368	33.8	34.5		32.2	28.1
366		32.6			
365	31.3			29.2	25.6
364	36.6	31.5			
362		32.9			
360		36.8	36.8	33.9	
359	38.2	37.1			
358	39.7	40.3	39.7	36.6	32.5
357	39.1	39.1	39.1		
356	37.8	38.4	38.2	36.1	
355		36.8			
354	34.7	36.6		33.2	
350	30.0	30.9	29.4	28.2	24.8
347		30.4			
346	32.8		31.8		
345	32.8	32.6	31.4	31.0	
344	31.9		30.2		
340		23.9			
338	22.9	23.0	21.8	21.7	18.7
337		22.6			
336		22.6			
335		22.8			
334	22.9	23.0	21.1	21.8	18.7
333	22.4				
330	18.5	18.5	16.7		
328	16.2	16.1		15.3	13.3
326		14.9			
325				14.0	12.4
324	14.9	14.8			
323	14.4			13.5	11.9

Table 16. (concluded)

Wave-length mμ	Molecular Extinction Coefficients VIB	IIB	VIIIB	IIIB	IVB
322		13.5			
320		12.1			
318	11.2	10.7		10.3	9.2
316	10.7	10.3			
314	10.2	9.9		9.4	8.5
312	9.7	9.4			
310		9.0		8.6	7.8
305	9.8	9.2		8.9	7.9
300	11.3	10.8	9.3	10.4	9.2
290	19.9	19.2	14.6		
280	38.4		28.4		
Apparent conc.	0.032	0.036	0.0077	0.033	0.033
Estimated conc.	0.032	0.032	0.013	0.029	0.029

Table 17. Absorption Maxima for Amyl Nitrite at Low Temperature

Wave-length A	Frequency cm^{-1}	Scale on Scale Inches*	Frequency Reported by Purkis and Thompson (45P)
3147.3	31764	7.60	32072
3235.1	30802	9.65	31133
3340.0	29932	12.10	30139
3446.1	29010	14.58	29180
3541.0	28231	16.8	28169
3652.5	27371	19.4	27130
3828.0	26116	23.5	26062

*These measurements were made from Trace #1 of Film #56. Curve #1 is photometered from spectrum #10 of that film--1 hr. exposure, 300μ slit, 50μ path length, at 70° absolute. Curve #2 is from spectrum #15--10 min. exposure - same as above. Curve #3 is from spectrum #28--iron arc with 30μ slit.

Calibration data: 3057.446 A = 5.50 inches on Trace.
3930.299 A = 25.89 inches on Trace, 1 inch = 42.8079 A
3225.8 A = 9.43 (calc. 3225.7)
3687.5 A = 20.21 (calc. 3687.2)

Table 18. Absorption Spectrum of Basic and Acidic Aqueous Sodium Nitrite

Wave-length mμ	Frequency cm^{-1}	Basic Solution D	Basic Solution ε	Acidic Solution D	Acidic Solution ε	Slit Width
400	24993	0.042	0.84	0.056	1.12	0.075mm
395	25309	0.099	1.98	0.257	5.14	
390	25634	0.199	3.98	0.940	18.80	
386	25900			1.29	25.86	
385	25967	0.344	6.88	1.28	25.60	
380	26308	0.511	10.22	1.08	21.60	
375	26659	0.760	15.20	1.60	32.00	
371	26947			1.97	39.36	
370	27019	0.930	18.60	1.95	39.00	
365	27389	1.09	21.80	1.60	32.00	
360	27770	1.20	24.00	1.90	38.00	
358	28005			2.05	41.00	
355	28161	1.24	24.80	1.90	38.00	
350	28563	1.22	24.40	1.58	31.60	
348	28728			1.64	32.80	
345	28977	1.14	22.80	1.58	31.60	
340	29403	1.03	20.60	1.15	23.00	
338	29579			0.97	19.40	
337	29666			1.05	20.90	
335	29842	0.902	18.04	1.03	20.06	
330	30294	0.782	15.64	0.748	14.98	
325	30760	0.680	13.60	0.594	11.88	
320	31241	0.608	12.16	0.424	8.48	
315	31737	0.549	10.98	0.315	6.30	
310	32249	0.514	10.28	0.227	4.54	0.10mm
305	32777	0.491	9.82	0.170	3.40	
300	33324	0.481	9.62	0.126	2.52	
295	33888	0.472	9.44	0.101	2.02	
290	34473	0.468	9.36	0.092	1.84	
285	35077	0.458	9.16	0.094	1.88	
280	35704	0.439	8.78	0.124	2.48	
275	36353	0.415	8.30	0.182	3.64	

Table 18. (concluded)

Wave-length mμ	Frequency cm^{-1}	Basic Solution D	Basic Solution ε	Acidic Solution D	Acidic Solution ε	Slit Width
270	37026	0.385	7.70	0.308	6.16	0.10 mm
265	37725	0.354	7.08	0.507	10.14	
260	38450	0.368	7.36	0.821	16.42	
255	39204	0.570	11.40	1.32	26.40	
250	39988	1.60	32.00	1.95	39.00	
245	40804		119.8*			
240	41654		408			
235	42540		904			
230	43465		2167			
225	44431		3800			
220	45440		5080			
215	46497		6440			
210	47604		7160			
205	48765		7480			
200	49735		7460			

*Measurements made in this laboratory by Wu-chieh Cheng (42C).

Table 19. Absorption Maxima of Nitrous Acid after Tarte (46T).

Designation (Tarte's)	Wave-length A	Frequency cm^{-1}
A	3840	26034
B	3680	27166
C	3541	28232
D	3417	29257
E	3306	30239
F	3206	31182
G	3144	32103
H	3030 (?)	32994

Table 20. Absorption Maxima of Nitrosyl Chloride after Goodeve and Katz (48G)

Designation (Goodeve's)	Wave-length A	Frequency cm^{-1}	Molecular Extinction Coefficients
A	1970	50800	2550
B	3350	29900	32.5
C	4400	22720	5.0
D	4750	21050	5.3
E	5385	18570	0.73 (?)
F	5495	18200	0.65
G	5612	17820	0.37
H	5879	17010	0.53
J	6017	16620	0.94
K	6158	16240	0.69
L	6431	15550	0.17 (?)

Table 21. Principal Maxima and Minima of Ozone at 18°C after Vigreux (51V)

Wave-length A	Frequency cm^{-1}	Ext. Coef.	Wave-length A	Frequency cm^{-1}	Ext. Coef. $x10^2$
3130	31940	16.8	4205	23775	0.964
3135	31889	17.9	4260	23468	1.86
3151	31727	12.7	4285	23331	1.72
3154	31697	14.1	4299	23255	1.63
3167	31567	10.1	4348	22993	2.46
3176	31477	10.2	4362	22919	2.13
3190	31339	6.9	4393	22757	3.00
3200	31241	8.7	4431	22562	4.15
3216	31086	4.8	4472	22355	3.56
3220	31047	6.7	4516	22137	5.22
3239	30865	3.14	4551	21967	5.06
3248	30779	5.02	4620	21639	11.0
3269	30582	2.06	4667	21421	8.84
3279	30488	3.65	4710	21226	11.6
3299	30304	1.26	4731	21131	10.9
3312	30185	2.42	4831	20694	23.3
3328	30039	0.78	4874	20511	20.9
3338	29949	1.73	5060	19757	45.0
3357	29780	0.45	5118	19533	40.3
3372	29648	1.04	5340	18721	72.8
3391	29481	0.314	5365	18634	71.5
3401	29395	0.627	5754	17374	125
3426	29130	0.166	5872	17025	113
3439	29070	0.340	6019	16609	133
3466	28843	0.105	6220	16073	99
3472	28794	0.136	6335	15781	85.2
3489	28653	0.061	6418	15577	74.2
3493	28621	0.095	6500	15380	64.0
3506	28514	0.053	6634	15070	51.7
3514	28449	0.101	6777	14752	37.6
3561	28074	0.015	6876	14539	30.9
3567	28027	0.030	7036	14209	22.4
3588	27863	0.012	7207	13872	17.0
3594	27816	0.018			

APPENDIX VII

THERMODYNAMIC CALCULATION OF CHARGE TRANSFER ENERGY

The transfer of an electron from a nitrite ion to a sodium ion in crystalline sodium nitrite or to a solvent molecule could be responsible for absorption of radiation. The process might be described by an equation (26F, 56R)

$$(Na^+ + NO_2^-)_{(solid)} \longrightarrow Na^*_{(gas)} + NO_2^*_{(gas)} \qquad (1)$$

where Na^* and NO_2^* indicate molecules in an excited state. The energy process

$$(Na^+ + NO_2^-)_{(solid)} \longrightarrow Na_{(gas)} + NO_{2\,(gas)} \qquad (2)$$

may be calculated from known thermodynamic values. Similar equations may be written for the process in solution

$$NO_2^-{}_{(aqueous)} + H_2O_{(liquid)} \longrightarrow NO_2^*{}_{(gas)} + e^{-*} \qquad (3)\ (26F)$$

where NO_2^* and e^{-*} represent the radical in its excited state unsolvated and e^{-*} the electron. The energy for the process

$$NO_2^-{}_{(aqueous)} + H_2O_{(liquid)} \longrightarrow NO_{2(gas)} + H_{(gas)} + OH^-_{(aqueous)} \qquad (4)$$

may be determined from heats of formation. The energy of the processes

$$Na^*_{(gas)} + NO_2^*{}_{(gas)} \longrightarrow Na_{(gas)} + NO_{2\,(gas)} \quad \text{and}$$

$$NO_2^{*}(gas) + e^{-*} + H_2O(liquid) \longrightarrow NO_2(gas) + H(gas) + OH^{-}(aqueous)$$

is not known. Excited states of Na and NO_2 suggest that it might be in the neighborhood of 10,000 to 15,000 cm^{-1} above the energies for the thermodynamic process. The following table lists a number of nitrites and nitrates and the calculated energies for processes like (2) and (4). These may be considered as a lower limit for the energy of the charge transfer. Higher energies would mean that the wave-length for the charge transfer absorption would be found from 300 to 800 A below that indicated in Table 22.

Table 22. Calculated Thermodynamic Energies for Electron Transfer[a].

Substance	A
NO_2^- (aqueous)	2880 A
$Ca(NO_2)_2$	2380
$Sr(NO_2)_2$	2930
$Ba(NO_2)_2$	2460
$LiNO_2$	2018
$NaNO_2$	2380
KNO_2	2420
NO_3^- (aqueous)	2770
$Mg(NO_3)_2$	2280
$Ca(NO_3)_2$	1930
$Sr(NO_3)_2$	1980
$Ba(NO_3)_2$	1870
$Ra(NO_3)_2$	1940
$LiNO_3$	1725
$NaNO_3$	1970
KNO_3	1873
$RbNO_3$	1890
$CsNO_3$	1905

[a]Process (2) is $(M^+ + NO_2^-) \longrightarrow M_{gas} + NO_2(gas)$ and process (4) is NO_2^- (aqueous) + H_2O(liquid) $\longrightarrow NO_2(gas) + H(gas) + OH^-$(aqueous).

Column A gives the value for the energy in terms of the wave-length of the radiation needed to excite it, calculated from data listed in Table 23 for process (2) or (4).

Table 23. Heat of Formation at 25°C From National Bureau of Standards Table (66R)

Substance	H_f^o	Substance	H_f^o
$H_{(gas)}$	52.089 kcal/mole	$Ca(NO_2)_2$	-178.3 kcal/mole
$OH_{(aqueous)}$	-54.957	$Sr(NO_2)_2$	-179.3
$H_2O_{(liquid)}$	-68.3174	$Ba(NO_2)_2$	-174.0
$NO_{2(gas)}$	8.091	$LiNO_2$	- 96.6
$NO_{3(gas)}$	13	$NaNO_2$	- 85.9
$NO_{2(aqueous)}^-$	-25.4	KNO_2	- 88.5
$NO_{3(aqueous)}^-$	-49.372	$Mg(NO_3)_2$	-188.72
$Mg_{(gas)}$	35.9	$Ca(NO_3)_2$	-224.0
$Ca_{(gas)}$	46.04	$Sr(NO_3)_2$	-233.25
$Sr_{(gas)}$	39.2	$Ba(NO_3)_2$	-237.06
$Ba_{(gas)}$	41.96	$Ra(NO_3)_2$	-237.
$Ra_{(gas)}$	31	$LiNO_3$	-115.279
$Li_{(gas)}$	37.07	$NaNO_3$	-101.54
$Na_{(gas)}$	25.98	KNO_3	-117.76
$K_{(gas)}$	21.51	$RbNO_3$	-117.04
$Rb_{(gas)}$	20.51	$CsNO_3$	-118.11
$Cs_{(gas)}$	18.83		

APPENDIX VIII

CORRELATION OF REFRACTIVE INDEX AND POLARIZATION

The difference in the refractive indices of crystalline sodium nitrite is caused by the electronic transitions which absorb radiation polarized along different axes. It is true in general that the refractive index of a substance increases as the frequency of the radiation approaches an absorption band. Using the Heisenberg-Kramer formula Mulliken (67M) derives the relationship

$$n-1 = (e^2N/2\pi mc^2) \sum_j f_{ij}/(\nu^2_{ij} - \nu^2),$$

where n is the refractive index, N is the number of molecules per cubic centimeter, f_{ij} is the mean oscillator strength for the transition $i \rightarrow j$, ν is the frequency of the radiation for which n is measured and ν_{ij} is the frequency of the radiation inducing the transition. If it is assumed that the refractive index along the a axis (n_α) is due primarily to the absorption band at 3500 A (it is polarized along the a axis) and the refractive index along the b axis (n_γ) is due primarily to the band at 2050 A (it is polarized along the b axis), then it is possible to predict the relative intensity of these two bands.

$$\frac{f_{3500}}{f_{2050}} = \frac{(n_\alpha - 1)\,(2\pi mc^2/e^2N)\,(\nu^2_{3500} - \nu^2)}{(n_\gamma - 1)\,(2\pi mc^2/e^2N)\,(\nu^2_{2050} - \nu^2)}$$

where $n_\alpha = 1.35$

$n_\gamma = 1.62$

$\nu_{3500} \sim 30{,}000\ cm^{-1}$

$$\nu_{2050} \sim 50{,}000 \text{ cm}^{-1}$$
$$\nu \sim 20{,}000 \text{ cm}^{-1}$$

$$\frac{f_{3500}}{f_{2050}} \sim \frac{1}{7.5}$$

This is approximately the ratio of the estimated intensities for the crystal (Chapter IV, p. 40), but for the solution the ratio is nearer to 1/300 (the ratio of $\int \epsilon \delta\nu$ for each band was estimated by plotting the absorption curves and weighing the paper between the abscissa and the curves). This result gives added support to the assignment by Friedman (26F) that this band in solution is due (at least in part) to an electron transfer process.

APPENDIX IX

A REPRINT OF A PUBLICATION RESULTING FROM THIS WORK

Reprinted from THE JOURNAL OF CHEMICAL PHYSICS, Vol. 22, No. 8, 1462, August, 1954
Printed in U. S. A.

Electronic Transitions in the Nitrite Ion

WILLIAM G. TRAWICK AND W. H. EBERHARDT
School of Chemistry, Georgia Institute of Technology, Atlanta, Georgia
(Received June 14, 1954)

A STUDY of the polarized ultraviolet absorption spectra of single crystals of sodium nitrite at liquid nitrogen temperature has yielded the following information:

1. The absorption band with maximum around 3500A appears to have an origin at 3851.4A and is polarized in the *a* direction of the crystal, i.e., perpendicular to the plane of the nitrite ion.[1] This absorption is believed to be due to a transition in which one of the unshared electrons on the nitrogen atom is raised to an antibonding π orbital of the ion ($n_N \rightarrow \pi^*$). This assignment is consistent with the fact that this band is absent in the nitroalkyls, nitryl chloride, and the nitrate ion where the corresponding electrons on the nitrogen are shared with other atoms and hence stabilized. We have also found the band to be absent in crystalline silver nitrite where the crystal structure is similar, but the internuclear distances[2] and chemical properties suggest a weak electron-pair bond between the silver ion and the nitrogen of the nitrite ion. However, absorption in this region is present in nitrous acid and the alkyl nitrites both in solution and in the gas.

2. On the basis of some incomplete measurements, the 2050A band appears to be polarized in the *c* direction, i.e., in the plane of the ion and perpendicular to the C_2 axis of the ion. It is assigned as a $\pi \rightarrow \pi^*$ transition and is comparable to the strong bands in the nitrate ion, NO_2, NO_2Cl, the nitroalkyls, and alkyl nitrites at approximately the same place in the spectrum.

3. The absorption band that is found about 3100A in the nitrate ion, NO_2Cl, nitric acid, and the nitroalkyls and which McConnell[3] believes to be an $n \rightarrow \pi^*$ transition appears in the alkaline nitrite ion solution also at about 3000A. In the crystal at liquid nitrogen temperature we find a weaker absorption in this region polarized in the *a* direction which at room temperature gives the effect of broadening the 3600A band. We ascribe this band to a transition in which one of the nonbonding oxygen electrons jumps to the antibonding π orbital of the ion, i.e., $n_O \rightarrow \pi^*$. This assignment is based on the difference in valence state ionization potentials[4] of oxygen and nitrogen which suggests a displacement of the order of one electron volt (or about 800A) to the blue from the $n_N \rightarrow \pi^*$ band. Such a calculation is only a crude estimate at best, but the direction and order of magnitude suggested seem significant. In addition an appreciable difference is found between neutral and acidified solutions of ethyl nitrite in water-ethanol mixtures in the vicinity of 3100–3400A where certain maxima in neutral solutions are greatly weakened in acidic solutions. Maxima above 3400A which are attributed to the $n_N \rightarrow \pi^*$ transitions are not as strongly affected by such a change in acidity.

A more detailed report of this study and its significance in the interpretation of the electronic spectra of other triatomic molecules will be presented in the near future.

[1] G. E. Ziegler, Phys. Rev. **38**, 1040 (1931); Gene B. Carpenter, Acta Cryst. **5**, 132 (1952); Mary R. Truter, Acta Cryst. **7**, 73 (1954).
[2] J. A. A. Ketelaar, Z. Krist. **95**, 383 (1936).
[3] Harden McConnell, J. Chem. Phys. **20**, 700 (1952).
[4] R. S. Mulliken, J. Chem. Phys. **2**, 792 (1934).

BIBLIOGRAPHY

BIBLIOGRAPHY

1S. H. Sponer and E. Teller, "Electronic Spectra of Polyatomic Molecules," Reviews of Modern Physics 13, 76 (1941).

2B. H. Bethe, "Termaufspaltung in Kristallen," Annalen der Physik 3 (5), 133 (1929).

3H. Ralph S. Halford, "Motion of Molecules in Condensed Systems: I Selection Rules, Relative Intensities, and Orientation Effects for Raman and Infrared Spectra," The Journal of Chemical Physics 14, 8 (1946).

4N. Roger Newman, "Polarized Infrared Spectrum of Sodium Nitrite," The Journal of Chemical Physics 20, 444 (1952).

5C. D. P. Craig and P. C. Hobbins, "Polarized Ultraviolet Absorption of Anthracene," Nature 171, 566 (1953).

6S. Otto Schnepp and Donald S. McClure, "Symmetry Assignments for the First Two Excited Singlet Electronic States of the Naphthalene Molecule," The Journal of Chemical Physics 21, 959 (1953).

7A. A. C. Albrecht and W. T. Simpson, "The Excited Electronic State of the 2600 A Transition in Benzene," The Journal of Chemical Physics 22, 940 (1953).

8L. L. E. Lyons, "Absorption by Pyrimidines of Plane Polarized Ultraviolet Light," The Journal of Chemical Physics 20, 1814 (1952).

9N. Kazuro Nakamoto, "Dichroism of Benzene Rings. I The Dichroism of Hexamethylbenzene and Hexabromomethylbenzene," The Journal of the American Chemical Society 74, 390 (1952).

10N. Kazuro Nakamoto, "Dichroism of Benzene Rings. II The Dichroism of m-Dinitrobenzene and Anthraquinone," The Journal of the American Chemical Society 74, 392 (1952).

11N. Kazuro Nakamoto and Keisake Suzaki, "Direct Evidence for the $n \rightarrow \pi$ Electronic Transition of the Nitroso-Absorption," The Journal of Chemical Physics 20, 1971 (1952).

12Y. S. Yamada, H. Yoneda and R. Tsuchida, "Absorption Spectra of Coordination Compounds. VIII. Dichroism of Planar Complexes." Journal of the Chemical Society of Japan, Pure Chemistry Section 69, 145 (1948).

13S. Edward V. Sayre, Kenneth M. Stancier and Simon Freed, "The Absorption Spectrum of Single Crystals of Anhydrous Praseodymium Chloride," A Paper Presented at Discussions of Physical and Inorganic Chemistry, American Chemical Society, September 1953.

14G. D. M. Gruen and M. Freed, "Crystalline Field Effects in Uranium Fluorides," A Paper Presented at Discussions of Physical and Inorganic Chemistry, American Chemical Society, September 1953.

15C. C. A. Coulson, Valence. London: Oxford at the Clarendon Press, 1952, Chapter VIII.

16E. H. Eyring, J. Walter and Geo. E. Kimball, Quantum Chemistry, New York: John Wiley and Sons, Inc., 1944, Appendix VII.

17C. Gene B. Carpenter, "The Crystal Structure of Sodium Nitrite," Acta Crystallographica 5, 132 (1952).

18H. G. Herzberg, Infrared and Raman Spectra of Polyatomic Molecules, New York: D. Van Nostrand Co., Inc., 1945, p. 104f.

19M. R. S. Mulliken, "Magic Formula, Structure of Bond Energies and Isovalent Hybridization," The Journal of Physical Chemistry 56, 295 (1952).

20M. R. S. Mulliken, C. A. Rieke, D. Orloff and H. Orloff, "Formulas and Numerical Tables for Overlap Integrals," The Journal of Chemical Physics 17, 1248 (1949).

21S. H. Sponer and E. Teller, op. cit., p. 75.

22S. Ibid., pp. 79-80.

23M. R. S. Mulliken, "Electronic Structures and Spectra of Triatomic Oxide Molecules," Reviews of Modern Physics 14, 204 (1942).

24Z. G. E. Ziegler, "Crystal Structure of Sodium Nitrite," The Physical Review 38, 1040 (1931).

25W. A. D. Walsh, "The Electronic Orbitals, Shapes and Spectra of Polyatomic Molecules," Journal of the Chemical Society (London) 1953, 2260.

26F. H. L. Friedman, "On the Ultraviolet Absorption Spectra of Uninegative Ions," The Journal of Chemical Physics 21, 319 (1953)

27K. Michael Kasha, "Characterization of Electronic Transitions in Complex Molecules," Discussions of the Faraday Society, 1950, No. 9, 14.

28N. R. J. Newman and R. S. Halford, "Motion of Molecules in Condensed Systems. VII The Infrared Spectra for Single Crystals of Ammonium Nitrate and Thallious Nitrate in Polarized Radiation," The Journal of Chemical Physics 18, 1276 (1950).

29G. T. R. P. Gibb, Optical Methods of Chemical Analysis, New York: McGraw-Hill Book Co., Inc., 1942, p. 245.

30W. Ernest E. Wahlstrom, Optical Crystallography, New York: John Wiley and Sons, Inc., 1943, pp. 48f.

31W. Ralph W. G. Wycoff, Crystal Structures, Vol. I, New York: Interscience Publishers, Inc., 1948, Chapter VI, text p. 10.

32W. Ernest E. Wahlstrom, op. cit., pp. 93f.

33K. J. A. A. Ketelaar, "Die Kristallstruktur des Silbernitrites," Zeitschrift fur Kristallographie 95, 383 (1936).

34W. Ernest E. Wahlstrom, op. cit., p. 128 and pp. 160ff.

35W. F. S. Wilson, A Study of the Effect of Pressure on the Visible Spectrum of Ozone. Unpublished M. S. Thesis, Georgia Institute of Technology, 1949, p. 14.

36S. John Strong, Procedures in Experimental Physics, New York: Prentice-Hall Inc., 1939, p. 462.

37R. Gunther Rodloff, "Uber die Ultraviolett Absorption an Kalium nitrite Nitriten and Schwefekohlenstoff bei treten Temperaturen," Zeitschrift fur Physik 91, 511 (1934).

38M. I. Maslakowez, "Zur Lichtabsorption in Kristallen bei spurenweiser Anwesenheit von Fremdionen," Zeitschrift fur Physik 51, 696 (1928).

39D. A. S. Davydov, "Theory of Absorption Spectra of Molecular Crystals," Zhurnal Eksperimental'noi i Teorticheskoi Fiziki 18, 210 (1948); Chemical Abstracts 43, 4575f (1949).

40B. M. Belenky and W. P. Juse, "Photochemie des Silbernitrites," Zeitschrift fur anorganische und allgemeine Chemie 190, 277 (1930).

41H. R. N. Haszeldine, "Studies in Spectroscopy. Part IV. The Infrared and Ultraviolet Spectra of Some Aliphatic Nitro-compounds," Journal of the Chemical Society 1953, 2525.

42C. Wu-chieh Cheng, Private Communication.

43K. K. S. Krishnan and A. C. Guha, "Absorption Spectra of Nitrates in Relation to Their Photodissociation," Proceedings of the Indian Academy of Sciences 1A, 242 (1934), and "Pleochroism and Crystal Structure," Nature 126, 12 (1930).

44M. Harden McConnell, "Effect of Polar Solvents on the Absorption Frequency of $n \rightarrow \pi$ Electronic Transitions," The Journal of Chemical Physics 20, 700 (1952).

45P. C. H. Purkis and H. W. Thompson, "Photochemistry of Nitrates, Nitrites and Nitro Compounds. II," Transactions of the Faraday Society 32, 1466 (1936).

46T. P. Tarte, "Recherches Spectroscopiques sur l'acide nitreus," Bulletin de la Societe de chimique de Belgique 59, 365 (1950).

47K. G. Kortum, "Uber die Zuordung von Elektronen banden in Losungs-spektren. III. Die Lichtabsorption der salpetrigen Saure, der Salpetersaure, ihrer Ester and Salze," Zeitschrift fur physikalische Chemie B43, 418 (1939).

48G. C. E. Goodeve and S. Katz, "The Absorption Spectrum of Nitrosyl Chloride," Proceedings of the Royal Society (London) A172, 102 (1930).

49E. W. H. Eberhardt, Private Communication.

50A. Robert J. Athey, The Absorption Spectrum of Nitryl Chloride. Unpublished M. S. Thesis, Georgia Institute of Technology, 1950.

51V. Ernest Vigreux, "Contribution a l'Etude Experimentale de l'Absorption de l'Ozone," Annales de physique 8, 709 (1953).

52H. L. Harris and G. W. King, "The Rotational Structure of the Ultraviolet Bands of NO_2," The Journal of Chemical Physics 8, 775 (1940).

53N. Mario Nardelli, Lugi Cavaka and Antonio Braibant, "Contributo alla conoscen za degli argentonitriti. Nota III. Equilibri nelle soluzioni sature di nitrito di argento in presenza di ioni NO_2 in excesso," Gassetta chimica italiana 83, 483 (1953).

54G. Maximilien Grunfeld, "Absorption dans l'Ultraviolet et Reactivite Chimique de Certains Classes de Composes Organiques," Annales de Chimie 20, 304 (1933).

55H. T. C. Hall and F. E. Blacet, "Separation of the Absorption Spectrum of NO_2 and N_2O_4 in the Range 2400-5000 A," The Journal of Chemical Physics 20, 1745 (1952).

56R. Eugene Rabinowitch, "Electron Transfer Spectra and Their Photochemical Effects," Reviews of Modern Physics 14, 112 (1942).

57C. C. A. Coulson, Valence. London: Oxford at the Clarendon Press, 1952, p. 194.

58E. H. Eyring, J. Walter and Geo. E. Kimball, Quantum Chemistry. New York: John Wiley and Sons, Inc., 1944, pp. 184f.

59M. R. S. Mulliken, "A New Electroaffinity Scale; Together with Data on Valence States and on Valence Ionization Potentials and Electron Affinities," The Journal of Chemical Physics 2, 782 (1934).

60E. W. H. Eberhardt, Private Communication.

61E. H. Eyring, J. Walter and Geo. E. Kimball, op. cit., pp. 143f.

62B. R. F. Bacher and Samuel Goudsmit, Atomic Energy States. New York: McGraw-Hill Book Co., Inc., 1932.

63W. Ernest E. Wahlstrom, op. cit., p. 111.

64H. George R. Harrison, Massachusetts Institute of Technology Wavelength Tables. New York: John Wiley and Sons, Inc., 1939.

65K. H. Kayser, Tabelle der Schwingungzahlen. Revised by W. F. Meggers, Ann Arbor, Michigan: Edwards Brothers, 1944.

66R. F. D. Rossini, National Bureau of Standards Tables of Selected Values of Chemical Thermodynamic Properties. Washington, D. C.: 1947.

67M. R. S. Mulliken, "Intensities of Electronic Transitions in Molecular Spectra I. Introduction," The Journal of Chemical Physics 7, 18 (1939).

VITA

The author was born on August 16, 1924 in Sandersville, Georgia to George T. and Ruth T. Trawick. He lived in the farm community of Linton, Hancock County, Georgia until the fall of 1936. He entered the Linton Consolidated School in 1931 and Hazlehurst High School in 1936. In 1941 he was graduated as valedictorian of his class. He entered Georgia Institute of Technology as a co-op student in chemical engineering in June of 1941 and in April of 1943 was called into the armed forces. He served until January, 1946, in this country and in Europe. In February, 1946 he returned to Georgia Institute of Technology and completed the work for a bachelor's degree in chemistry in the fall of 1947. For seven months he was employed by American Bakeries Company as a chemist. On August 7, 1948 he was married to Margaret Gheesling and they entered Southern Baptist Theological Seminary to study theology and Bible. In September, 1950 he returned to Georgia Institute of Technology to begin work toward a doctorate in chemistry. On April 26, 1954 a son, Robert Jesse, was born. In October, 1954 the author began work as a chemist with Carbide and Carbon Chemicals Company, K-25 Plant, in Oak Ridge, Tennessee.